Ecological Tipping Points in the Mississippi Sound in Response to Modeled Bonnet Carré Spillway Openings

Project Personnel

Kim de Mutsert, PhD

Associate Professor, School of Ocean Science and Engineering

The University of Southern Mississippi

Aaron Ridall, PhD

Postdoctoral Scholar, School of Ocean Science and Engineering

The University of Southern Mississippi

Scott Milroy, PhD

Associate Professor, School of Ocean Science and Engineering

The University of Southern Mississippi

Report Citation:

De Mutsert, K., Ridall, A. & Milroy, S. 2026, Ecological Tipping Points in the Mississippi Sound in Response to Modeled Bonnet Carré Spillway Openings, 107 pp, The University of Southern Mississippi, Ocean Springs, MS.

Acknowledgements

We want to thank the Mississippi Sound Coalition who requested this research and funded it through GOMESA funds appropriated by the Mississippi Legislature to the Mississippi Department of Marine Resources. MDMR granted the funds to Harrison County, Mississippi, Board of Supervisors, which selected NGI in a competitive procurement process. We want to thank the USM physical modeling team (Brandy Armstrong, Jerry Wiggert, Kemal Cambazoglu, Mohsena Lopa, and Marc Diard) for providing us with the salinity and temperature output of the Bonnet Carré Spillway opening scenarios as drivers in the ecological models. A separate report contains the details of the hydrodynamic modeling work of the overarching project. The authors also acknowledge HPC at The University of Southern Mississippi supported by the National Science Foundation under the Major Research Instrumentation (MRI) program via Grant # ACI 1626217. We also appreciate the efforts of the Mississippi-Alabama Sea Grant Consortium in arranging for external reviews. We thank the reviewers for providing a critical assessment which was truly insightful and guided our efforts to substantially improve this report. The overall guidance of Dr. Paul Mickle and assistance of the staff at the Northern Gulf Institute, in report formatting and logistics, facilitation of the peer-review process, and review of this final report is gratefully recognized.

Executive Summary

Background and Objectives

This project examines ecological effects of the current operational strategy of the Bonnet Carré Spillway (BCS), a Mississippi River flood-control structure located about 21 miles northwest of New Orleans, Louisiana, and managed by the U.S. Army Corps of Engineers. The BCS is part of the larger Mississippi River and Tributaries Project, a network of levees and control structures designed to minimize flooding from the American plains to southern Louisiana. The spillway is opened when river discharge at New Orleans is forecasted to exceed 1,250,000 cubic feet per second, diverting significant volumes of Mississippi River water into the Mississippi Sound.

The Mississippi Sound normally maintains salinities of 5–18 parts per thousand, fluctuating with seasonal wet and dry periods. While natural salinity deviations can occur due to local factors, these are usually brief. Extended BCS openings, however, have reduced salinity to zero for over 39 consecutive days across much of the estuary. Past BCS openings have been linked to elevated mortality in marine species, including oysters. Over the past 14 years, the BCS has been opened seven times, which is more frequent than during the previous six decades. After the two BCS openings in 2019, it became clear that spillway operations can have severe impacts on ecosystems and fisheries, as harvestable oyster reefs in the Mississippi Sound experienced up to 100% mortality based on MDMR field surveys during the summer of that year. Mississippi's on-bottom oyster fishery was closed for five years after this event. With increasing rainfall trends at both local and national scales, there is an urgent need to explore alternative flood-control strategies and management approaches that minimize ecological harm and protect Mississippi's marine resources.

This is the report on the ecological component of the project "Development of an operational alternative to the Bonnet Carré Spillway accounting for ecological tipping points in the Mississippi Sound". The objective of this component is to identify where and when environmental stressors (e.g., low salinity) lead to the ecological tipping points

whereby (or salinity thresholds when) oyster mortality is significantly increased due to BCS releases, and at what discharge these occur.

Approach

We analyzed MDMR oyster survey data from 2006 to 2022 to determine what the average percent natural mortality is. The tipping point per life stage was determined to be one standard deviation away from natural mortality. To create a common metric between the field data and the model simulations, we translated the percent mortality observed in the field into a percent biomass loss. We developed an Ecopath with Ecosim model to simulate biomass changes of settled life stages of oysters—spat (0.33-24 mm), seed (25-76 mm), and sack oysters (>76 mm)—under 7 different scenarios that are reconstructions of past BCS openings plus one scenario without a BCS opening. We compared the biomass change in each scenario for each life stage at eight different Mississippi oyster reefs (Figure E1) to the ecological tipping point of each life stage. We also developed habitat suitability index (HSI) models for oyster larvae, spat, seed and sack. The models determine the suitability of the habitat based on salinity and temperature on a scale from 0 (completely unsuitable habitat) to 1 (ideal habitat suitability) and were calculated daily based on salinity and temperature output from the seven BCS scenarios. These HSI's informed the salinity and temperature response of spat, seed, and sack oysters in the Ecosim simulations, and allowed for a deeper dive into the suitability changes at each reef daily in response to the BCS opening scenarios.

We used a hydrodynamic modeling framework to simulate scenarios based on "hindcasts" - flow conditions (river flow as well as BCS release) that have occurred in the past - to reduce uncertainty about what the environmental conditions are during BCS release events. To make the scenarios comparable and focused on the effects of the BCS openings, the atmospheric forcings of the same year (2018) were used in each scenario, and the BCS opened at the same time in each scenario. These historical openings reflect seven scenarios, detailed below and characterized in Table E1, Figure E2.

1. Scenario 1: The first scenario recreates the 2011 opening, which spanned 43 days with a total freshwater discharge volume of 329.6% of Lake Pontchartrain.
2. Scenario 2: The second scenario recreates the 2018 opening, which spanned 21 days with a total freshwater discharge volume of 86.6% of Lake Pontchartrain.
3. Scenario 3: The third scenario recreates the 2019 first opening, which spanned 43 days with a total freshwater discharge volume of 219.5% of Lake Pontchartrain.
4. Scenario 4: The fourth scenario recreates the 2019 second opening, which spanned 79 days with a total freshwater discharge volume of 346.9% of Lake Pontchartrain.
5. Scenario 5: The fifth scenario recreates the combined 2019 openings, which spanned 122 days with a total freshwater discharge volume of 566.4% of Lake Pontchartrain.
6. Scenario 6: The sixth scenario recreates the river inflow only from the climatology (average conditions based on 2011-2020), without BCS openings.
7. Scenario 7: The seventh scenario recreates the 2020 opening, which spanned 29 days with a total freshwater discharge volume of 59.9% of Lake Pontchartrain.

The resulting salinity and temperature output from running these scenarios with the hydrodynamic model was applied to the habitat suitability and ecosystem models, to determine suitability and ecological tipping points for oysters within the Mississippi Sound and Bight.

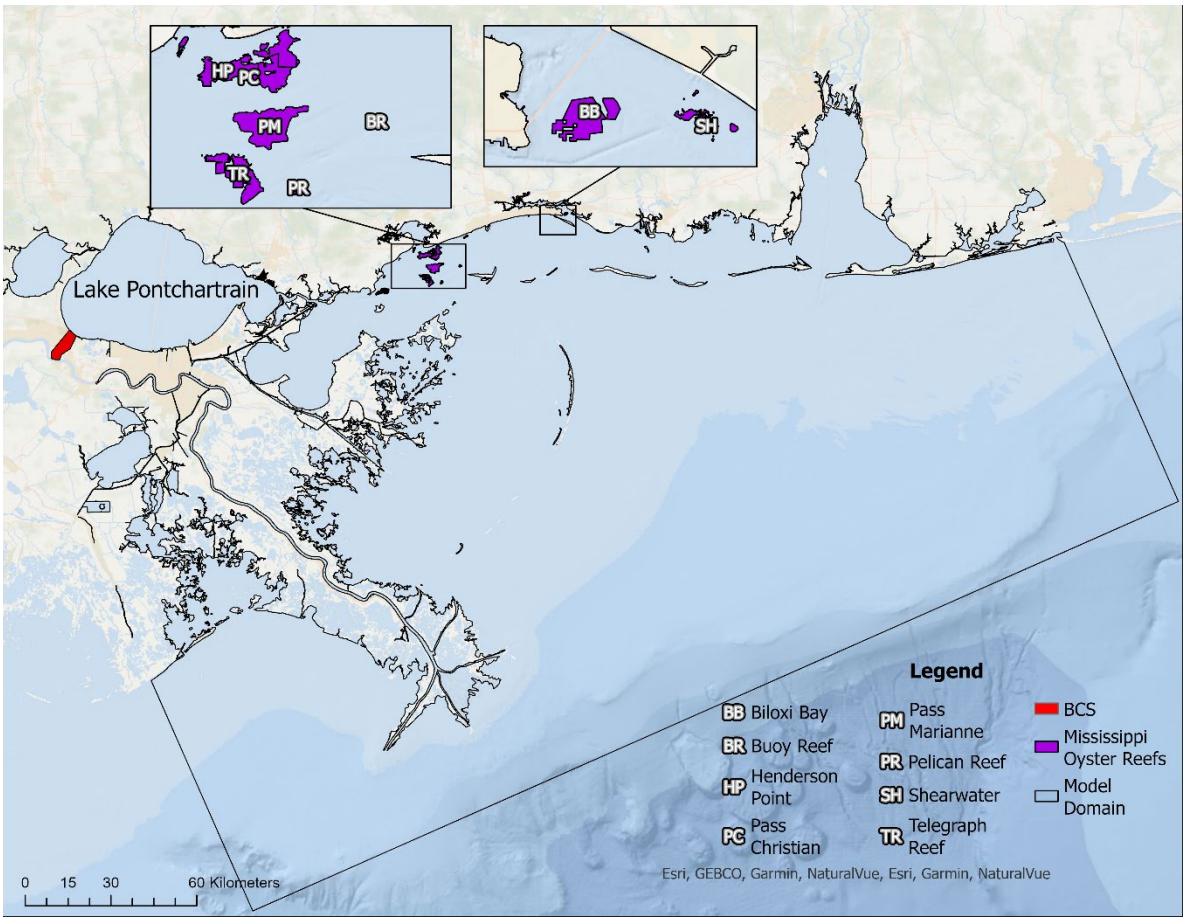

Figure E1. Locations of Mississippi oyster reefs that are the focus of this study.

Table E1. BCS operations used for hydrodynamic model experiments to inform water temperature and salinity for habitat suitability and Ecosim model runs. Scenario 2019A: first 2019 opening; *Scenario* 2019B: second 2019 opening; *Scenario* 2019Full: 2019 with both the first and second openings; *Scenario* 2019 RO: 2019 with rivers-only forcing and no BCS operations.

Opening Scenario	Opening Duration (days)	Opening Volume (% Lake Pontchartrain)	Avg. Discharge (m^3/s)	Est. Total Discharge (km^3)	Volume/Intensity Category
2011	43	329.6	5891	21.9	Extreme
2018	21	86.6	3035	5.8	Below Average
2019A	44	219.5	3967	15.1	Above Average
2019B	79	346.9	3374	23	Extreme
2019Full	123	566.4	3587	38.1	Extreme
2020	29	59.9	1536	3.98	Lowest
2019 RO	NA	NA	NA	NA	NA

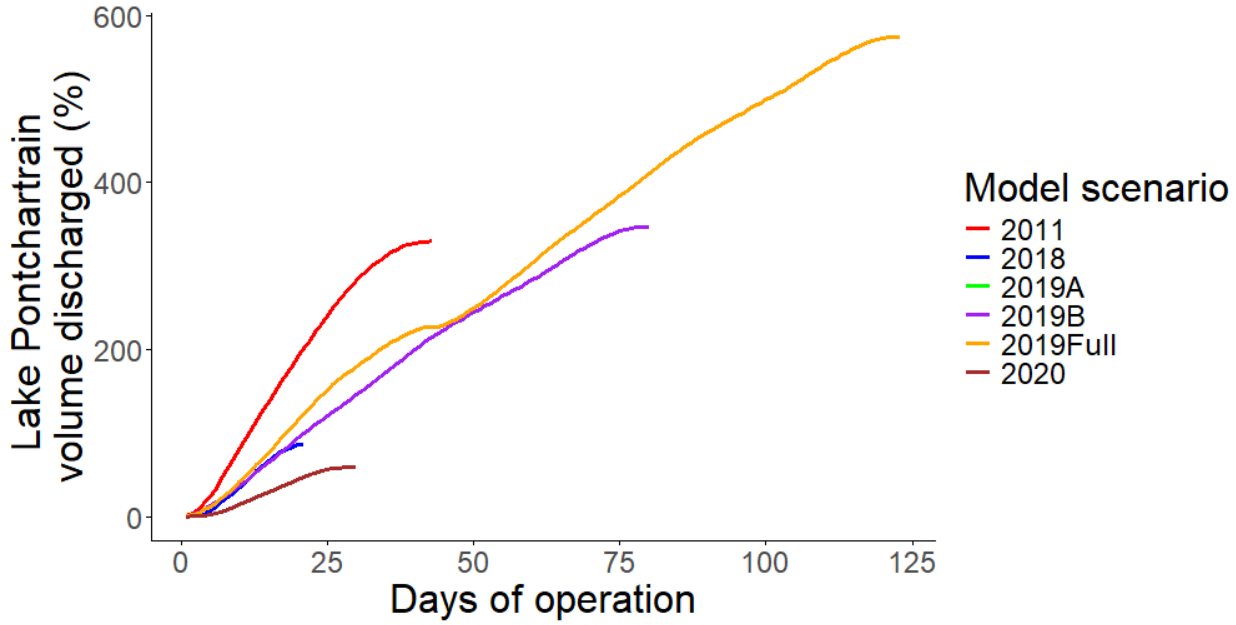

Figure E2. Duration (days of operation) and diverted river volume (as percentage of Lake Pontchartrain) of historic BCS operations used for the hydrodynamic model scenarios.

Key Findings and Recommendations

Ecological tipping points for each oyster stanza were calculated as 19.4%, 32.3%, and 38% of spat, seed, and sack biomass, respectively, remaining after one year. This means that recovery of each of the life stages is severely impaired if over one year the biomass of spat, seed oysters and sack oysters is reduced by 80.6%, 67.7% and 62% respectively. Environmental conditions leading to these ecological tipping points represent unsuitable conditions beyond tolerance thresholds for the oysters.

Hydrodynamic model results from the various historical BCS releases tested indicated that the age-class of settled oysters that was most sensitive to BCS-induced environmental stress was newly-settled spat, for all BCS release scenarios and all reef locations tested (Figure E3).

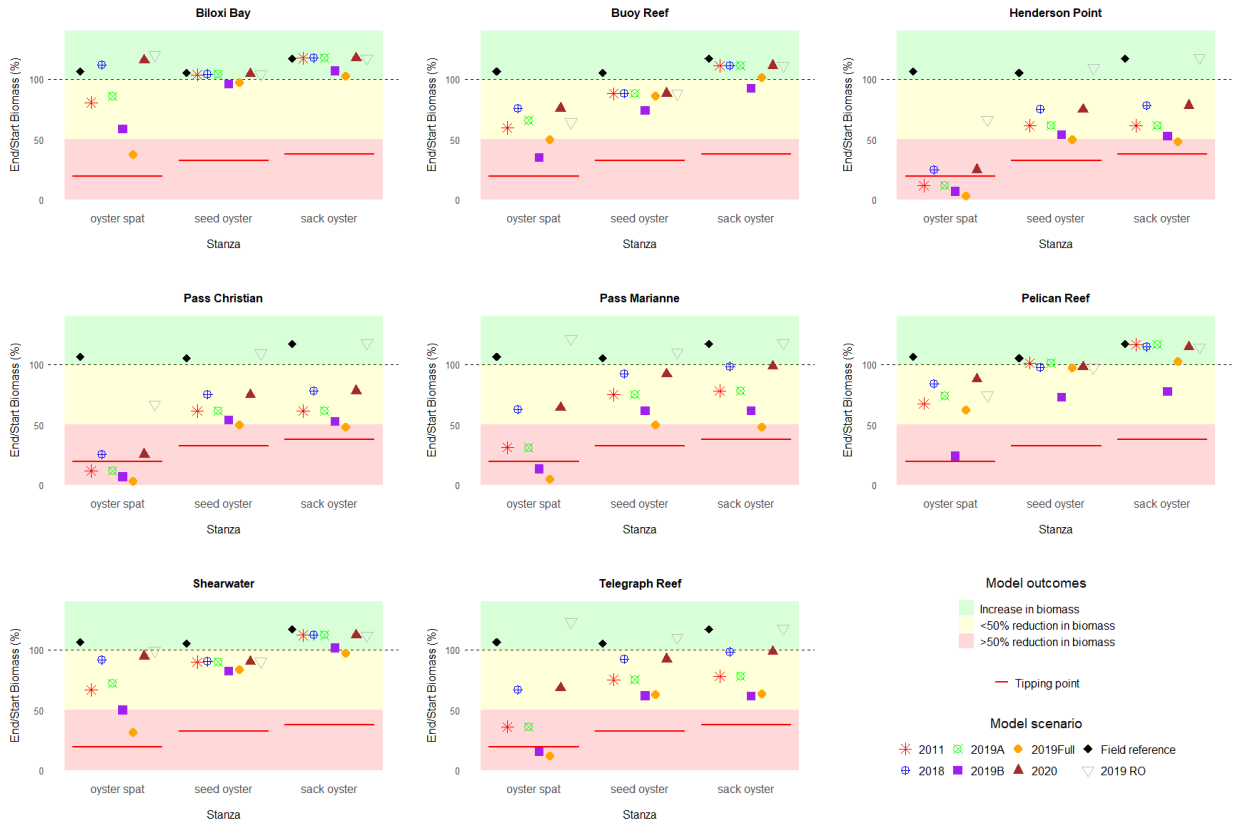

Figure E3. Ecosim estimates of oyster biomass trends (by age-class) at various reef sites throughout the Mississippi Sound in response to the historical BCS release scenarios tested, compared to field reference data. Note the horizonal red lines which represent the ecological tipping point for each age-class of settled oyster, calculated as one standard deviation below the average field biomass loss for years when mortality occurred.

BCS operations have led to ecological tipping points for eastern oysters in the Mississippi Sound. The double opening of the spillway in 2019 severely affected oyster biomass, with the modeled double opening scenario leading to the lowest oyster biomass values at six of the eight Mississippi oyster reefs included in this study (Biloxi Bay, Henderson Point, Pass Christian, Pass Marianne, Shearwater and Telegraph Reef). Ecological tipping points occurred for oyster spat during the simulated 2011 BCS opening scenario, the simulated 1st 2019 BCS opening scenario, the simulated 2nd 2019 BCS opening scenario, and the simulated 2019 BCS double opening scenario at Henderson Point and Pass Christian reefs. This includes scenarios where the BCS was open for 43 days with a total freshwater discharge volume of 329.6% of Lake Pontchartrain (2011), the BCS was open for 43 days with a total freshwater discharge volume of 219.5% of Lake

Pontchartrain (2019A), the BCS was open for 79 days with a total freshwater discharge volume of 346.9% of Lake Pontchartrain (2019B), and the BCS was open for 122 days with a total freshwater discharge volume of 566.4% of Lake Pontchartrain (2019Full). While spat oysters located at the Pass Marianne and Telegraph Reef locations had seemingly avoided reaching their ecological tipping point during the simulated 2011 BCS opening scenario and the simulated 1st BCS opening scenario of 2019, the simulated 2nd 2019 opening scenario and the simulated 2019 double opening scenario did result in losses past this ecological threshold.

Reefs in the eastern portion of the model domain—Biloxi Bay and Shearwater—were less affected by all opening scenarios than reefs in the west, demonstrating proximity effects of the BCS opening on oyster mortality. Seed and sack oysters experienced good conditions in Biloxi Bay during all BCS openings, indicating that Biloxi Bay is a good oyster relay location when a BCS opening appears inevitable. The biomass at Buoy Reef and Pelican Reef was less negatively affected by freshwater inflow as compared to Henderson Point, Pass Christian, Pass Marianne, and Telegraph Reef as well. However, these reefs are only 0.192 and 0.408 km^2, respectively, and have not been as historically productive compared to the larger, western MS Sound reefs. The extreme reductions in environmental quality and oyster biomass experienced at the western reefs during long and voluminous discharges through the BCS are impactful, given that the two most historically productive and largest reefs in the Mississippi Sound, Pass Christian and Pass Marianne, are western reefs.

The 2018 and 2020 opening scenarios had the least impact on oyster biomass across all size classes at all reefs compared to all other BCS openings scenarios, which is reflective of the shorter duration and lower freshwater discharge volume for these two scenarios. These openings did not cause ecological tipping points for any of the size classes at any of the reefs, only resulted in poor conditions for spat at two reefs (Henderson Point and Pass Christian), and resulted in fair to good conditions at all other reefs for all life stages. Thus, it is indeed possible that conservative spillway operations can result in acceptable – even beneficial – effects on oysters in the Mississippi Sound. While

this study demonstrates that ecological tipping points are specific to size classes of oysters and locations of the reefs, the developed models allow us to determine ahead of time which reefs are most likely to be affected, and to what extent, when a BCS opening is proposed in future years. The shortest opening duration when tipping points for spat occurred in our scenarios was 43 days, and the smallest discharge volume when tipping points for spat occurred was 219.5% of Lake Pontchartrain. Using the information from the scenarios we have run in this study, a BCS opening duration up to 29 days (2020) with a total freshwater discharge volume up to 86.6% of Lake Pontchartrain (2018) would allow for oyster biomass losses to remain above their ecological tipping points for all life stages at all reefs included in our study.

Table of Contents

Abbreviations

A

Akaike Information Criterion **(AIC)**

Alabama Department of Conservation and Natural Resources **(ADCNR)**

B

Bonnet Carré Spillway **(BCS)**

C

Catch per Unit Effort **(CPUE)**

Coupled Ocean-Atmosphere-Wave-Sediment Transport Modeling System **(COAWST)**

Cubic Feet per Second **(cfs)**

E

Ecopath with Ecosim and Ecospace Ecosystem Modeling Software **(EwE)**

Ecotrophic Efficiency **(EE)**

F

Florida **(FL)**

H

Habitat Suitability Index Model **(HSI)**

L

Left Bottom **(LB)**

Left Top **(LT)**

Locally Estimated Scatterplot Smoothing **(LOESS)**

Louisiana **(LA)**

Louisiana Department of Wildlife and Fisheries **(LDWF)**

Lower Limit Threshold **(LL)**

Lower Optimal Threshold **(LO)**

M

Mississippi **(MS)**

Mississippi Department of Marine Resources **(MDMR)**

Mississippi Sound and Bight **(MSB)**

Mississippi Sound and Bight Regional Application of the COAWST Model Domain **(msbCOAWST)**

N

National Oceanic and Atmospheric Administration **(NOAA)**

P

Pre-balance **(PREBAL)**

R

Regional Ocean Modeling System **(ROMS)**

Right Bottom **(RB)**

Right Top **(RT)**

Rivers Only Hydrodynamic Model Experiment **(RO)**

S

Salinity **(Sal)**

Southeast Area Monitoring and Assessment Program **(SEAMAP)**

Sum of Squares **(SS)**

U

United States Geological Survey **(USGS)**

Upper Limit Threshold **(UL)**

Upper Optimal Threshold **(UO)**

V

Variable **(Var)**

W

Weighted Incidence **(WI)**

Western Mississippi Sound **(wMSS)**

List of Figures and Tables

Figure 8. The primary productivity driver in Ecosim based on total nitrogen load measured in the Mississippi River at Tarbert Landing, MS.

Figure 9. Salinity and temperature drivers used to calibrate the model.

Figure 10. Calibration plots of spat, seed, and sack oyster biomass and landings.

Figure 11. Locations of Mississippi oyster reefs that are the focus of this study.

Figure 12. Duration (days of operation) and diverted river volume (as percentage of Lake Pontchartrain) of historic BCS operations used for the hydrodynamic model scenarios.

Figure 13. Bottom salinity output from the msbCOAWST model scenarios at the eight different reefs we have included in our research.

Figure 14. Bottom temperature output from the msbCOAWST model scenarios at the eight different reefs we have included in our research.

Figure 15. Ecosim modeling estimates of oyster biomass trends (by age-class) at various reef sites throughout the Mississippi Sound in response to the historical BCS release scenarios tested, compared to field reference data.

Figure 16. Scenario 2011 near-bottom mean daily salinities (top row) and the resultant calculation of HSI_{Sal} for spat-sized oysters (bottom row) at those locations where Ecosim model results indicated a “tipping point” had been reached.

Figure 17. Scenario 2019A near-bottom mean daily salinities (top row) and the resultant calculation of HSI_{Sal} for spat-sized oysters (bottom row) at those locations where Ecosim model results indicated a “tipping point” had been reached.

Figure 18. Scenario 2019B near-bottom mean daily salinities (rows 1,3) and the resultant calculation of HSI_{Sal} for spat-sized oysters (rows 2,4) at those locations where Ecosim model results indicated a “tipping point” had been reached.

Figure 19. Scenario 2019Full near-bottom mean daily salinities (rows 1,3) and the resultant calculation of HSI_{Sal} for spat-sized oysters (rows 2,4) at those locations where Ecosim model results indicated a "tipping point" had been reached.

Table E1. BCS operations used for hydrodynamic model experiments to inform water temperature and salinity for habitat suitability and Ecosim model runs.

Table 1. Model data source information for forcing parameters and ecological variables applied in performing the simulations.

Table 2. Initial parameters used to develop the Ecopath model. $\frac{P}{B}$ = Production to Biomass ratio, $\frac{Q}{B}$ = Consumption to Biomass ratio, stanza break = age in months when juveniles become adults, VBGF K = curvature parameter in von Bertalanffy growth function.

Table 3. Length-weight regressions and data sources used to calculate g_i m^{-2}.

Table 4. Parameters for the balanced Ecopath model. $\frac{P}{B}$ = Production to Biomass ratio, $\frac{Q}{B}$ = Consumption to Biomass ratio, EE = ecotrophic efficiency, and $\frac{P}{Q}$ = Production to Consumption ratio.

Table 5. Trapezoidal response curve values for salinity and temperature.

Table 6. Model output locations and associated reefs used to evaluate ecological tipping points model runs.

Table 7. BCS operations used for hydrodynamic model experiments to inform water temperature and salinity for Ecosim model runs. Scenario 2019A: first 2019 opening; Scenario 2019B: second 2019 opening; Scenario 2019Full: 2019 with both the first and second openings; Scenario 2019 RO: 2019 with rivers-only forcing and no BCS operations.

Table 8. Hydrodynamic model results from the various BCS discharge scenarios tested, indicating the total number of days when mean daily near-bottom salinity ≤ 5.0 (or the maximum number of consecutive days when mean daily near-bottom salinity ≤ 5.0, in parentheses).

List of Figures and Tables from Appendix

Introduction

Background

Eastern oyster, *Crassostrea virginica*, have long been a preferred target for management and restoration efforts in coastal waters, particularly for the wide-ranging economic and ecological benefits they provide. For example, commercial oyster landings within U.S. Gulf waters have generated an average of $85M revenue per year over the last decade, representing more than 50% of all U.S. oyster value from 2011-2020 (NOAA Office of Science and Technology, 2023). Beyond their economic significance, oysters also provide a host of valuable ecosystem services, such as their capacity to: enhance shoreline protection and mitigate coastal erosion in low-energy environments (La Peyre et al., 2017; Morris et al., 2021; Piazza et al., 2005), accelerate carbon sequestration (Fodrie et al., 2017; Veenstra et al., 2021), improve water quality via nutrient removal (Ayvazian et al., 2021; Humphries et al., 2016; Kellogg et al., 2013; Parker & Bricker, 2020), enhance water clarity via clearance of suspended particulate matter (Coen et al., 2007; Kreeger et al., 2018; Turner, 2021), and provide critical habitat to other economically- and ecologically-important species (Coen et al., 2007; Gilby et al., 2018; Mann, 2001).

The eastern oyster plays a defining role in the economic and ecological function of Mississippi coastal waters and is a critical focus of MS state restoration efforts. The need for dramatically more effective restoration strategies has become especially acute in recent years, as the Mississippi oyster fishery suffered a precipitous three-fold decrease in year-to-year commercial landings from 2017 to 2018, and then dwindling to zero by 2019, where it remains to-date (NOAA Office of Science and Technology, 2023). While the decimation of the Mississippi oyster fishery has largely been attributed to the ecological impacts from Hurricane Katrina in 2005 (Buck, 2005; Mackenzie Jr., 2006; Sheikh, 2005; Supan & Voisin, 2006) and the Deepwater Horizon oil spill in 2010 (Baker et al., 2017; Blancher II et al., 2017; Grabowski et al., 2017; Vignier et al., 2018), prolonged exposure to excessive river effluent has also served as a dominant threat to oyster recovery and restoration in northern Gulf waters (Gledhill et al., 2020; La Peyre et al., 2013; Posadas,

2020; Soniat et al., 2013). In fact, freshwater flooding impacts to the shrimp and oyster fisheries within MS state waters have led to two federal disaster declarations in 2011 and again in 2019, with another declaration in 2020 pending decision (NOAA Office of Sustainable Fisheries, 2023).

Bonnet Carré Spillway History and Environmental Effects

The Bonnet Carré Spillway (BCS) was constructed in 1931 in response to the catastrophic Mississippi River flood of 1927 and remains the largest freshwater diversion influencing the Mississippi Sound and Bight (United States Army Corps of Engineers, 2021). Located approximately 52 km upstream of New Orleans, the BCS consists of 350 floodgates that can divert up to 7,079 $m^3 s^{-1}$ (250,000 cfs) of Mississippi River water into Lake Pontchartrain, which then flows into Lake Borgne and ultimately into the northern Gulf via the Mississippi Sound and Chandeleur Sound. The U.S. Army Corps of Engineers is mandated to open the spillway when Mississippi River discharge at New Orleans exceeds 35,396 $m^3 s^{-1}$ (1.25 million cfs) (United States Army Corps of Engineers, 2021). Since its construction, the BCS has been opened 15 times, averaging one opening every six years, but the frequency has increased markedly in recent decades. Five openings occurred between 2016 and 2020 alone, including the first-ever three consecutive annual openings from 2018–2020 as well as the first instance of dual openings within a single calendar year in 2019 (Parra et al., 2020).

Although designed as a flood-control structure to protect New Orleans, the BCS has far-reaching ecological effects when operated. High-volume releases of freshwater alter circulation, stratification, and water quality in Lake Pontchartrain and the Mississippi Sound, often reducing salinities to near zero for extended periods (Parra et al., 2020; Wiggert et al., 2022). These changes are accompanied by the delivery of nutrient-rich water that can intensify eutrophication, promote harmful algal blooms (Soto Ramos et al., 2023), and exacerbate hypoxia (Wiggert et al., 2022). The 2019 openings, which lasted a combined 123 days and discharged an estimated 38.1 km^3 of water, caused massive oyster mortality (approaching 100% at most harvest reefs), harmful algal blooms, beach closures, and

hypoxia that forced mobile fauna to flee and subjected benthic species such as oysters to lethal physiological stress (Gledhill et al., 2020; Hendon et al., 2019).

As described above, BCS operations affect more than just salinity and temperature; they also alter nutrient loads, sediment delivery, turbidity, and pathogen dynamics, all of which can further impact oyster populations through mechanisms such as food dilution, burial, and reduced clearance and respiration rates (Davis & Hidu, 1969; Lenihan, 1999; Loosanoff, 1962; Loosanoff & Tommers, 1948; Park & Clough, 2018; Poirier et al., 2021). However, the modeling work presented here focuses exclusively on the effects of BCS-driven temperature and salinity changes on oyster habitat suitability and biomass changes. As such, our results should be viewed as representing the minimum expected ecological impact of spillway operations, with future modeling efforts needed to fully incorporate the impacts of nutrient loadings, hypoxia, and sediment-related stressors for a more complete understanding of BCS effects.

Primary Objective and Goals

This project will provide the Mississippi Sound Coalition with the scientific information needed to determine how much freshwater diverted through the BCS is too much for eastern oyster (*Crassostrea virginica*) at several historically and currently important oyster reefs in the Mississippi Sound. The core objective is to develop model-based guidance on the critical salinity threshold and BCS operation and duration that lead to environmental conditions where oyster mortality is significantly increased to such an extent that recovery is severely impaired. The ultimate goal of this project is to provide the best available scientific information needed to accurately address public concerns regarding the potential effects of BCS flood diversions on the shellfisheries within the jurisdictional waters of Mississippi. The report presented herein provides model-based guidance on the impacts that various historical BCS flood diversion scenarios have had on habitat suitability and biomass of oysters in Mississippi's jurisdictional waters.

Study Area

Located in the northern Gulf, the Mississippi Sound (Figure 1) is a shallow (~3 m), predominantly well-mixed estuarine basin with microtidal range (~0.6 m) (C. K. Eleuterius, 1978), extending from Grand Island, Louisiana to Dauphin Island, Alabama, spanning the entire Gulf coast of the state of Mississippi (U.S. Fish and Wildlife Service (USFWS), 1982). Water exchange with the Gulf is restricted by five major barrier islands (Cat, Ship, Horn, Petit Bois, and Dauphin Islands), with natural freshwater fluxes largely dominated by the Pascagoula River in the eastern Sound and the Pearl River in the western Sound (C. K. Eleuterius, 1978), although the Mobile and Tensaw rivers can contribute fresh water to the eastern Sound as well (Cambazoglu et al., 2017). When the Mississippi River reaches flood stage upstream of New Orleans, the Bonnet Carré Spillway is used to divert flood waters into Lake Pontchartrain, resulting in episodic (but quite significant) freshwater fluxes which ultimately flow into the western MS Sound (Cambazoglu et al., 2017; Greer et al., 2018).

As an obligate estuarine organism, the eastern oyster is found throughout the entire Mississippi Sound, and in the neighboring coastal waters of Breton and Chandeleur Sounds of Louisiana and within Mobile Bay, Alabama (Figure 1). While it has been noted that oyster physiology and ecology are governed almost entirely by temperature, salinity, and food availability (La Peyre et al., 2021), the greatest density of oysters within the Mississippi Sound are relegated to those areas which are also host to substrate of suitable firmness to support the weight of accreting oyster reefs. In Mississippi waters, the most productive oyster reefs have historically been restricted to the western Mississippi Sound, south of Bay St. Louis and nestled between Cat Island, MS and Grand Island, LA.

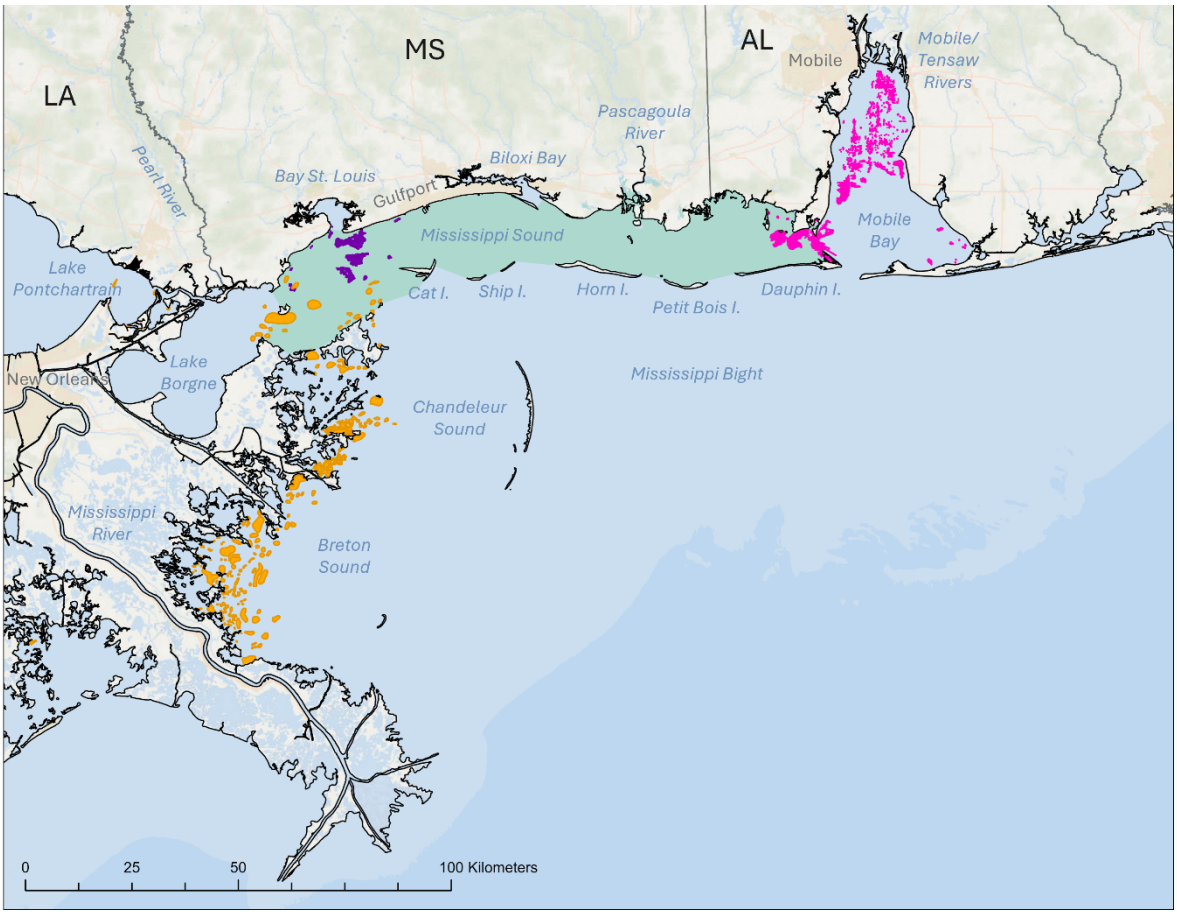

Figure 1. Map of the general study area and model domain (adapted from NOAA Office of Science and Technology, 2011). Current locations of known reef and/or on-bottom lease areas for the eastern oyster (Crassostrea virginica) are indicated in orange (Louisiana), purple (Mississippi), or fuchsia (Alabama).

Methods

Model Data and Integration

A coupled modeling framework was used to determine the effects of BCS operations on oyster biomass across Mississippi Sound reefs. As part of this coupled approach, a hydrodynamic model for the Mississippi Sound was run, from which the salinity and temperature data were used to inform oyster habitat suitability and to drive the temperature and salinity dynamics within the Ecosim model. The data sources and their resolution for each model forcing parameter are provided in Table 1, and each model component is subsequently described in the following sections. Briefly, daily bottom water salinity and bottom water temperature data at all reefs within the study were exported from the msbCOAWST model and integrated into HSI calculations. The monthly average HSI along with monthly bottom water temperature and monthly bottom water salinity at each reef from the msbCOAWST model were used to inform oyster habitat suitability and the environmental suitability for each Ecosim model group for each scenario.

Hydrodynamic Model Framework

In order to resolve the spatio-temporal variability of temperature and salinity which were used to define oyster habitat suitability, Wiggert et al. (2022) implemented changes to their application of the Coupled Ocean-Atmosphere-Wave-Sediment Transport (COAWST) modeling system (Warner et al., 2010), with the Regional Ocean Modeling System (ROMS; Haidvogel et al., 2008; Shchepetkin & McWilliams, 2005) at its core, to refine their regional circulation model specifically calibrated for application within the Mississippi Sound and Bight (Greer et al. 2018) and ultimately in response to the needs of this project (Wiggert et al., 2022; Figure 2). The Mississippi Sound and Bight regional application of the COAWST (msbCOAWST) model domain encompasses the Mississippi Sound and Bight southward to the continental shelf break, westward to Lake Maurepas, LA and eastward to Perdido Bay, FL at 400 m horizontal resolution (580 x 370 horizontal grid points) and 24 vertical layers (Cambazoglu et al., 2024; Wiggert et al., 2022), with finer vertical resolution in the top/bottom layers to better resolve boundary layer processes (Cambazoglu et al., 2020).

Table 1. Model data source information for forcing parameters and ecological variables applied in performing the simulations.

Model type	Model Forcing	Source	Spatial Resolution	Temporal Resolution	Reference and Web Link (if available)
Hydrodynamic	River forcing	USGS Stream Gage Data	Point data	Daily averages	U.S. Geological Survey (2021) http://waterdata.usgs.gov/nwis
Hydrodynamic	River temperature	Group for High Resolution Sea Surface Temperature (GHRSST)	6 km 0.05˚	Daily averages	Govekar et al. (2022)
Hydrodynamic	Atmospheric forcing	NOAA High Resolution Rapid Refresh (HRRR)	3 km	Hourly	Benjamin et al. (2016)
Hydrodynamic	Open boundary conditions	Navy Coastal Ocean Model – Gulf of Mexico (NCOM – GOM) regional model	1 km	3 hourly	Jacobs et al. (2016) Jacobs (2017)
Ecopath and Ecosim	Initial biomass and time series	ADCNR, LDWF, MDMR, SEAMAP	Point data	1995-2017	
HSI Ecosim	Bottom water temperature	Mississippi Sound and Bight application of a Coupled Ocean Atmosphere Wave Sediment Transport modeling system (msbCOAWST)	400 m	Daily Monthly	Cambazoglu et al. (2024) https://oceancube.usm.edu
HSI Ecosim	Bottom water salinity	msbCOAWST	400 m	Daily Monthly	Cambazoglu et al. (2024) https://oceancube.usm.edu

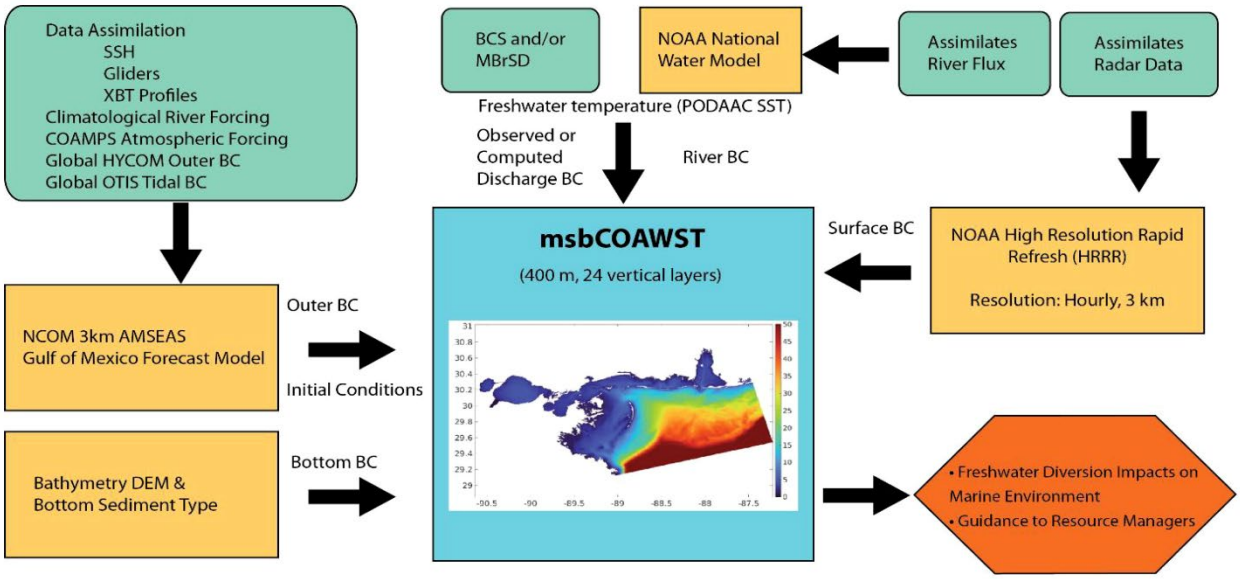

Figure 2. Conceptual diagram of the elements that comprise the msbCOAWST model. Freshwater inputs from MS River diversion structures (specifically, BCS) were computed from U.S. Army Corps of Engineers historical flow records (from Stanic et al., 2024).

Note that the biogeochemical, sediment, and wave modeling capacities of the msbCOAWST model were not employed in the hydrodynamic model implementation used in this project, as msbCOAWST model estimates of daily, weekly, and monthly average salinity gradients were sufficient for the HSI model analyses conducted herein. The reader is invited to refer to Wiggert et al. (2022) for a more comprehensive description of the hydrodynamic model used to estimate the spatio-temporal evolution of critical environmental parameters (specifically, salinity) which were most relevant to the HSI modeling framework below.

Habitat Suitability Index (HSI) Model Framework

General HSI Framework

Although HSI response curves can take any geometric shape, the HSI model calculations herein followed a simple trapezoidal geometry (U.S. Fish and Wildlife Service (USFWS), 1981) defined by four critical threshold values: 1) the lower limit (*LL*) of survival; 2) the lower threshold of optimal condition (*LO*); 3) the upper threshold of optimal

condition (*UO*); and 4) the upper limit (*UL*) of survival (Figure 3), such that HSI scores were computed for each age-class of oyster according to their respective sensitivities to modeled variable (*var*) such as salinity and temperature.

Thus, HSI scores were calculated in response to a given environmental variable (*var*) following Equations 1-4, where:

$$HSI = 0 \; when \; var \; \leq LL \mid var \geq UL \tag{1}$$

$$HSI = 1 \; when \; LO \; \leq var \leq UO \tag{2}$$

$$HSI_{LL \rightarrow LO} = \left[\frac{1}{(LO - LL)} \cdot var\right] + \frac{LL}{(LL - LO)} when \; LL < var < LO \tag{3}$$

$$HSI_{UO \rightarrow UL} = \left[\frac{1}{(UO - UL)} \cdot var\right] + \frac{UL}{(UL - UO)} when \; UO < var < UL \tag{4}$$

Each HSI score was calculated to explore the relative significance of salinity (HSI_{Sal}) in the determination of habitat suitability for each age-class of oyster. Resultant HSI_{Sal} scores were then translated into a more intuitive stoplight color scheme to visually identify areas/thresholds of "poor" (red; 0.00 – 0.29), "fair" (yellow; 0.30 – 0.59), or "good" (green; 0.60 – 1.00) habitat suitability, as suggested by Volety et al. (2009).

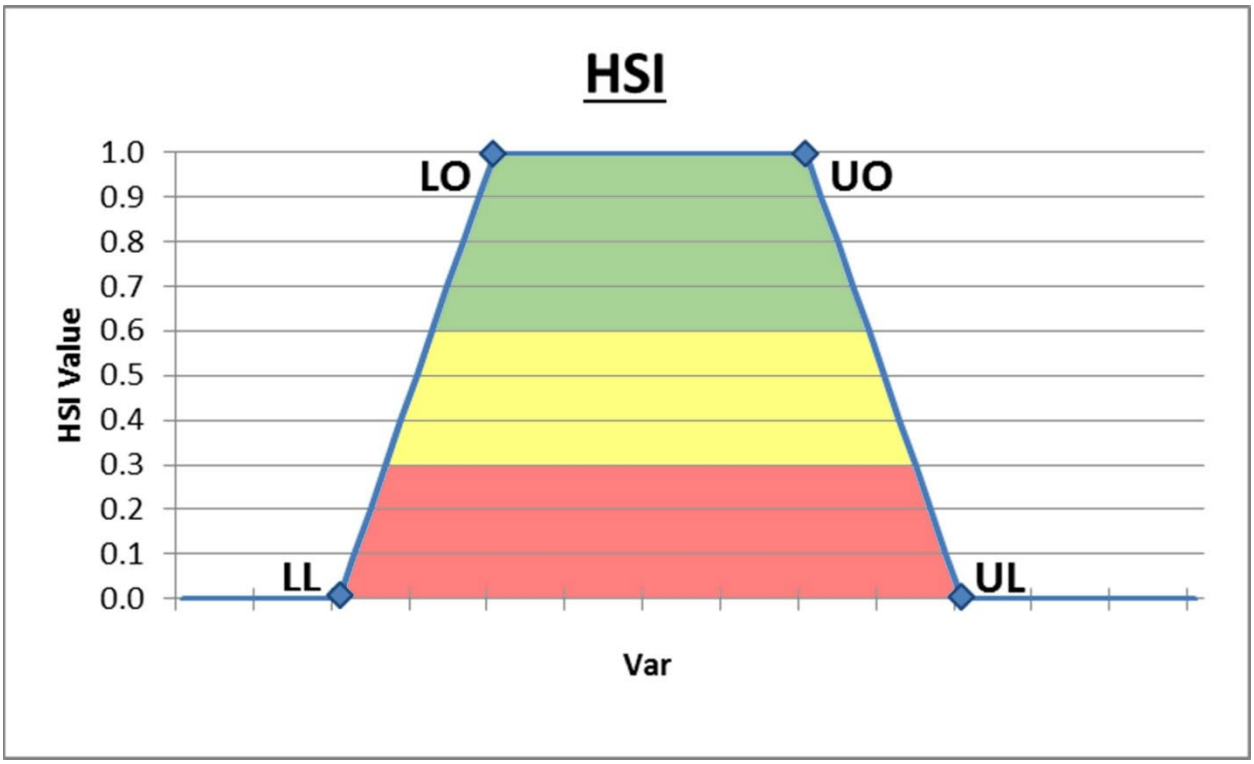

Figure 3. Trapezoidal geometry of habitable eco-space as prescribed by the HSI model, defined by the four critical threshold values (LL, LO, UO, UL) of sensitivity in response to variable environmental conditions (Var). Note that the "stoplight" scheme defining poor (0.00 – 0.29), fair (0.30 – 0.59), or good (0.60 – 1.00) habitat suitability follows Volety et al. (2009).

Oyster Age-classes Modeled

Oyster larvae are planktonic and have a minimum length dimension of approximately 50 μm (Galtsoff, 1964) soon after fertilization (by trochophore stage) and grow somewhat linearly with respect to fractional development time (Dekshenieks et al., 1993), reaching a maximum length dimension of 300-350 μm (Galtsoff, 1964) prior to settlement as spat. Assuming larvae settle as spat upon reaching 330 μm (Dekshenieks et al., 1993), the "Larv" age-class represents all planktonic oysters across all trochophore-veliger-pediveliger stages of development, ranging from 50-330 μm in size (190 μm median).

Among the three age-classes of settled oysters, the "Spat" age-class was chosen to represent small, newly-settled oysters ranging from 0.33 – 25 mm in size (Hofman et al., 1994; Powell et al., 1994; Rybovich, 2014), with a median size of 12.7 mm. The "Seed" age-

class (25-76 mm; median size of 50.5 mm) represents a combination of sexually immature juvenile (25-50 mm) and sexually mature sub-adult (50-76 mm) oysters (Hofman et al., 1994; Powell et al., 1994) which have not yet grown to market size (Rybovich, 2014; Soniat et al., 1998). The "Sack" age-class is used to represent all those sexually mature adult oysters which have grown large enough (>76 mm) for commercial exploitation (Hofman et al., 1994; Powell et al., 1994; Soniat et al., 1998).

Oyster Habitat Thresholds of Temperature and Salinity

A comprehensive review of the scientific literature was performed to glean the most appropriate values of *LL*, *LO*, *UO*, *UL* based on published values of intrinsic preference for temperature and salinity minima, maxima, and optima among larval, spat, seed, and sack oysters throughout the U.S. Gulf and Atlantic coastal waters (Tables A1-A2). Ultimately, a total of 160 published threshold values among 21 citations were used to calculate mean threshold values defining HSI_{Tmp} (Figure 4) and HSI_{Sal} (Figure 5) representing the temperature and innate (i.e. osmoregulation) salinity tolerances (respectively) among all oyster age-classes in waters free from predation and/or disease.

However, when occurring in natural waters, the *UO* and *UL* of settled oysters are more appropriately constrained by the salinity tolerance of co-occurring marine predators, most notably the southern oyster drill, *Stramonita* (=*Thais*) *haemastoma floridana*. Oyster drill frequency and predation rates have both been linked to an increasing salinity gradient (Garton & Stickle, 1980) within waters of greater marine influence, such that oyster drills – while rarely found below the 15 salinity isocline (Louisiana Sea Grant, 1996; St. Amant, 1957) – exhibit maximal predation rates at 20 salinity (Garton & Stickle, 1980) and can swiftly decimate oyster populations in polyhaline (18-30 salinity) waters. Spat- and seed-sized oysters are particularly vulnerable, which are ~3.375X more likely to suffer predation losses by oyster drills than are sack-sized oysters (Butler, 1985).

To more accurately reflect settled oysters' exposure to predatory losses to oyster drills at polyhaline salinities, the UO_{Sal} and UL_{Sal} thresholds for spat- and seed- (and to a lesser extent, sack-) sized oysters were modified to reflect the diminished oyster habitat

suitability in waters which are more favorable to oyster drills. Since all but the largest oysters are particularly susceptible to oyster drill predation, the UO_{Sal} for both spat- and seed-sized oysters were set to 15.0, to coincide with the LL_{Sal} of the oyster drill (Louisiana Sea Grant, 1996; St. Amant, 1957).

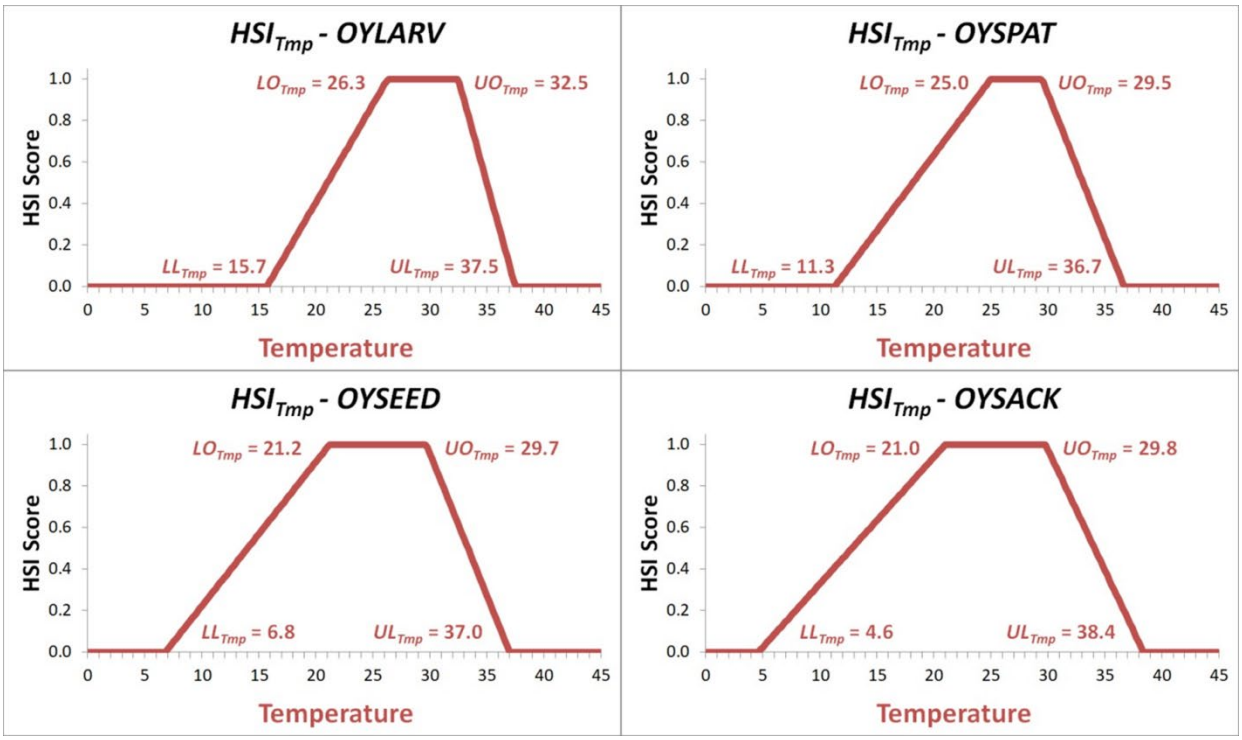

Figure 4. Chosen temperature thresholds which define HSI_{Tmp} for larval (top left), spat (top right), seed (bottom left), and sack (bottom right) oysters.

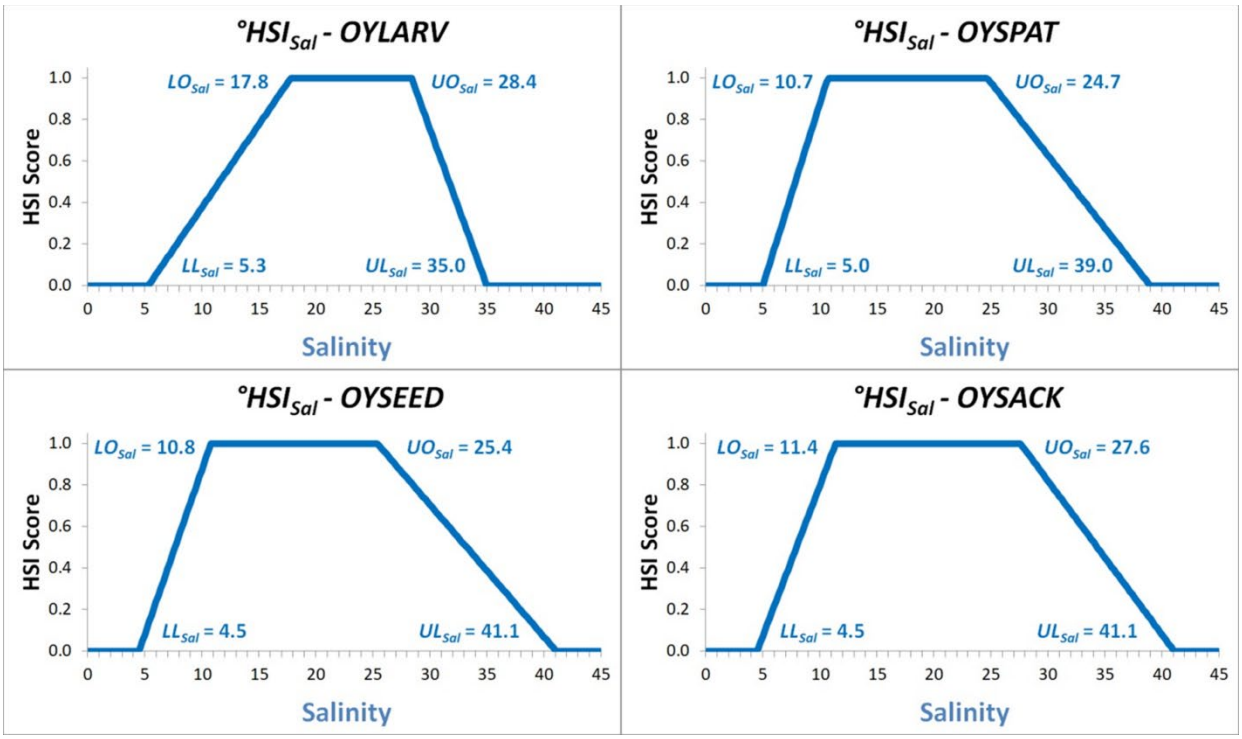

Figure 5. Salinity thresholds which define HSI_{Sal} for larval (top left), spat (top right), seed (bottom left), and sack (bottom right) oysters based solely on innate salinity tolerance (i.e. $°HSI_{Sal}$).

Using 15.0 salinity as the effective UO_{Sal} for spat exposed to oyster drill predation and the original value of 39.0 salinity (Figure 4) as the innate spat UL_{Sal} in Eq. 4, the resultant linear equation of spat *UO→UL* was simply:

$$Spat\ HSI_{Sal}(UO \rightarrow UL; no\ predation) = -0.0417Sal + 1.625 \qquad (5)$$

Since spat are 3.375X more susceptible to oyster drill predation than sack-sized oysters (Butler, 1985), the slope of Eq. 5 was "steepened" by a factor of 3.375, yielding a new slope of -0.1406 which was then used in Eq. 4 to estimate a new value for spat UL_{Sal} (= 22.1), updating Eq. 5 to now become:

$$Spat\ HSI_{Sal}(UO \rightarrow UL; with\ predation) = -0.1406Sal + 3.109 \qquad (6)$$

to represent a diminution of habitat suitability when spat are exposed to oyster drill predation.

In similar fashion, the effective UO_{Sal} for seed-sized oysters exposed to oyster drill predation was also set to 15.0 salinity, and the original value of 41.1 salinity (Figure 4) as the innate seed UL_{Sal} in Eq. 4, the resultant linear equation of seed *UO→UL* was:

$$Seed\ HSI_{Sal}(UO \rightarrow UL; no\ predation) = -0.0383Sal + 1.575 \quad (7)$$

Since seed-sized oysters are also 3.375X more susceptible to oyster drill predation compared to sack oysters (Butler, 1985), the slope of Eq. 7 was similarly steepened by a factor of 3.375, yielding a new slope of -0.1293 which was used in Eq. 4 to estimate the new value for seed UL_{Sal} (= 22.7), such that Eq. 7 was replaced by:

$$Seed\ HSI_{Sal}(UO \rightarrow UL; with\ predation) = -0.1293Sal + 2.948 \quad (8)$$

to represent diminished habitat suitability when seed are exposed to oyster drill predation.

The sensitivity of sack oysters to oyster drill predation was handled somewhat differently, whereby the difference between the innate sack UO_{Sal} (= 27.6; Figure 4) and drill LL_{Sal} (= 15.0; Louisiana Sea Grant, 1996; St. Amant, 1957) was modified by a factor of 0.2963 (= 1/3.375) and added to the drill LL_{Sal} threshold value (= 15.0) to obtain a new estimate for sack UO_{Sal} (= 18.7) to more appropriately constrain the range of refuge salinities for sack oysters subject to predation, so:

$$Sack\ UO_{Sal} = \left[(innate\ Sack\ UO_{Sal} - Drill\ LL_{Sal}) \cdot \left(\frac{1}{3.375}\right)\right] + Drill\ LL_{Sal} \quad (9)$$

Similarly, the new estimate for UL_{Sal} among sack-sized oysters subject to oyster drill predation was computed by taking the difference between the innate sack UL_{Sal} (= 41.1; Figure 4) and drill LO_{Sal} (= 20.0; Garton & Stickle, 1980), modified by the same factor of 0.2963 (1/3.375), and then added to the drill LO_{Sal} threshold value (= 20.0), to yield a new

estimate for sack UL_{Sal} (= 25.0), thereby defining the salinity limit beyond which oyster drill predation would likely preclude sack-sized oyster success, such that:

$$Sack\ UL_{Sal} = \left[(innate\ Sack\ UL_{Sal} - Drill\ LO_{Sal}) \cdot \left(\frac{1}{3.375}\right)\right] + Drill\ LO_{Sal} \qquad (10)$$

In all, these new estimates for UO_{Sal} and UL_{Sal} were used to redefine the HSI_{Sal} for spat, seed, and sack oysters (Figure 6) in this analysis, as they are more reflective of the true habitat suitability with respect to settled oysters in natural waters, where marine predators (particularly the southern oyster drill) represent a significant constraint on oyster habitat suitability in polyhaline (18-30 salinity) waters. They are also more consistent with local observations in the U.S. Gulf, where productive oyster reefs are rarely found in waters with typical salinities exceeding 20-25 (Hendon 2019, pers. comm.; Powell 2019, pers. comm.; Hendon & Mickle 2020, pers. comm.).

While predators (such as oyster drill) represent a more obvious biological control on oyster mortality, lethal infections by the protozoan endoparasite *Perkinsus marinus* can also have devastating effects on oyster populations. Under normal conditions, mortality from *P. marinus* infections (i.e. Dermo disease) typically do not outpace oyster population growth (Powell et al., 1996). When significant oyster mortality events from *P. marinus* do occur, they are usually linked to break-out infections associated with periods (and locations) of high salinity waters coincident with high temperatures (Powell et al., 1996; Soniat, 1985). However, it is interesting to note that Soniat (1985) also found that the weighted incidence (WI) of *P. marinus* infections (following Mackin, 1961) were significantly correlated with salinity when considered in isolation (but temperature alone was not significantly correlated with WI). Indeed, subsequent work by Soniat et al. (2012) demonstrated that Dermo disease (caused by *P. marinus*) seems to respond to climate signals specifically in relation to salinity.

Models of *P. marinus* growth have indicated that parasite division (i.e. growth) just equal losses at 20° C temperature and 20 salinity (Powell et al., 1996), suggesting that *P. marinus* populations may exist, but may persist indefinitely, in waters consistently <20

salinity (which suggests a LO_{Sal} = 20 for *P. marinus*). However, La Peyre et al. (2006) found that *P. marinus* exhibited optimal growth parameters (e.g. viability, metabolic rate, and cell abundance) at experimental salinities of 15, 25, and 35, suggesting a lower optimal salinity threshold of 15 may be more appropriate. This threshold is further supported by Ragone Calvo et al. (2000) who suggest that the specific rate of *P. marinus* transmission is optimal at salinities of 15 and higher.

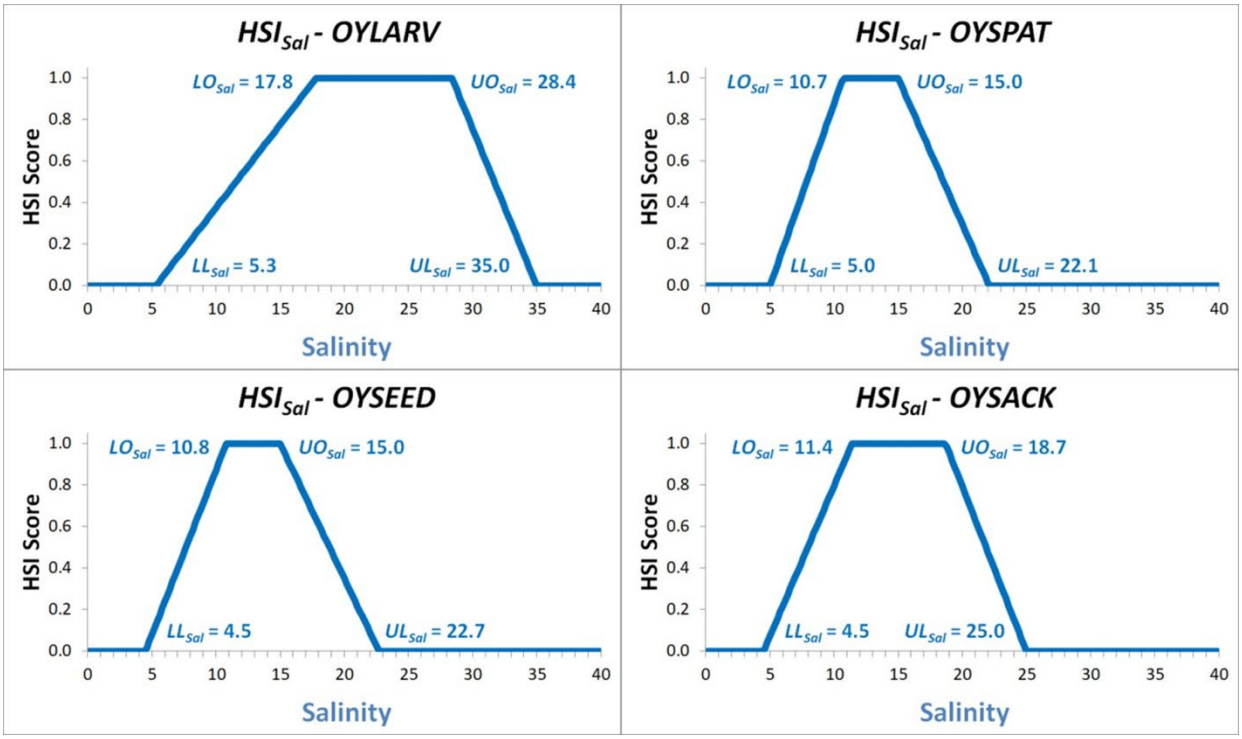

Figure 6. Chosen salinity thresholds which define HSI_{Sal} for larval (top left), spat (top right), seed (bottom left), and sack (bottom right) oysters when considering habitat suitability constraints due either to predation pressure from marine carnivorous snails, primarily from the southern oyster drill, Stramonita (=Thais) haemastoma floridana or from mortalities associated with Perkinsus marinus infections.

Nevertheless, the earlier work of Andrews and Hewatt (1957) found that *P. marinus* infections were absent from Chesapeake Bay oysters in waters with mean summer salinities of 15, were rarely found in salinities of 17, but were quite common in salinities of 19. In more recent investigations, Soniat et al. (2012) indicated that Dermo does not become additive to oyster mortality until salinities of 20 or greater are reached. These salinity thresholds suggest Dermo disease (from *P. marinus* infection) should be parameterized using LL_{Sal} = 15 and LO_{Sal} = 20, salinity thresholds which are identical to

those chosen to represent the southern oyster drill. Thus, the modeled compression/reduction of oyster habitat suitability caused by oyster drill predation (as discussed earlier) was applied as simultaneously inclusive of potential *P. marinus* impacts as well.

Ecopath with Ecosim Modeling Framework

We used the Ecopath with Ecosim (EwE) modeling framework to evaluate trophic interactions and energy flow within the study system. Ecopath is a mass-balance, steady-state model that represents an ecosystem as a network of interacting functional groups, including primary producers, consumers, and detritus. Each group is characterized by parameters such as biomass, production/biomass (P/B), consumption/biomass (Q/B), and diet composition. The model solves a set of linear equations to balance production, consumption, predation, and mortality for all groups simultaneously, ensuring that the energy input and output within the system are accounted for.

This mass-balance approach provides a static snapshot of trophic structure that can be used to quantify ecosystem productivity, evaluate the relative importance of different prey items, and estimate key ecological indicators (e.g., trophic level, transfer efficiency). We then paired this with Ecosim, the time-dynamic module of EwE, to evaluate the effects on different life stages of oyster biomass of freshwater inflow from the BCS and determine where the threshold of biomass loss due to this inflow occurs.

The Mississippi Sound and Bight (MSB) EwE Model is composed of 74 groups that represent species, life stages of species, and species aggregates (Table 2). Major nekton groups were characterized with juvenile and adult life stages to better represent the ontogenetic changes through a species' life history. Oysters were represented in the model with three life stages: spat, seed oysters, and sack oysters. The life stages are linked with a von Bertalanffy growth curve and follow the age-structure dynamics as described in Christensen and Walters (2024). Estimates of initial biomass were obtained from fisheries-independent monitoring programs and the sources indicated in Table 2. In addition to initial

biomass values, production to biomass ($\frac{P}{B}$), consumption to biomass ($\frac{Q}{B}$), multi-stanza age classifications (age breaks), and von Bertalanffy growth function K values were entered for each functional group.

The Ecopath (start) model represents the year 2000. Species biomasses (in t km^{-2}) are based on the average biomass estimated with fish and shellfish survey carried out by state and federal agencies from 1995-2000 (or the earliest year available if no data was collected during this time for a species) within the Mississippi Sound and Bight, Mobile Bay, and the Lower Mississippi River Delta. The average of six years were used for the start model rather than the exact biomass in 2000, to have a start model that is representative of the ecosystem at that time, and to avoid basing the start model on data from one year that could be different than average conditions around that time.

Table 2. Initial parameters used to develop the Ecopath model. $\frac{P}{B}$ = Production to Biomass ratio, $\frac{Q}{B}$ = Consumption to Biomass ratio, stanza break = age in months when juveniles become adults, VBGF K = curvature parameter in von Bertalanffy growth function.

Group No	Group Name	Parameters based on species	Biomass (t km^{-2})	$\frac{P}{B}$	$\frac{Q}{B}$	Stanza Break (mo.)	VBGF K
1	juvenile large coastal sharks	*Sphyrna lewini; Carcharhinus leucas*	0.007[1]	2.00[2]	17.961[2]		
2	adult large coastal sharks			0.51[2]		174[3]	0.08[3,4,5]
3	juvenile dolphins	*Tursiops truncatus*	0.001[6]	3.408[7]	25.3[7]		
4	adult dolphins			0.10[8]		150[9]	0.42[10]
5	juvenile small coastal sharks	*Rhizoprionodon terraenovae*	0.085[11]	2.00[2]			
6	adult small coastal sharks			0.53[12]	4.51[13]	84[14]	0.3[4]
7	juvenile large pelagics	*Scomberomorus maculatus; Trichiurus lepturus*	0.031[15]	4.00[16]			
8	adult large pelagics			0.95[13]	5.6[17]	24[18]	0.64[19]
9	juvenile small pelagics	*Peprilus triacanthus; Chloroscomburs chrysurus*	0.108[15]	3.00[20]			
10	adult small pelagics			2.00[12]	10.4[12]	12[21]	1.744[4,22]
11	sea birds		0.007[15]	1.00[23]			
12	juvenile red snapper	*Lutjaneus campechanus*		3.00[16]	9.2[24]		
13	adult red snapper		0.085[25]	0.60[16]		24[26]	0.147[25]

Group No	Group Name	Parameters based on species	Biomass (t km^{-2})	$\frac{P}{B}$	$\frac{Q}{B}$	Stanza Break (mo.)	VBGF K
14	juvenile red drum	*Sciaenops ocellatus*		2.20[16]			
15	adult red drum		0.006[15]	0.62[16]	3.9[17]	36[27]	0.464[28]
16	juvenile black drum	*Pogonias cromis*		2.00[23]			
17	adult black drum		0.005[15]	0.50[23]	6.36[24]	66[29]	0.17[30]
18	juvenile spotted seatrout	*Cynoscion nebulosus*		3.70[16]			
19	adult spotted seatrout		0.001[15]	0.70[16]	5.4[17]	30[31]	0.22[28,30,32]
20	juvenile other seatrout	*Cynoscion arenarius; Cynoscion nothus*		3.70[16]			
21	adult other seatrout		0.048[15]	0.70[16]	5.4[24]	12[33]	0.31[34]
22	juvenile sciaenids	*Leiostomus xanthurus*		2.00[23]			
23	adult sciaenids		0.124[15]	1.10[16]	7.2[17]	30[35]	0.43[36]
24	juvenile largemouth bass	*Micropterus salmoides*		2.00[23]			
25	adult largemouth bass		0.001[15]	0.60[23]	2.81[24]	12[37]	0.267[38]
26	juvenile gulf sturgeon	*Acipenser oxyrinchus desotoi*	0.002[39]	2.00[23]			
27	adult gulf sturgeon			0.15[39]	2.1[17]	132[40]	0.06[41]
28	juvenile blue catfish	*Ictalurus furcatus*		2.00[23]			
29	adult blue catfish		0.002[15]	0.80[23]	3.3[17]	48[42]	0.12[43]
30	juvenile sea catfish	*Ariopsis felis; Bagre marinus*		2.00[23]			
31	adult sea catfish		0.089[15]	0.80[16]	3.3[17]	12[44]	0.15[17]
32	juvenile Atlantic croaker	*Micropogonias undulatus*	0.260[15]	2.00[23]			
33	adult Atlantic croaker			1.50[16]	8.02[17]	12[45]	0.35[36]
34	juvenile southern flounder	*Paralichthys lethostigma*		2.00[23]			
35	adult southern flounder		0.003[15]	0.42[24]	4.5[17]	36[46]	0.23[28]
36	juvenile near-coastal consumers	*Lagodon rhomboides; Archosargus probatocephalus*		1.02[16]	19.19[23]		
37	adult near-coastal consumers		0.022[15]	0.30[17]		12[47]	0.32[48]
38	rays and skates	*Hypanus sabinus*	0.049[15]	0.70[16,24]	4.7[17]		
39	juvenile demersals	*Calamus leucosteus*		2.52[24]			
40	adult demersals		0.156[15]	0.55[49]	5.7[17]	12[50]	0.28[51]
41	juvenile squid	*Loligo plei*	0.016[15]	4.00[12]			
42	adult squid			3.00[8]	13.12[49]	12[52]	0.59[53]
43	Gulf menhaden 0yr	*Brevoortia patronus*		2.30[16]	19.38[54]		
44	Gulf menhaden 1yr		2.397[55]	1.396[55]		12	0.331[56]
45	Gulf menhaden 2yr			1.723[55]		24	0.331[56]
46	Gulf menhaden 3yr			1.497[55]		36	0.331[56]

Group No	Group Name	Parameters based on species	Biomass (t km^{-2})	$\frac{P}{B}$	$\frac{Q}{B}$	Stanza Break (mo.)	VBGF K
47	Gulf menhaden 4yr			1.497[55]		48	0.331[56]
48	juvenile striped mullet	*Mugil cephalus*	0.003[15]	2.40[16]			
49	adult striped mullet			0.80[16]	12.28[17]	18[57]	0.3[17]
50	juvenile sunfishes	*Lepomis macrochirus; Lepomis microlophus*		2.00[23]			
51	adult sunfishes		0.001[15]	0.80[23]	4.97[58]	24[59]	0.296[60]
52	juvenile forage fish	*Anchoa mitchilli*	0.052[15]	3.00[23]	37.779[23]		
53	adult forage fish			2.53[16]		4[61]	0.6[62]
54	juvenile blue crab	*Callinectes sapidus/similis*		3.00[23]	17.037[43]		
55	adult blue crab		0.022[15]	2.40[16]		15[63]	1.057[64]
56	juvenile brown shrimp	*Farfantepenaeus aztecus*		3.00[23]			
57	adult brown shrimp		0.052[65]	2.40[16]	19.2[16]	10[66]	3.423[67]
58	juvenile white shrimp	*Litopenaeus setiferus*		3.00[23]			
59	adult white shrimp		0.573[68]	2.40[16]	19.2[16]	10[69]	2.493[70]
60	jellyfish		0.082[15]	15[71]	56[72]		
61	oyster spat	*Crassostrea virginica*		2.00[23]			
62	seed oyster	*Crassostrea virginica*		1.80[23]	14.651[54]	4[23]	1.2[23]
63	sack oyster	*Crassostrea virginica*	1.482[15]	2.40[23]		16	1.2[23]
64	oyster drill	*Thais haemastoma*	0.012[15]	4.5[16]	18[16]		
65	grass shrimp	*Palaemonetes spp.*	0.45[23]	4.5[16]	18[16]		
66	benthic crabs	*Rhithropanopeus harrisii*	1[23]	2[12]	18[16]		
67	zoobenthos	*Mellita quinquiesperforata; Luidia clathrata*; Annelids	3.96[23]	4.5[16]	22[16]		
68	benthic crustaceans	Amphipods, Isopods	4.39[23]	4.5[16]	22[16]		
69	mollusks	Clams	4.03[23]	4.5[16]	22[16]		
70	zooplankton		4.124[23]	28.772[58]	84.87[58]		
71	phytoplankton		12.838[23]	81.7[7]			
72	benthic algae		29.778[23]	3.909[58]			
73	SAV		9.778[23]	9.014[12]			
74	detritus		100				

Sources: [1]SEDAR (2024b); [2]Geers (2012); [3]Branstetter & Stiles (1987); [4]Froese (2022); [5]Hoenig (1979); [6]NOAA Office of Science and Technology (2025); [7]www.sealifebase.org (2025); [8]Okey et al. (2004); [9]Sergeant et al. (1973); [10]Palomares et al. (2008); [11]SEDAR (2013); [12]Geers et al. (2016); [13]Sinnickson et al. (2021); [14]Frazier et al. (2014); [15]Pooled agency data from ADCNR, LDWF, MDMR, and SEAMAP monitoring surveys; [16]Walters et al. (2008); [17]www.fishbase.org (2025); [18]Nakamura & Parin (1993); [19]Baker et al. (2001); [20]Sagarese et al. (2017); [21]DuPaul & McEachran (1973); [22]Murphy & Chittenden Jr (1991); [23]De Mutsert et al. (2017); [24]Lewis et al. (2022); [25]SEDAR (2024a); [26]NOAA Fisheries (2025); [27]Satterfield (2017); [28]Matlock & Garcia (1983); [29]Wells & Jones (2002); [30]Pauly (1978); [31]Bester (2025b); [32]Erzini (1991); [33]Shlossman & Chittenden (1981); [34]Nemeth et al. (2006); [35]Bare (2001); [36]Rao (2011); [37]Boudreaux (2013); [38]Beamesderfer & North (1995); [39]Kirk (2008); [40]Bester (2025a); [41]Stevenson & Secor (1999); [42]Carlander (1969); [43]Hilling et al. (2018); [44]Indian River Lagoon National Estuary Program (n.d.); [45]De Mutsert et al. (2012); [46]Reagan Jr & Wingo (1985); [47]Texas Parks and Wildlife Department (n.d.); [48]Nelson (2002); [49]Chagaris et al. (2020); [50]Waltz et al. (1982); [51]Potts & Manooch III (2002); [52]Perez et al. (2002); [53]Pauly (1985); [54]von Bertalanffy (1938); [55]GDAR (2024); [56]SEDAR (2018); [57]Collins (1985); [58]Althauser (2003); [59]Peterson et al.

(2010); [60]Pauly (1979); [61]Luo & Musick (1991); [62]Acosta (2000); [63]GDAR (2013); [64]Sumer et al. (2013); [65]Hart (2015b); [66]Aragão et al. (2021); [67]Parrack (1979); [68]Hart (2015a); [69]Muncy (1984); [70]Klima (1974); [71]Ruzicka et al. (2007); [72]Chiaverano et al. (2018)

The area from which the biomass data are collected includes portions of southeastern Louisiana – including Lakes Maurepas, Pontchartrain, Borgne, Salvador, Little Lake, Barataria Bay, West Bay, East Bay, Black Bay, and the Chandeleur Sound – the Mississippi Sound and Bight, and southern Alabama – including Mobile and Perdido Bays, and is approximately 40,200 km^2 (Figure 7). This larger model domain allows for the use of this model for different projects and is the model domain for future Ecospace model scenarios.

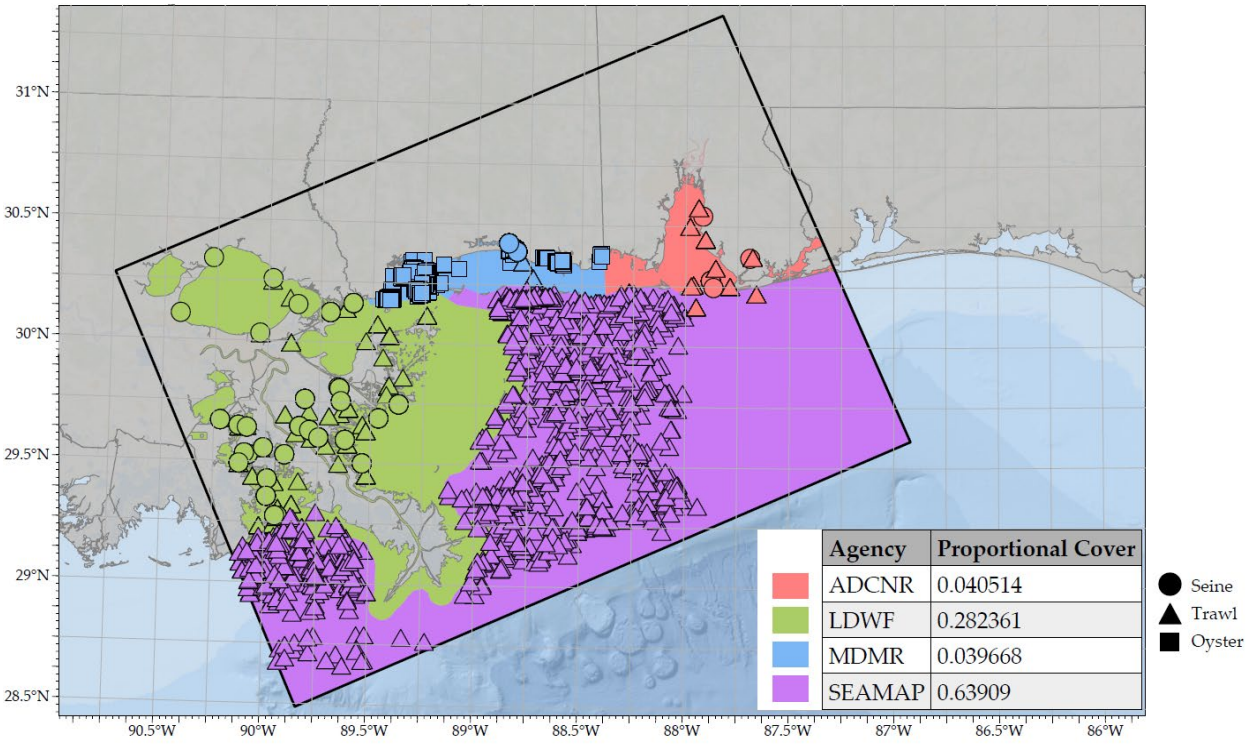

Figure 7. EwE model domain. The symbols indicate the locations of the survey sampling sites the Ecopath model biomass data is based on. The color coding indicates the different agencies collecting the data, and the shape of the symbols indicates the gear type.

Biological Input Data Wrangling

Many species were split into age classes to better reflect ontogenetic changes in a species' life history, resulting in 74 groups that vary in representation of a life stage of a single species (e.g. juvenile red snapper), to a guild (e.g. zoobenthos). For a complete list of model groups, see Table 2.

Two primary inputs required for Ecopath and Ecosim are initial biomasses and a time series of biomasses for each species or species group, respectively. Time series are used for model calibration, allowing for evaluation of model fit with historical data before introducing hypothetical scenarios for which time series data may not exist.

Most of the data used to create the Ecopath model were derived from four fisheries independent monitoring programs: the Mississippi Department of Marine Resources – Fisheries Assessment and Monitoring program (MDMR), the Southeast Area Monitoring and Assessment Program (SEAMAP), the Louisiana Department of Wildlife and Fisheries – Fisheries Independent Monitoring Program (LDWF), and the Alabama Department of Conservation and Natural Resources – Marine Resources Division Fisheries Assessment and Monitoring Program (ADCNR). The fisheries-independent monitoring programs use different gear types in their efforts to target certain species and life stages. For inclusion in the Ecopath model, we need to use gear types that are used by the different agencies, and a collection method that allows for calculating the biomass per area sampled (g m^{-2}). Data collected from the 4.88 m otter trawl, the 15.24 m seine, and the square meter oyster quadrats were used to develop the initial conditions and biomass time series in our model. For all gear types, all sampling events located within the spatial extent of the model domain were included in the initial biomass and time series biomass calculations.

Abundance and length data were used to convert the fisheries-independent monitoring data to g m^{-2} yr^{-1} biomass values, as is required by EwE. Abundance per unit effort data were converted to g m^{-2} for each species in the model by using length-weight relationships and estimating the area sampled with each gear type. Biomass per sample was determined by using abundance and length data in a length-weight regression,

$$W_i = aTL_i^b, \quad (11)$$

where a and b are species-specific parameters, TL is the length measured as total length, and i is each species of interest (Table 3). All species' biomasses were then divided by the sampling area of each gear type to determine the g_i m^{-2}, where i defines each functional group or species.

The area sampled using the 15.24 m seine was calculated by determining the area of a rectangle created during sampling. The length of the seine net represents the short side of the rectangle, while the distance the seine is towed once it is set offshore (30.48 m) represents the long side of the rectangle. As such, the area sampled was calculated by:

$$seine\ area\ sampled\ (m^2) = (15.24 \cdot 30.48) \quad (12)$$

The area sampled using the 4.88 m otter trawl was calculated using methods similar to Brown et al. (2013) and Sparre and Venema (1998) for ADCNR, LDWF, and MDMR trawl efforts. The area sampled equation used in this study was $a = DhX$, where a is the area sampled, D is the distance covered during the tow, h is the length of the headrope, and X is the fraction of the headrope length that is equal to the width of the path.

$$trawl\ area\ sampled\ (m^2) = (925.99 \cdot 4.88 \cdot 0.8) \quad (13)$$

Distance was determined by converting 3.0 knots to 1.54333 m s^{-1} and converting a 10-minute tow time to 600 seconds. Therefore, $D = (1.54333\ x\ 600)$ or 925.99 meters

covered. Headrope length (h) is 4.88 m and X was determined to be 0.8 in this study since the length of the headrope and the width of the path were similar.

For SEAMAP trawl data, the area sampled was calculated by first converting the start and end points for each tow to a towing distance (D. Chagaris, personal communication):

$$distance\ towed\ (NM) = 60\sqrt{(lat_{start} - lat_{end})^2 + (lon_{start} - lon_{end})^2 \cdot cos\theta^2} \qquad (14)$$

where: $\theta = 0.5(lat_{start} + lat_{end}) \cdot \frac{\pi}{180}$, and represents the towing angle in radians. The towing distance was used to determine the area sampled by multiplying by the tow width (0.012192 km) and converting from nautical miles to trawl area sampled in m^2. The trawl area sampled was subsequently calculated as:

$$trawl\ area\ sampled_{SEAMAP}\ (m^2) = 1.852 \cdot distance\ towed\ (NM) \cdot 0.012192 \cdot 1000000 \qquad (15)$$

The catch (in biomass) per unit effort of each species is then divided by this sampling area value.

To correct for gear inefficiencies, calculated biomasses and time series data were increased using correction factors obtained from Rozas and Minello (1997) for both seine (33% correction) and trawl (17% correction) samplings.

Since each of the four fisheries independent monitoring programs only surveys a subset of the model domain, a spatial sampling coefficient was multiplied by the biomass data prior to summing the biomasses for each species or model group across the four monitoring programs. The spatial sampling coefficient was derived by calculating the

proportion of the model domain sampled by each agency ($\frac{area\ sampled\ by\ agency}{total\ model\ area}$). Therefore, total biomass per species *i* in g m^{-2} was determined as:

$$\frac{\sum(aTL_i^b)\cdot S_{ADCNR}}{\sum A}+\frac{\sum(aTL_i^b)\cdot S_{LDWF}}{\sum A}+\frac{\sum(aTL_i^b)\cdot S_{MDMR}}{\sum A}+\frac{\sum(aTL_i^b)\cdot S_{SEAMAP}}{\sum A}, \qquad (16)$$

where aTL_i^b represents the length-weight regression for species *i* as described above on page 41, S represents the spatial sampling coefficient per agency, and A represents the area sampled per gear deployment.

For some model groups, estimates of biomass based on the fisheries independent survey data were not appropriate based on sampling bias or false absence data. Therefore, biomass estimates for such groups were obtained from other sources (Table 2). When initial biomasses could not be obtained from field data, estimates from stock assessments, other published studies, and/or other ecosystem models from similar systems were used as initial conditions in our model. For eastern oysters, biomass estimates came from square meter quadrat sampling by MDMR from the start of this survey in 2006 to 2017. Oyster abundance data from MDMR sampling efforts were converted to g m^{-2} using the oyster L-W relationship described in Table 3. Oyster biomass was then multiplied by the proportion of model domain covered by Mississippi oyster reefs to reflect the spatial extent to which oysters are found within the model domain. Sack oyster biomass was used along with the von Bertalanffy growth function to calculate spat and seed biomasses.

Table 3. Length-weight regressions and data sources used to calculate g_i m^{-2}. Species indicated with an asterisk (*) mark taxa that used FL-TL and SL-TL conversions to calculate these parameters using the data provided. (CW = carapace width; FL = fork length; ML = mantle length; SL = standard length; TL = total length; WD = wing diameter).

Functional Group	Length-Weight Regression	Data Source	Units	
Large coastal sharks	$W_{lcs} = 0.00631TL_{lcs}^{3.06}$	Fishbase	g	cm
Dolphins	$W_{dol} = 0.58TL_{dol}$	(Ridgway & Fenner, 1982)	kg	cm

Functional Group	Length-Weight Regression	Data Source	Units	
Small coastal sharks	NA†			
Large pelagics	$W_{lp} = 0.001TL_{lp}^{2.908}$	Fishbase	g	cm
Small pelagics	$W_{sp} = 0.0356TL_{sp}^{2.612}$	Fishbase	g	cm
Red snapper	$W_{rs} = 0.00749TL_{rs}^{3.16}$	Fishbase	g	cm
Red drum	$W_{rd} = 0.0143TL_{rd}^{3}$	Fishbase	g	cm
Black drum	$W_{bd} = 1.19x10^{-5}TL_{bd}^{3.04}$	(Murphy & Taylor, 1989)	g	mm
Spotted seatrout	$W_{sst} = 0.0073TL_{sst}^{3.139}$	Fishbase	g	cm
Other seatrout*	$W_{ost} = 0.0308SL_{ost}^{2.892}$	Fishbase	g	cm
Sciaenids	$W_{sci} = 0.00921TL_{sci}^{3.072}$	Fishbase	g	cm
Largemouth bass	$W_{lmb} = 0.0144TL_{lmb}^{2.96}$	Fishbase	g	cm
Gulf sturgeon	NA*			
Blue catfish	$W_{bcat} = 0.0185TL_{bcat}^{3}$	Fishbase	g	cm
Sea catfish	$W_{scat} = 0.0181TL_{scat}^{2.99}$	Fishbase	g	cm
Atlantic croaker	$W_{ac} = 0.00918TL_{ac}^{3.09}$	Fishbase	g	cm
Southern flounder	$W_{sf} = 0.00427TL_{sf}^{3.295}$	Fishbase	g	cm
Near-coastal consumers*	$W_{ncc} = 0.0296SL_{ncc}^{3.045}$	Fishbase	g	cm
Rays and skates	$W_{rays} = 0.05WD_{rays}^{3.09}$	Fishbase	g	cm
Demersals	$W_{dem} = 0.0148TL_{dem}^{2.894}$	Fishbase	g	cm
Squid	$W_{sq} = 0.1673ML_{sq}^{2.525}$	Sealifebase	g	cm
Gulf menhaden	$W_{gm} = 0.008TL_{gm}^{2.45}$	(De Mutsert, 2010)	g	cm
Striped mullet	$W_{sm} = 0.0213TL_{sm}^{2.75}$	Fishbase	g	cm
Sunfishes	$W_{sun} = 0.0218TL_{sun}^{2.96}$	Fishbase	g	cm
Forage fish	$W_{ff} = 0.0171SL_{ff}^{2.814}$	Fishbase	g	cm
Blue crab	$W_{bc} = 0.108CW_{bc}^{2.775}$	Sealifebase	g	cm
Brown shrimp	$W_{bs} = 0.006TL_{bs}^{2.938}$	(Fontaine & Neal, 1971)	g	cm
White shrimp	$W_{ws} = 0.003TL_{ws}^{3.247}$	(Fontaine & Neal, 1971)	g	cm
Jellyfish	NA†			
Oysters	$W_{oy} = 9x10^{-5}TL_{oy}^{2}$	(Powell et al., 2016; Rose et al., 1989)	g	mm
Oyster drill	NA†			
Grass shrimp	$W_{grass} = 0.0107BL_{grass}^{2.73}$	Sealifebase	g	cm
Benthic crabs	$W_{benth} = 0.5703CW_{benth}^{2.279}$	Sealifebase	g	cm

*†Species in this functional group were massed by the monitoring agencies and therefore did not require L-W regression calculations. *Gulf sturgeon biomass input data was sourced from Kirk (2008) and therefore a L-W regression calculation was not required.*

The calculated and adjusted annual averaged biomasses from 1995 – 2000 were used as initial input parameters in the Ecopath model for all model groups. For each species we used the survey data for to develop the Ecopath model, we created time series from 2000-2017 based on the annual average biomass for each of those years for model calibration in Ecosim.

Ecopath

Ecopath is based on two mass-balance equations that ensure production and consumption are balanced for each functional group in the modeled ecosystem (Christensen & Pauly, 1992):

1. Production (Energy Balance) Equation:

$$\left(\frac{P_i}{B_i}\right) \cdot B_i \cdot EE_i - \sum_{j=1}^{n} B_j \cdot \left(\frac{Q_j}{B_j}\right) \cdot DC_{ji} - Y_i - E_i - BA_i = 0, \quad (17)$$

where $\left(\frac{P_i}{B_i}\right)$ is the production to biomass ratio for group i, EE_i is the ecotrophic efficiency (the proportion of production used in the system), B_i and B_j are the biomasses of the prey and predators respectively, $\left(\frac{Q_j}{B_j}\right)$ is the consumption to biomass ratio, DC_{ji} is the fraction of prey i in predator j's diet, Y_i is catch rate for the fishery for group i, E_i is the net migration rate, and BA_i is the biomass accumulation for group i.

2. Consumption (Energy Use) Equation:

$$Consumption = Production + Respiration + Unassimilated\ energy \quad (18)$$

This equation ensures that the consumption of each group is balanced by its production, metabolic costs, and waste (unassimilated material).

Together, these equations provide a mass-balanced representation of trophic flows in the system, where energy inputs equal outputs for every group over a year. After initial input parameters were entered (listed in Table 2), a diet matrix was completed. The diet of each model group consists of the proportional consumption of some set of other groups in the model, summing to one. The diet matrix is based on the diet matrix created for the

Delta Management EwE Model (De Mutsert et al., 2017), with adjustments made to account for the proportional availability of prey species in the current model and the changes made to the species list in the model.

Relevant local fisheries fleets and landings were included in the model as well. Two types of fishery-dependent data were used in our model: commercial and recreational landings data. The data were sourced from the NOAA Fisheries One Stop Shop. The commercial fisheries included in the model were: shrimp, black drum, blue crab, Gulf menhaden, and eastern oyster. The recreational fishery included adult small coastal sharks, adult large pelagics, adult red snapper, adult red drum, adult black drum, adult spotted seatrout, adult other seatrout, adult sciaenids, adult largemouth bass, adult sea catfish, adult Atlantic croaker, adult southern flounder, adult near-coastal consumers, and adult blue crab. The landings were divided by the spatial extent of the model domain to calculate g m^{-2}. Landings used as initial inputs in Ecopath were averaged between 1995 and 2000 to account for temporal variability in the data. Time series of average annual landings were created for calibration in Ecosim and spanned the years 2000 – 2017. Fishing mortality time series were included for adult red snapper, adult red drum, adult black drum, Gulf menhaden (1yr, 2yr, 3yr, 4yr), adult brown shrimp, and adult white shrimp sourced from stock assessment reports.

With all Ecopath parameters entered the Ecopath model was balanced. The balancing process ensures that no more biomass of any of the model groups is used in the system by predation or fishing than is produced. The amount of biomass used for each group in the model is reflected in their ecotrophic efficiency (EE), represented as a fraction from 0 to 1. Ecopath uses its first master equation to calculate the EE; the model is balanced when all EEs are between 0 and 1. Adjustments made to balance the model mainly entailed reducing predation pressure to more reasonable levels when it initially resulted in more biomass consumed of a specific species than is produced in the model. During the PREBAL diagnostics (Link, 2010), benthic algae biomass, which was not measured in the system but copied from a different model, was reduced from 29.788 t km^{-2}

to 18.778 t km^{-2}. A balanced representation of the full Mississippi Sound and Bight ecosystem was developed in Ecopath with the parameters indicated in Table 4.

Table 4. Parameters for the balanced Ecopath model. $\frac{P}{B}$ = Production to Biomass ratio, $\frac{Q}{B}$ = Consumption to Biomass ratio, EE = ecotrophic efficiency, and $\frac{P}{Q}$ = Production to Consumption ratio. Values in bold are estimated by Ecopath.

Group No	Group Name	Trophic Level	Biomass (t km^{-2})	$\frac{P}{B}$	$\frac{Q}{B}$	EE	$\frac{P}{Q}$
1	juvenile large coastal sharks	**3.489**	0.007	2.00	17.961	**0.002**	**0.111**
2	adult large coastal sharks	**3.676**	**8.961E-12**	0.51		**0.125**	**0.194**
3	juvenile dolphins	**3.419**	0.001	3.408	25.3	**0.003**	**0.135**
4	adult dolphins	**3.626**	**2.015E-18**	0.10		**0.000**	**0.015**
5	juvenile small coastal sharks	**3.227**	0.085	2.00	4.51	**0.029**	**0.149**
6	adult small coastal sharks	**3.587**	**2.287E-05**	0.53		**0.017**	**0.118**
7	juvenile large pelagics	**3.186**	0.031	4.00		**0.113**	**0.272**
8	adult large pelagics	**3.369**	**0.002**	0.95	5.6	**0.428**	**0.17**
9	juvenile small pelagics	**3.087**	0.108	3.00		**0.029**	**0.179**
10	adult small pelagics	**2.869**	**0.074**	2.00	10.4	**0.027**	**0.192**
11	sea birds	**3.255**	0.007	1.00		**0.017**	**0.056**
12	juvenile red snapper	**3.013**	**0.038**	3.00	9.2	**0.098**	**0.326**
13	adult red snapper	**3.148**	0.085	0.60		**0.076**	**0.262**
14	juvenile red drum	**2.349**	**0.035**	2.20		**0.717**	**0.326**
15	adult red drum	**2.981**	0.006	0.62	3.9	**0.378**	**0.159**
16	juvenile black drum	**2.52**	**0.434**	2.00		**0.102**	**0.088**
17	adult black drum	**2.704**	0.005	0.50	6.36	**0.415**	**0.079**
18	juvenile spotted seatrout	**2.78**	**0.011**	3.70		**0.837**	**0.171**
19	adult spotted seatrout	**3.306**	0.001	0.70	5.4	**0.762**	**0.13**
20	juvenile other seatrout	**3**	**0.003**	3.70		**0.795**	**0.175**
21	adult other seatrout	**2.867**	0.048	0.70	5.4	**0.341**	**0.13**
22	juvenile sciaenids	**2.606**	**0.402**	2.00		**0.284**	**0.133**
23	adult sciaenids	**2.361**	0.124	1.10	7.2	**0.101**	**0.153**
24	juvenile largemouth bass	**2.982**	**1.151E-05**	2.00		**0.687**	**0.184**
25	adult largemouth bass	**2.791**	0.001	0.60	2.81	**0.416**	**0.214**
26	juvenile gulf sturgeon	**2.613**	0.002	2.00		**0.000**	**0.117**
27	adult gulf sturgeon	**2.613**	**1.364E-08**	0.15	2.1	**0.000**	**0.071**

Group No	Group Name	Trophic Level	Biomass (t km^{-2})	$\frac{P}{B}$	$\frac{Q}{B}$	EE	$\frac{P}{Q}$
28	juvenile blue catfish	**2.543**	**0.020**	2.00		**0.0291**	**0.188**
29	adult blue catfish	**2.733**	0.002	0.80	3.3	**0.146**	**0.242**
30	juvenile sea catfish	**2.303**	**0.002**	2.00		**0.406**	**0.144**
31	adult sea catfish	**2.659**	0.089	0.80	3.3	**0.078**	**0.242**
32	juvenile Atlantic croaker	**2.818**	0.260	2.00		**0.233**	**0.1**
33	adult Atlantic croaker	**2.874**	**1.590**	1.50	8.02	**0.026**	**0.187**
34	juvenile southern flounder	**2.672**	**0.003**	2.00		**0.520**	**0.151**
35	adult southern flounder	**3.038**	0.003	0.42	4.5	**0.548**	**0.093**
36	juvenile near-coastal consumers	**2.650**	**1.129E-04**	1.02	19.19	**0.831**	**0.053**
37	adult near-coastal consumers	**2.948**	0.022	0.30		**0.468**	**0.063**
38	rays and skates	**3.017**	0.049	0.70	4.7	**0.068**	**0.149**
39	juvenile demersals	**2.708**	**0.003**	2.52		**0.68**	**0.109**
40	adult demersals	**2.859**	0.156	0.55	5.7	**0.016**	**0.097**
41	juvenile squid	**2.908**	0.016	4.00		**0.604**	**0.142**
42	adult squid	**3.061**	**0.011**	3.00	13.12	**0.020**	**0.229**
43	Gulf menhaden 0yr	**2.000**	**0.861**	2.30	19.38	**0.221**	**0.119**
44	Gulf menhaden 1yr	**2.2**	2.397	1.396		**0.88**	**0.15**
45	Gulf menhaden 2yr	**2.3**	**1.686**	1.723		**0.966**	**0.266**
46	Gulf menhaden 3yr	**2.5**	**0.624**	1.497		**0.822**	**0.286**
47	Gulf menhaden 4yr	**2.7**	**0.287**	1.497		**0.366**	**0.335**
48	juvenile striped mullet	**2.696**	0.003	2.40		**0.448**	**0.07**
49	adult striped mullet	**2.684**	**0.011**	0.80	12.28	**0.163**	**0.065**
50	juvenile sunfishes	**2.9**	**5.89E-04**	2.00		**0.116**	**0.163**
51	adult sunfishes	**2.684**	0.001	0.80	4.97	**0.618**	**0.161**
52	juvenile forage fish	**2.5**	0.052	3.00	37.779	**0.563**	**0.075**
53	adult forage fish	**2.433**	**2.829**	2.53		**0.321**	**0.242**
54	juvenile blue crab	**2.040**	**0.052**	3.00	17.037	**0.502**	**0.176**
55	adult blue crab	**2.433**	0.022	2.40		**0.319**	**0.25**
56	juvenile brown shrimp	**2.040**	**0.102**	3.00		**0.377**	**0.115**
57	adult brown shrimp	**2.161**	0.052	2.40	19.2	**0.672**	**0.125**
58	juvenile white shrimp	**2.05**	**0.798**	3.00		**0.037**	**0.105**
59	adult white shrimp	**2.161**	0.573	2.40	19.2	**0.227**	**0.125**
60	jellyfish	**2.256**	0.082	15	56	**0.001**	**0.268**
61	oyster spat	**2**	**0.077**	2.00		**0.129**	**0.05**
62	seed oyster	**2.05**	**2.6**	1.80	14.651	**0.039**	**0.123**
63	sack oyster	**2.05**	1.482	2.40		**0.032**	**0.24**
64	oyster drill	**2.62**	0.012	4.5	18	**0.048**	**0.25**
65	grass shrimp	**2.051**	0.45	4.5	18	**0.395**	**0.25**
66	benthic crabs	**2.000**	1	2	18	**0.859**	**0.111**
67	zoobenthos	**2.011**	3.96	4.5	22	**0.536**	**0.205**

Group No	Group Name	Trophic Level	Biomass (t km^{-2})	$\frac{P}{B}$	$\frac{Q}{B}$	EE	$\frac{P}{Q}$
68	benthic crustaceans	**2.051**	4.39	4.5	22	**0.358**	**0.205**
69	mollusks	**2**	4.03	4.5	22	**0.378**	**0.205**
70	zooplankton	**2**	4.124	28.772	84.87	**0.263**	**0.339**
71	phytoplankton	**1**	12.838	81.7		**0.454**	
72	benthic algae	**1**	18.778	3.909		**0.497**	
73	SAV	**1**	9.778	9.014		**0.365**	
74	detritus	**1**	100			**0.275**	

Ecosim

Ecosim is the time-dynamic module of EwE, which transforms the static set of Ecopath mass-balance equations into a system of coupled differential equations to simulate temporal changes in biomass:

$$\frac{dB_i}{dt} = g_i \sum_j c_{ji} - \sum_j c_{ij} + I_i - (M_i + F_i + e_i) \cdot B_i, \quad (19)$$

where g_i is the net growth efficiency of group i; I_i is the biomass immigration rate; M_i is the nonpredation mortality rate; F_i is the fishing mortality rate; e_i is the emigration rate; and C_{ij} the consumption rate of group i by group j.

To allow the model groups to respond to changes in salinity and temperature, response curves were developed and included. Frequency distributions of model groups from the fisheries-independent monitoring data were evaluated against salinity and temperature, and the absolute minimum, minimum preferred, maximum preferred, and absolute maximum value for each driver were determined to make trapezoid-shaped response curves. The minimum preferred and maximum preferred represent the 10th and 90th percentiles, respectively. In the trapezoid-shaped response curves, the absolute minimum is the left bottom, the minimum preferred is the left top, the maximum preferred

is the right top, and the absolute maximum is the right bottom (Table 5). Since these response curves are akin to HSIs, no new response curves were created for oysters in this way, and the above-described HSI's were applied directly to the oyster spat, seed and sack groups.

*Table 5. Trapezoidal response curve values for salinity and temperature. Values indicate the left bottom (LB), left top (LT), right top (RT), and right bottom (RB) of a trapezoid in the unit of the parameter. Sources are indicated to the right of each set of values, where A = pooled agency data from ADCNR, LDWF, MDMR, and SEAMAP; A[1] = pooled agency data from ADCNR, LDWF, MDMR, and SEAMAP. Due to the absence of data from fish surveys on lengths of individuals > 3yrs, the menhaden 3yr data and trapezoid vertices were used for the 4yr individuals; B = Aquamaps; B[1] = Aquamaps. Due to the absence of data on adult gulf sturgeon, data for adult Atlantic sturgeon were used; C = Pooled data from literature searches; D = Hijuelos et al. (2016); D[1]= Hijuelos et al. (2016) largemouth bass HSI use for sunfishes as well; E = Nepal & Fabrizio (2019); F = Murray (pers. communication); G = Phyto'pedia (2012). *The HSIs described earlier in the report were used for oysters.*

Group Name	Salinity					Temperature				
	LB	LT	RT	RB	Source	LB	LT	RT	RB	Source
juvenile large coastal sharks	0.1999	0.6999	35.950	36.46	A	13.9	14.68	27.374	28.570	A
adult large coastal sharks	19.16	32.1	36.23	39.08	B	12.4	20.61	27.72	32.22	B
juvenile dolphins	1	15	23	32	A	8	16	28	32	A
adult dolphins	3.42	31.97	36.5	40.11	B	0	8.65	26.65	40.15	C
juvenile small coastal sharks	4.889	30.706	36.47	38.56	A	14.13	20.19	28.772	30.8	A
adult small coastal sharks	0.3	31.14	36.822	37.06	A	12.59	19.181	27.767	31.3	A
juvenile large pelagics	0	2.799	30.32	39.94	A	1.5	18.4	30.5	39.9	A
adult large pelagics	0.1	4.619	36.22	37.59	A	11.7	19.196	31.3	34.3	A
juvenile small pelagics	0	3.099	31.84	40	A	0	16.7	30.7	39.9	A
adult small pelagics	0.0999	26.36	36.45	39.04	A	9	19.704	27.8	34.6	A
juvenile red snapper	0.1999	30.49	36.32	39.89	A	1.6999	21.83	28	39.9	A
adult red snapper	18.940	30.610	36.19	39.46	A	11.89	22.97	27.62	31.82	A
juvenile red drum	0	1.0999	25	39.3	A	4.2999	10.6999	30	35.5	A
adult red drum	0.0999	3.7999	26.0999	36.65	A	7.3999	11.0999	26.2999	31.7999	A
juvenile black drum	0	1.0999	22.6999	36.6	A	2.6999	10.3999	30.5999	36	A
adult black drum	0.0999	2.43994	30.824	34.78	A	9.5999	12.7199	25.6599	31.4	A
juvenile spotted seatrout	0	1.7999	22.5	38.3999	A	1.6999	10.3999	29.2999	39	A
adult spotted seatrout	0	6.5	25	34	A	2.2999	12.7999	28.6999	32.8	A
juvenile other seatrout	0	1.5999	23.2999	40	A	0	21.0999	31.1999	39.8999	A
adult other seatrout	0	3.8999	35.77	40	A	1.5	19.48	30.5	35.8999	A
juvenile sciaenids	0	1.6999	25	40	A	0	16.2	30.4	39.8999	A
adult sciaenids	0	2.0999	28.92	40	A	0	15.7	30.7999	39.8999	A

Group Name	Salinity					Temperature				
	LB	LT	RT	RB	Source	LB	LT	RT	RB	Source
juvenile largemouth bass	0	0.5	5	24	D	2.8	25.7	31.7	35.5	A
adult largemouth bass	0	0.5	5	24	D	2.8	29	30.16	35.5	A
juvenile gulf sturgeon	0.2	0.7	20.73991	31.8	A	10.6	12.19	23.51	27.8999	A
adult gulf sturgeon	18.97	22.78	35.94	36.53	B[1]	0	6.31	22.39	34.45	C
juvenile blue catfish	0	0	11.557	17.671	E	3.3999	13.5999	30.3999	38	A
adult blue catfish	0	0	13.654	20.058	E	7.8999	13.7199	24.38	27.0999	A
juvenile sea catfish	0	2.6999	23.7999	38.3999	A	1.5	20.5999	31.3999	39.8999	A
adult sea catfish	0	2	23.3999	38	A	0	19.0999	30.9	39.8999	A
juvenile Atlantic croaker	0	1.0999	21.5	40	A	0	15.7999	30	39.8999	A
adult Atlantic croaker	0	2	36.19	39.3	A	0	17.26	29.6999	38	A
juvenile southern flounder	0	1.3999	21.7999	39.3	A	0	16.3999	30.7999	37.0999	A
adult southern flounder	0	1.19999	34.001	37.04	A	6.2999	14.0999	31.1999	35.7999	A
juvenile near coastal consumers	0	2.0999	32.41	39.92	A	1.6999	17.3	31	39	A
adult near coastal consumers	0	1.9	36.03	39.3	A	1.6999	15.2999	30.5	39.8999	A
rays and skates	0	1.2	23.0999	39.3	A	1.6999	12.8999	30.5	37.5	A
juvenile demersals	0	2.3999	35.28	40	A	0	16.3	30.2999	39.8999	A
adult demersals	0.0999	10	36.44	39.81	A	2.5	19.84	30	39.8999	A
juvenile squid	0	4.5	33.18	40	A	0	16.3999	30.3999	39.8999	A
adult squid	0	7.2999	36.42	38.62	A	1.5	18.5	30.7999	36	A
menhaden 0yr	0	0	28	38.01	A	4.2	12.2	29.8	35	A
menhaden 1yr	1.47	21.8	35.72	37	A	16	21.305	26.95	32	A
menhaden 2yr	0	21.803	35.63	39.94	A	16	21.305	26.95	32	A
menhaden 3yr	4	18.2	35.188	36.96	A	11.5	18.664	27.26	32	A
menhaden 4yr	4	18.2	35.188	36.96	A[1]	11.5	18.664	27.26	32	A[1]
juvenile striped mullet	0	0.7999	21.5	37.2999	A	2.0999	9.2999	30.3	37.1	A
adult striped mullet	0	2.7599	22.93994	31.6999	A	2.7999	5.2999	22.7999	30.1	A
juvenile sunfishes	0	0.5	5	24	D	1.2999	12.6	31.0999	38	A

Group Name	Salinity					Temperature				
	LB	LT	RT	RB	Source	LB	LT	RT	RB	Source
adult sunfishes	0	0.5	5	24	D	1.2999	13.0999	31.19999	35.8999	A
juvenile forage fish	0	1.5	23.2999	40	A	0	15.1999	30.7999	39.8999	A
adult forage fish	0	3.5	36.11	39.94	A	0	16.5	30.0999	38	A
juvenile blue crab	0	1.0999	23	40	A	0	15.5999	30.7999	39.8999	A
adult blue crab	0	1.1999	21.8999	40	A	0	17.5999	31.2999	39.8999	A
juvenile brown shrimp	0	2	22.2999	40	A	0	21.2999	30.4	39.8999	A
adult brown shrimp	0.0999	12.2999	36.46	40	A	6.8	20.2	29.5	35.8999	A
juvenile white shrimp	0	1.6999	23.5	39.3	A	0	15.5999	31.0999	39.8999	A
adult white shrimp	0	1.6999	25.8999	40	A	0	19.0999	30.3	38	A
jellyfish	0.2	4.2	32	38	A	6.3	13.4	30	34.2	A
oyster spat seed oyster sack oyster										
oyster drill	16.66	25	31.829	36.05	A	14.1	18.9	28.7	29.7	A
grass shrimp	0	2	20	40	F	0	11.6999	29.5999	39.8999	A
benthic crabs	0	2.7999	30.1999	40	A	2.0999	13	29.7999	35.8	A
zoobenthos	1	24	35	38	A	6.4	15.9	29.1	35.8	A
benthic crustaceans	5.5	7.01	26.7	27.3999	A	9.77	13.99	25.42	28.41	B
mollusks	0	1.2999	19.0999	39.04	A	3	11.5999	30.5	34.6999	A
zooplankton	19.99	30.06	36.17	38.13	B	8.93	15.61	26.72	31.69	B
phytoplankton	19.59	21.4085	35.9565	37.775	G	-1.541	1.5599	26.3671	29.468	G
benthic algae	3.85	32.473	35.924	40.57	B	-2	19.627	26.389	33.65	B
SAV	14.99	33.6	36.05	38.51	B	8.13	22.944	28.152	32.38	B

Calibration

The model was calibrated in Ecosim before the scenario runs were performed. During calibration, the model's biomass and landings outputs were fitted to observed biomass, landings, and fishing mortality for all groups with available data. In Ecosim, model fitting works by adjusting the vulnerability exchange rates related to predation and fishing until the outputs align closely with observations. This process continues until the model minimizes the sum of squared deviations (SS) between observed log-biomass

values and produces the lowest AIC score, resulting in the model that best reproduces historical biomass trends (Christensen et al., 2008).

Calibration was performed from 2000 – 2017 by fitting the biomass predicted by the model to time series of field observed biomass derived from the combined ADCNR, LDWF, MDMR, and SEAMAP fisheries-independent monitoring surveys for the species with biomass in the Ecopath model based on those data. Due to the high variability of monitoring data, LOESS (locally estimated scatterplot smoothing) curves were fitted to the raw data, and those values served as observations. For species biomass based on stock assessment data in the Ecopath model, stock assessment data on biomass and fishing mortality (when targeted) were used for calibration (large coastal sharks, bottlenose dolphin, red snapper, red drum, black drum, Gulf menhaden, brown shrimp, white shrimp). For those groups targeted with a fishery in the model, predicted landings were calibrated with reported fisheries landings. A time series from 2006-2017 based on the MDMR oyster survey data was used to calibrate oyster spat, seed and sack biomass. A biomass value for the year 2000 was generated using a surplus production model with the landings data to have the observed time series start at the start of the model run.

Environmental drivers and responses were included in the calibration process. The total nitrogen load measured by USGS at Tarbert Landing was used as a primary productivity driver applied to all primary producers in the model (Figure 8). The values are normalized to 1 in the first year so that just the trend drives the primary production. The msbCOAWST model was used to create an 11-year climatological average of the model area of temperature and salinity based on years 2011-2020. This climatology output, averaged over the model domain, was used to create a time series of average environmental conditions from 2000 to March 2015. The salinity and temperature were hindcasted with msbCOAWST to April 2015, so starting in April 2015, the resolved temperature and salinity model output was used up to December 2017. The model-generated salinity and temperature drivers were created in this way from 2000-2017 (Figure 9). Since the salinities created in this way are higher than what is generally experienced at the oyster reefs (because it is the average of the whole model area including the Mississippi

Bight), additional time series were created using MDMR field measurements of temperature and salinity at Pass Marianne Reef. For these field-based environmental drivers, multi-year averages were used for months that did not have any measured data. Since the oyster monitoring program started in 2006, and the salinity and temperature data collected during this survey were used, the average for each month of data collected from 2006 to 2016 was applied to the years 2000 to 2005. From 2006 to 2017 the field data collected during each month were used. When there was a month that had no measurement, the average of 2006-2016 was used. This resulted in salinity and temperature environmental drivers from 2000 to 2017 (Figure 9). The field-based environmental drivers were applied to all species that have trophic interactions with oysters. These field data were not suitable for the species that occupy the Mississippi Bight, which is why these two sets of environmental drivers were used. Environmental drivers were provided on a monthly time step to all organisms in the model.

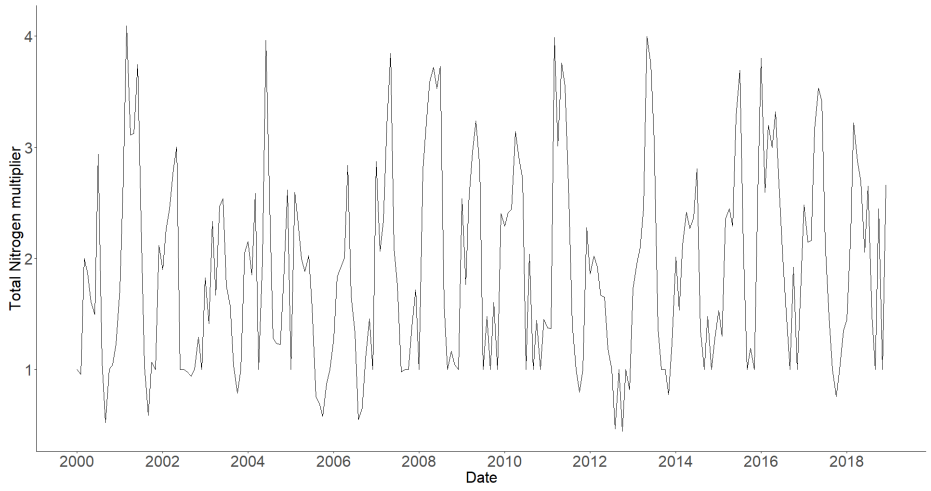

Figure 8. The primary productivity driver in Ecosim based on total nitrogen load measured in the Mississippi River at Tarbert Landing, MS.

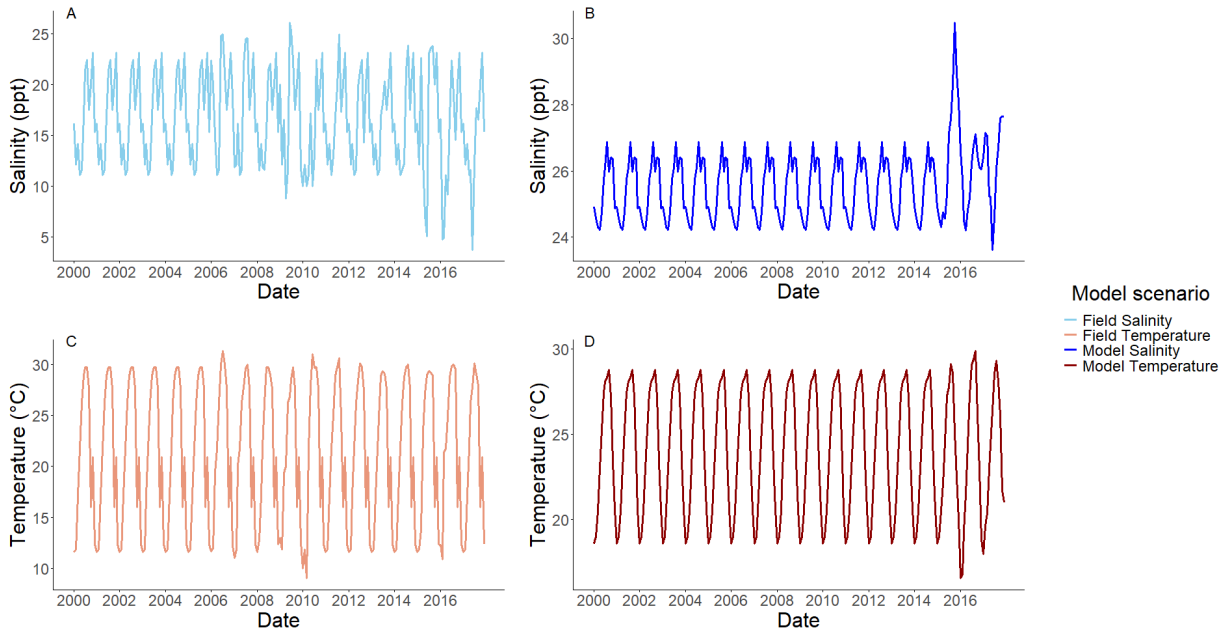

Figure 9. Salinity and temperature drivers used to calibrate the model. Panel A shows the salinity measured at the western reef sites by MDMR from 2000-2017, panel B the msbCOAWST model-generated salinity averaged over the model domain. Panel C shows the temperature measured at the western reef sites by MDMR from 2000-2017, panel D the msbCOAWST model-generated temperature averaged over the model domain.

Oysters do not directly respond to the monthly salinity and temperature values loaded in Ecosim. Instead, the HSIs described above are calculated from the daily temperature and salinity values (using the MDMR field data), and those daily HSI's are averaged by month. The resulting monthly HSI values for temperature and salinity for spat, seed and sack oysters were then loaded as drivers and applied to the three oyster life stages respectively with a 1:1 relationship. The habitat capacity model in Ecosim takes the product of each species-specific habitat suitability score, which means that interactions between temperature and salinity are included in the model (Christensen et al., 2014). Based on previous work, food availability can serve as a limiting factor to oysters in the Mississippi Sound (Klein et al., 2024); therefore a foraging anomaly was applied to all three life stages of oysters during the calibration process (Bentley et al., 2024; Serpetti et al., 2017).

The calibration process reduced the total sum of squared difference between predicted and observed from 16088 to 667 (AIC reduced from 3141 to -398). Very good fits were obtained for biomass of oyster spat and landings of sack oysters (Figure 10).

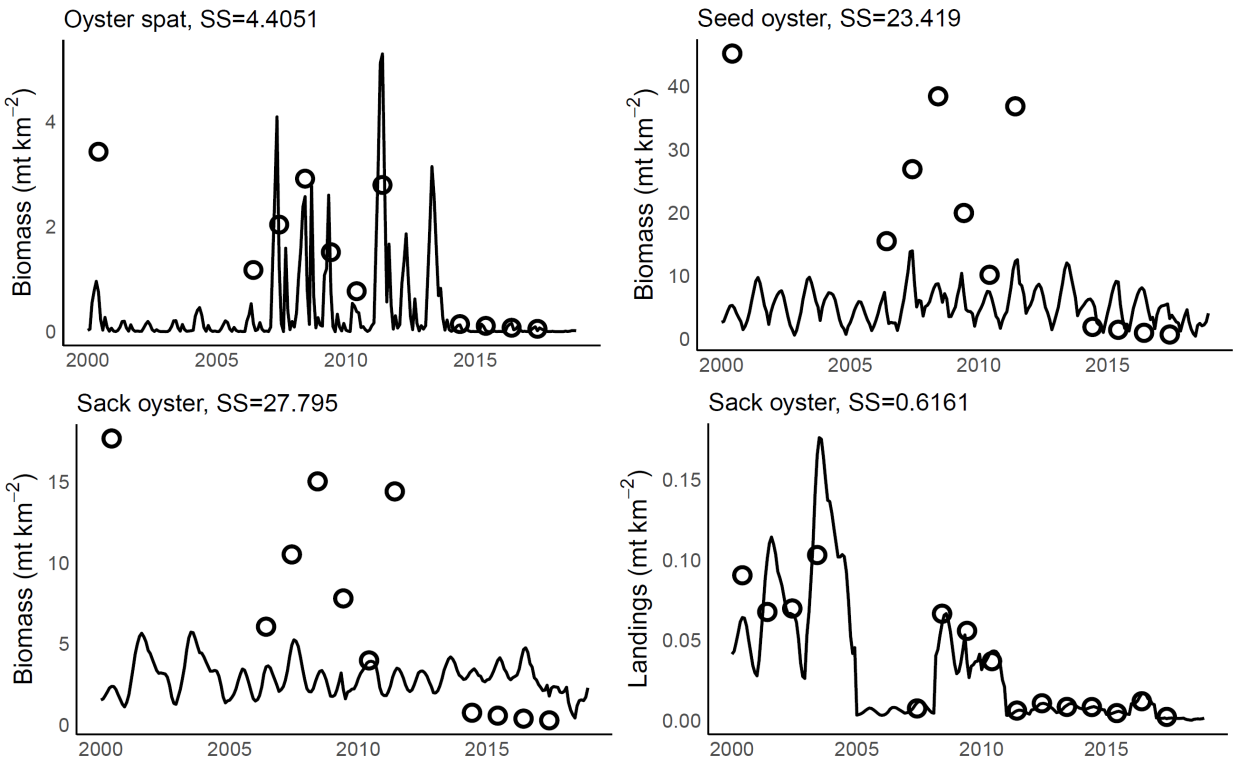

Figure 10. Calibration plots of spat, seed, and sack oyster biomass and landings. The circles are observed values, and the lines are predicted values. The SS indicates the sum of squared difference between observed and predicted.

The oyster survey started in 2006, so the poor fits of seed and sack oysters are a result of a lack of data from 2000-2005 in these calibration runs. Of the different life stages, spat most strongly responded to changes in environmental conditions and thereby had a better fit to observations. In the model the life stages are linked with a von Bertalanffy growth function, so the initial biomass of the seed and sack oyster will be determined by the biomass of spat, which means that having the leading stanza fit observations well will result in reasonable biomass predictions for the linked stanzas. Since spat is the most sensitive settled life stage to environmental conditions, and oyster landings are most informative regarding oysters as a resource, the good fits of spat biomass and sack oyster

landings make this a skillful model for the intent of determining salinity thresholds for oyster survival.

Tipping Point Evaluation

To determine the ecological tipping point of eastern oyster, defined as where mortality is so high that recovery is severely impaired, we analyzed the MDMR oyster field surveys from 2006 to 2022. Oyster mortality was evaluated for each settled oyster stanza: spat, seed, and sack oysters. To create a common metric between the field data and the Ecosim model simulations, we translated the percent mortality observed in the field into a percent biomass loss. Biomass loss was evaluated for each oyster life stage – spat, seed, sack – as $B_{(t)}/B_{(t-1)} \cdot 100\%$, where *t* represents the current year and *t-1* the year prior. Oyster biomass loss was not evaluated for field survey data for any year *t* where biomass was not measured in year *t-1,* which excluded 2006 and 2014. Biomass loss per year was averaged to determine the mean proportion of biomass loss across the sampling period, using all available years. The ecological tipping point for this work was defined as an operational threshold rather than a mechanistic ecological limit. Specifically, a tipping point was identified when annual biomass declined by more than one standard deviation relative to mean biomass loss. This approach incorporates natural interannual variability in oyster mortality and identifies anomalously high mortality events relative to those reported in MDMR oyster reef field monitoring data.

Model Coupling and Simulation Scenarios

Oyster reefs

We focused this project on eight important oyster reefs in Mississippi (Table 6, Figure 11) and extracted the environmental conditions from the model scenario outputs from those locations. The reefs include the historically most productive reefs in the western MS Sound that also receive the highest impact from BCS openings because of their proximity to the outfall through the Rigolets. They also include reefs in Biloxi Bay that

are further away from the outfall and are already being used as potential relocation sites when adverse conditions are expected in the western MS Sound.

Table 6. Model output locations and associated reefs used to evaluate ecological tipping points model runs.

Reef Name	Abbreviation	Latitude	Longitude	Reef Area (km^2)	Reef Depth (m)
Biloxi Bay	BB	30.39598677	-88.84509582	0.571	1.46
Buoy Reef	BR	30.25212087	-89.17911282	0.192	3.63
Henderson Point	HP	30.28231365	-89.27444096	5.240	3.56
Pass Christian	PC	30.27883611	-89.27336744	3.776	3.01
Pass Marianne	PM	30.24846241	-89.25969221	8.310	3.12
Pelican Reef	PR	30.20950553	-89.23477117	0.408	1.98
Shearwater	SH	30.39365548	-88.82287209	0.128	1.59
Telegraph Reef	TR	30.21764475	-89.28028625	5.032	2.80

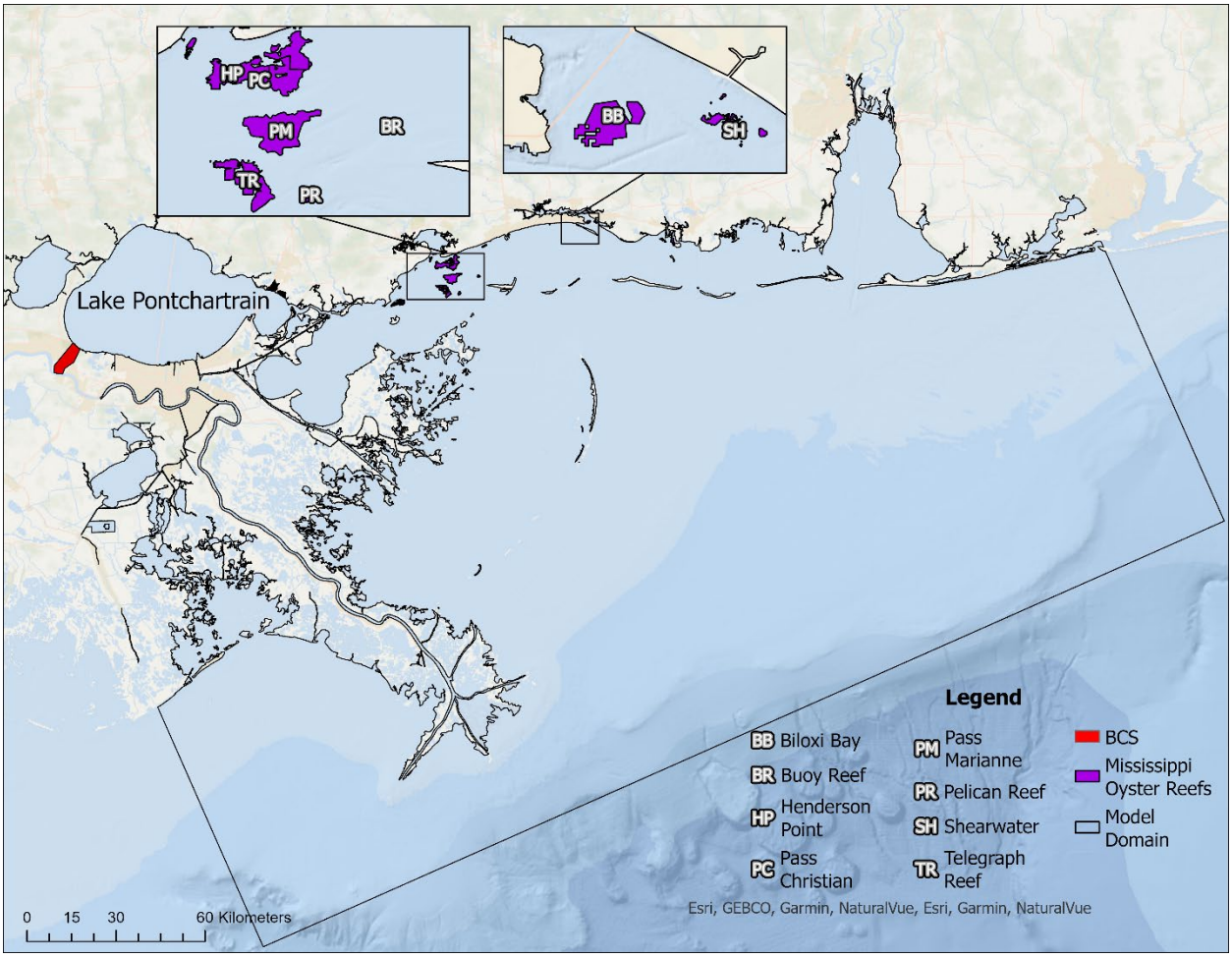

Figure 11. Locations of Mississippi oyster reefs that are the focus of this study.

Physical model

The msbCOAWST model was used to simulate scenarios based on "hindcasts" - flow conditions (river flow as well as BCS release) that have occurred in past years - to reduce uncertainty about what the environmental conditions are during BCS release events. To make the scenarios comparable and focused on the effects of the various BCS opening strategies, the atmospheric forcing for 2018 was consistently applied, and the BCS diversion was initiated at the same time in each scenario. Details on the physical model runs are provided in a separate report. These historical openings reflect seven hydrodynamic model scenarios, detailed below and characterized in Table 7, Figure 12.

1. Scenario 1: The first scenario recreates the 2011 opening, which spanned 43 days with a total freshwater discharge volume of 329.6% of Lake Pontchartrain.

2. Scenario 2: The second scenario recreates the 2018 opening, which spanned 21 days with a total freshwater discharge volume of 86.6% of Lake Pontchartrain.
3. Scenario 3: The third scenario recreates the 2019 first opening (2019A), which spanned 43 days with a total freshwater discharge volume of 219.5% of Lake Pontchartrain.
4. Scenario 4: The fourth scenario recreates the 2019 second opening (2019B), which spanned 79 days with a total freshwater discharge volume of 346.9% of Lake Pontchartrain.
5. Scenario 5: The fifth scenario recreates the combined 2019 openings (2019Full), which spanned 122 days with a total freshwater discharge volume of 566.4% of Lake Pontchartrain.
6. Scenario 6: The sixth scenario recreates the river inflow only from the climatology (average conditions based on 2011-2020), without BCS openings.
7. Scenario 7: The seventh scenario recreates the 2020 opening, which spanned 29 days with a total freshwater discharge volume of 59.9% of Lake Pontchartrain.

The resulting bottom salinity and temperature output from running these scenarios with the hydrodynamic model (Figures 13 and 14) was applied to the habitat suitability and ecosystem models, to determine suitability and ecological tipping points for oysters within the Mississippi Sound.

Table 7. BCS operations used for hydrodynamic model experiments to inform water temperature and salinity for Ecosim model runs. Scenario 2019A: first 2019 opening; *Scenario* 2019B: second 2019 opening; *Scenario* 2019Full: 2019 with both the first and second openings; *Scenario* 2019 RO: 2019 with rivers-only forcing and no BCS operations.

Opening Scenario	Opening Duration (days)	Opening Volume (% Lake Pontchartrain)	Avg. Discharge (m^3/s)	Est. Total Discharge (km^3)	Volume/Intensity Category
2011	43	329.6	5891	21.9	Extreme
2018	21	86.6	3035	5.8	Below Average
2019A	44	219.5	3967	15.1	Above Average
2019B	79	346.9	3374	23	Extreme
2019Full	123	566.4	3587	38.1	Extreme
2020	29	59.9	1536	3.98	Lowest
2019 RO	NA	NA	NA	NA	NA

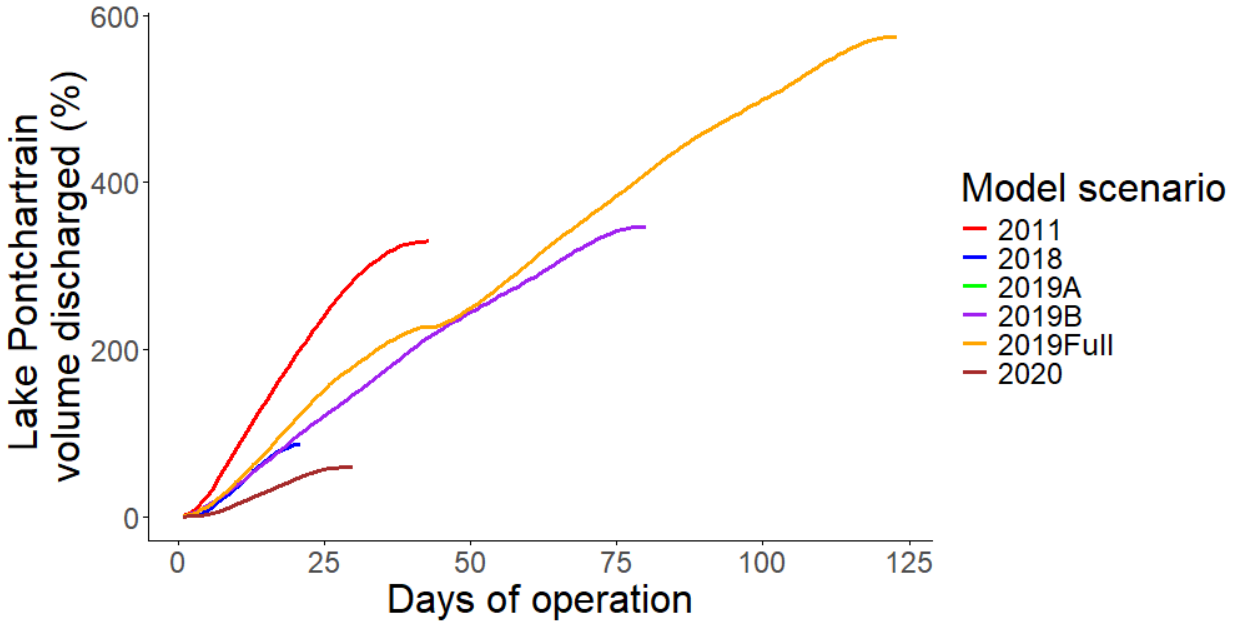

Figure 12. Duration (days of operation) and diverted river volume (as percentage of Lake Pontchartrain) of historic BCS operations used for the hydrodynamic model scenarios.

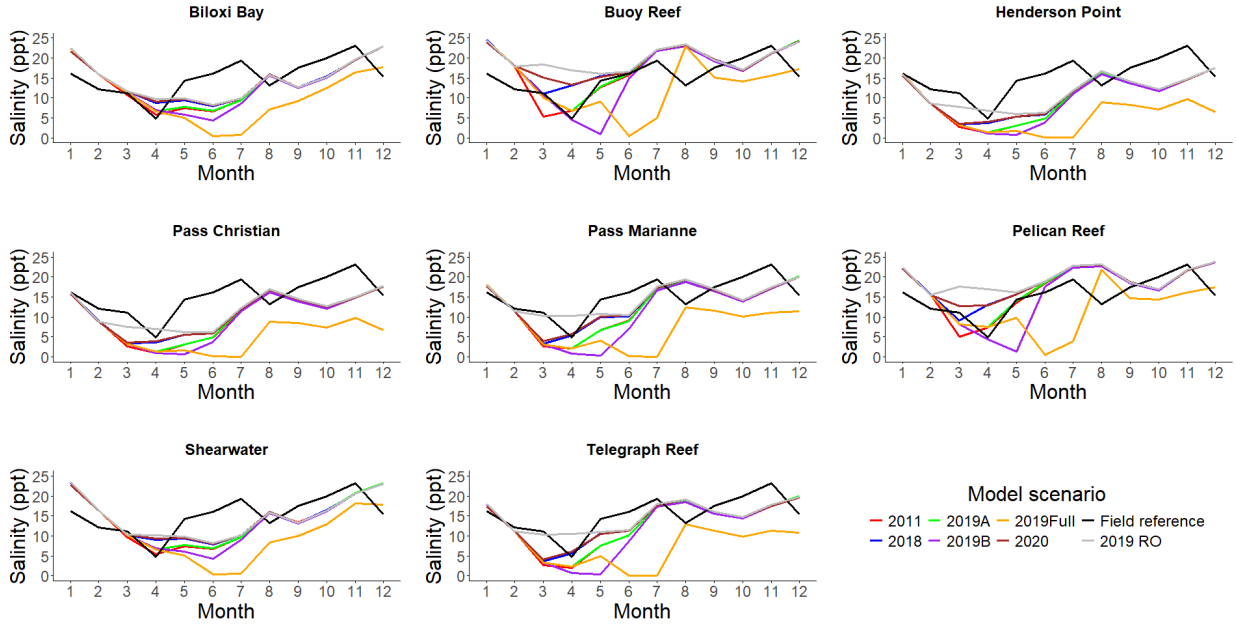

Figure 13. Bottom salinity output from the msbCOAWST model scenarios at the eight different reefs we have included in our research. The colors refer to the different model scenarios described in the report. Field reference is the average salinity measured at Pass Marianne in 2018.

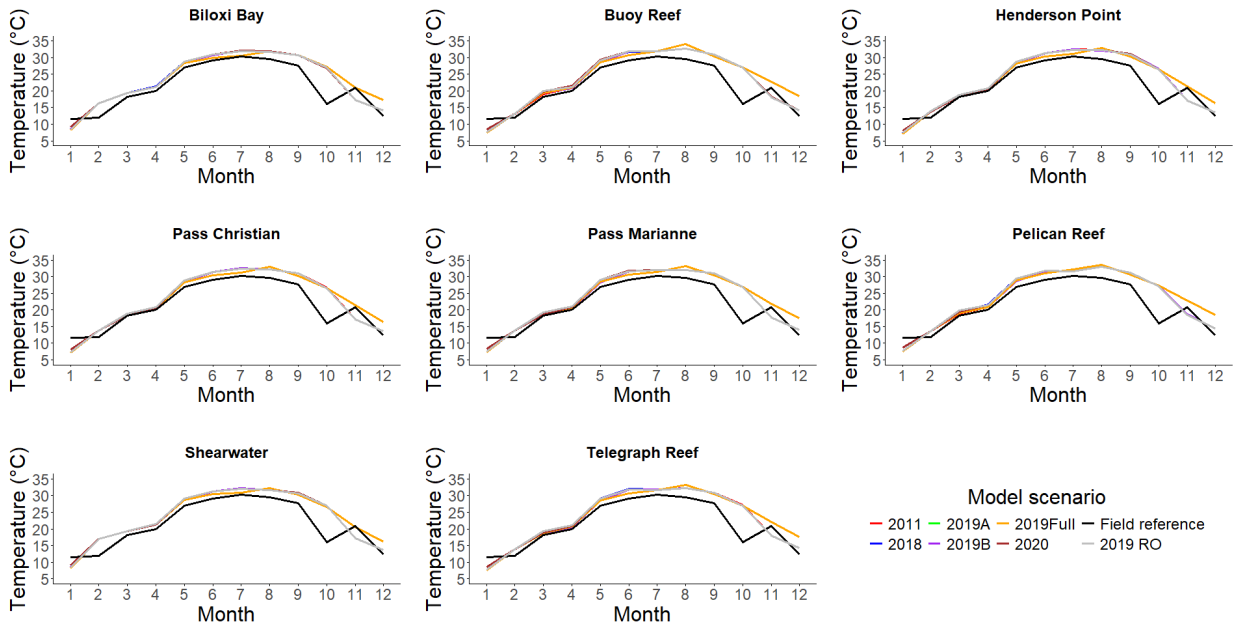

Figure 14. Bottom temperature output from the msbCOAWST model scenarios at the eight different reefs we have included in our research. The colors refer to the different model scenarios described in the report. Field reference is the average temperature at Pass Marianne in 2018.

Habitat suitability

Index score calculations for all HSI analyses were performed based on msbCOAWST model estimates of surface and bottom salinity within the model domain according to the seven (7) different BCS historical releases simulated via hydrodynamic model scenarios described above. For each hydrodynamic model experiment, mean monthly, weekly, and daily values of salinity (at the surface and just above the bottom) were extracted from the hydrodynamic model solution at the eight (8) oyster reef locations described above (Biloxi Bay, Buoy Reef, Henderson Point Reef, Pass Christian Reef, Pass Marianne Reef, Pelican Reef, Shearwater Reef, and Telegraph Reef) in order to resolve the daily evolution of habitat suitability at various historically- and economically-important oyster reef locations within the Mississippi Sound. In each case, HSI analyses were performed for each modeled age-class of oyster in specific response to their respective sensitivities to salinity – particularly with respect to their tolerance(s) for low salinity waters associated with the modeled BCS releases. All HSI analyses were conducted against the

conceptual backdrop of the timing, duration, and magnitude of freshwater discharge introduced to the model domain from the Bonnet Carré Spillway according to the historical cases modeled.

In each case, HSI analyses were performed for each modeled age-class of oyster in specific response to their respective sensitivities to salinity. This modeling strategy allowed us to investigate temporal and/or spatial gradients of change with respect to habitat suitability, induced either from natural vs. anthropogenic impacts to water quality, allowing us to compare the calculated index scores using differences between the hydrodynamic model solutions to isolate and quantify the relative effects of various historical BCS openings on oyster habitat suitability within the Mississippi Sound.

Ecosim simulations

The calibration run from 2000 to 2017 preceded each simulation scenario. Bottom salinity, temperature and HSI outputs from each msbCOAWST model scenario were applied in 2018 in the Ecosim model runs. The year 2018 was chosen because the atmospheric conditions of all model runs are representative of 2018. From an ecological perspective, 2018 was chosen for that so that the scenarios occur before the catastrophic mortality event in 2019, when a change in biomass would be difficult to evaluate since biomass was so close to zero. Model runs were performed from 2000 to 2018. The biomass loss for each sessile life stage in each model scenario was determined with Ecosim by evaluating end/start output biomass, calculated as $(B_{(end\_2018)}/B_{(start\_2018)}) \cdot 100\%$. These end/start values were compared to the ecological tipping point, defined as one standard deviation below the average field mortality in years of biomass decrease.

Model results were evaluated at the eight geographic points (Table 6), representing the location of harvestable oyster reefs within the western Mississippi Sound.

Results

Ecological tipping points

Ecological tipping points for each oyster stanza were calculated as 19.4%, 32.3%, and 38.0% of spat, seed, and sack biomass, respectively, remaining after one year. This means that recovery of each life stage is severely impaired if over one year the biomass of spat, seed oysters, and sack oysters is reduced by 80.6%, 67.6%, and 62% respectively. Environmental conditions leading to these ecological tipping points represent unsuitable conditions beyond tolerance thresholds for the oysters.

Ecosim output

Hydrodynamic model results from the various historical BCS releases tested indicated that the age-class of settled oyster that was most sensitive to BCS-induced environmental stress was newly-settled spat, for all BCS release scenarios and all reef locations tested (Figure 15). While Ecosim model results indicated that seed- and sack-sized oysters were indeed affected by BCS releases, none of the release scenarios (regardless of reef location) provided sufficient evidence that seed or sack oyster mortalities had exceeded the threshold of one standard deviation below the average field biomass loss, which was the uniform standard used to define the ecological tipping point. However, among spat-sized oysters, Ecosim model evidence suggests that among the reef locations tested, the spat at Henderson Point, Pass Christian, Pass Marianne, and Telegraph Reefs had indeed experienced excessive mortalities from BCS-induced effects wrought from the release scenarios of 2011 and 2019 (Figure 15).

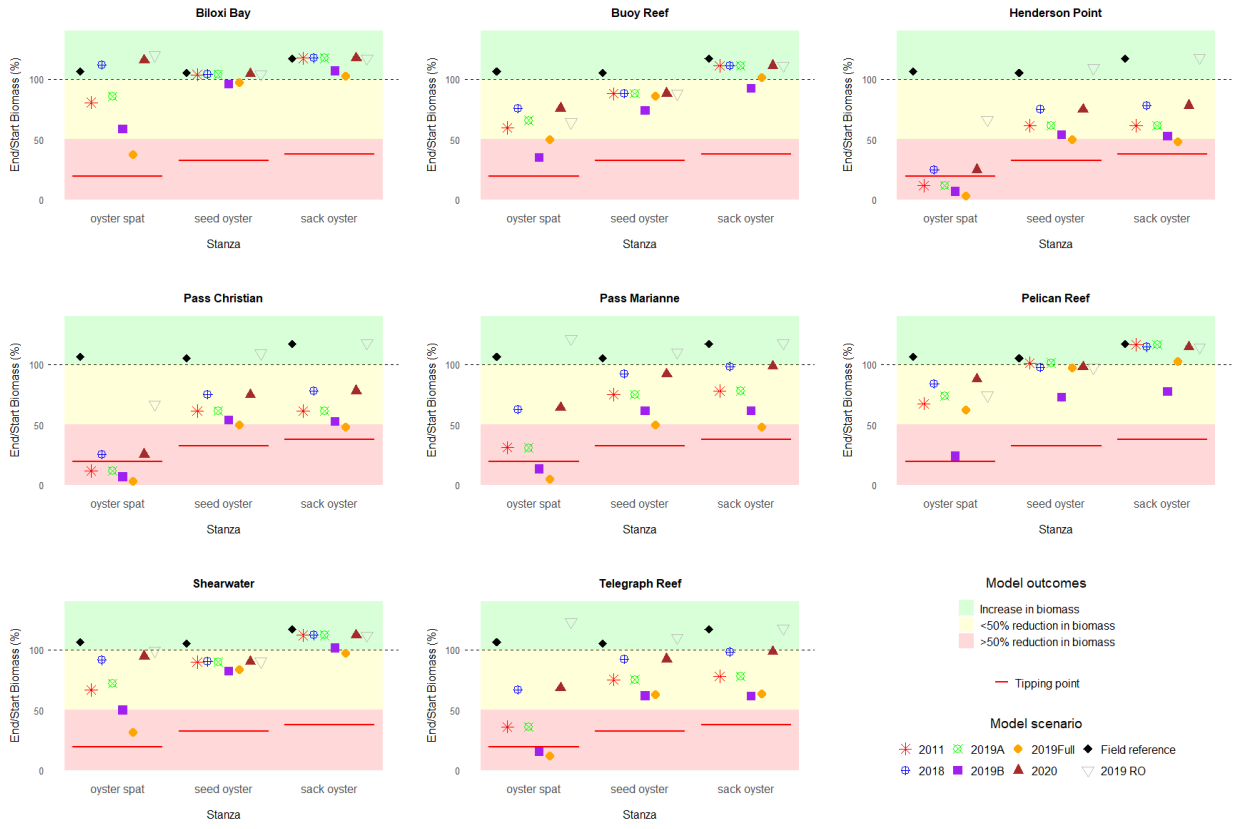

Figure 15. Ecosim modeling estimates of oyster biomass trends (by age-class) at various reef sites throughout the Mississippi Sound in response to the historical BCS release scenarios tested, compared to field reference data. Note the horizonal red lines which represent the ecological tipping point for each age-class of settled oyster, calculated as one standard deviation below the average field biomass loss for years when mortality occurred.

In fact, the reefs most sensitive/susceptible to the historical BCS release scenarios tested were Henderson Point and Pass Christian reefs, where Ecosim model results indicate that tipping points for spat oyster mortality had been reached in 2011, the 1st BCS opening of 2019 (2019A), the 2nd BCS opening of 2019 (2019B), and of course, throughout the entirety of the 2019 BCS releases (2019Full). While spat oysters located at the Pass Marianne and Telegraph reef locations had seemingly avoided reaching their ecological tipping point despite BCS releases of 2011 and the 1st opening of 2019 (2019A), the 2nd opening of 2019 (2019B) did indeed push them beyond their tipping point – a result also reflected in the full accounting of 2019 BCS releases (2019Full). At all other reef locations, spat mortalities were certainly augmented by the various BCS release scenarios tested (as

evidenced by the depressed biomasses), but no others rose to meet our technical definition of an ecological tipping point (Figure 15).

Oysters at the two eastern reefs and at Buoy Reef and Pelican Reef were regularly less affected by BCS openings than their western reef counterparts. During the 2019Full model runs, for instance, mean annual salinity at Pass Marianne was 7.94±5.80 (SD) ppt, while values at Buoy and Pelican Reefs were 13.20±7.18 ppt and 12.64±6.79 ppt, respectively. Another interesting finding at Buoy Reef and Pelican Reef is that the scenario with only the second 2019 opening (2019B) had a larger impact on oyster biomass at all size classes than the scenario with the double 2019 opening (2019Full). The reason for this is likely that since all BCS opening scenarios started at the same time of year in the msbCOAWST modeling environment, which meant that the longer lasting and higher volume second opening occurred earlier in the year than during the 2019Full scenario, reducing salinity earlier (Figure 13) which negatively affected oyster spat.

Oyster spat biomass losses right on the cusp of their ecological tipping point include Henderson Point and Pass Christian during the 2018 and 2020 BCS openings, Pass Marianne and Telegraph Reef during the 2011 and first 2019 opening (2019A), Pelican Reef during the 2nd 2019 opening (2019B), and Shearwater during the full 2019 release (2019Full). Scenarios that resulted in a 50% or more biomass loss (poor conditions) for spat while not quite reaching the tipping point were 2019Full at Buoy Reef, Biloxi Bay and Shearwater. Net 50% biomass loss within one year was also seen among seed and sack oysters at Henderson Point and Pass Christian for both the 2019Full and 2019B scenarios, and at Pass Marianne during the 2019Full scenario. Oyster spat showed a net loss of biomass (commensurate with fair conditions or worse) in all scenarios where the BCS was opened, except for the 2018 and 2020 scenarios at Biloxi Bay. Reefs where seed and sack oysters also only had net biomass losses when the BCS was opened include Henderson Point, Pass Christian, Pass Marianne, and Telegraph Reef. Reefs at other locations (Biloxi Bay, Buoy Reef, Pelican Reef, Shearwater) show that a net biomass loss or gain of seed and

sack oysters over a year with a BCS opening can depend on the duration and volume of the freshwater release (Figure 15).

The rivers only scenario (2019RO), which represents no BCS openings with freshwater inflow only from rivers during unusually wet 2019 conditions, mostly led to a gain in biomass (good conditions) for all reefs and life stages, and fair conditions for some (spat and seed oysters at Buoy Reef, Pelican Reef, and Shearwater, and only spat at Henderson Point and Pass Christian). A comparison between the rivers only scenario and the double BCS opening scenario (2019Full) allows for an evaluation of the percent biomass loss because of the 2019 BCS openings for each life stage at each reef evaluated. The field reference scenario does well for all life stages as well; this is the average salinity in the Mississippi Sound in 2018 and not specific to each reef location. This shows that in an average year, even with a conservative BCS opening, conditions in the Mississippi Sound are on average suitable for oyster growth at all life stages.

Detailed habitat suitability evaluation

In order to provide further insights into the timing and intensity of BCS-induced effects on spat mortality at each of the most affected reef locations (Henderson Point, Pass Christian, Pass Marianne, and Telegraph Reefs) for which Ecosim model results suggested a tipping point had been reached, it was necessary to employ a habitat suitability modeling approach to resolve the temporal dynamics of the most likely environmental stressor – salinity, rather than temperature – that had so negatively affected the habitat suitability of spat in response to changing freshwater inventories wrought from BCS releases. Thus, hydrodynamic model results of near-bottom salinity were extracted from the various BCS release scenarios with daily temporal resolution to not only link the chronology of BCS discharges with their commensurate impacts on oyster habitat suitability, but also to quantify the number of days the salinity had fallen below the critical threshold of 5.0, the lower limit (*LL*) of habitat suitability among spat oysters (Figure 6). While daily HSI_{Sal} calculations would indicate a habitat suitability score of 0.0 when salinity ≤ 5.0, HSI_{Sal} results by themselves cannot adequately resolve the effects of salinity ≤ 5.0. For that, the

results of the ecological model were needed to relate the total number of low-salinity days (to represent pulsed, or more acute effects) and consecutive low-salinity days (to represent cumulative, or more chronic effects) which were coincident with tipping point(s), across all sites and modeled scenarios.

Among all BCS release scenarios tested, it was apparent from Ecosim model results that spat-sized oysters were the only age-class of settled oyster that had reached an ecological tipping point in response to BCS freshwater discharges, specifically in 2011 and 2019 (Fig. 13). Henderson Point (HP) and Pass Christian (PC) oyster reefs were the most susceptible to BCS releases, as evidenced by the multiple scenarios (2011, 2019A, 2019B, 2019Full) which indicated that a tipping point had been reached for oyster spat. The Pass Marianne (PM) and Telegraph Reef (TR) sites were also indicative that a tipping point for spat oysters had been reached, although such excessive mortalities were limited to the 2019 2nd opening (2019B) and double-opening (2019Full) BCS scenarios (Figure 15).

Upon review of the mean daily values of near-bottom salinity at each reef location (Table 8), oyster spat did not seem to reach their respective tipping point until the total number of days per year when salinity ≤ 5.0 reached the minimum threshold of at least 96 days (TR, scenario 2019B; Table 8). This threshold was much lower when considering the number of *consecutive* days of salinity ≤ 5.0, as indicated by the minimum threshold of 59 consecutive days (HP and PC, scenarios 2011 and 2019A; Table 8). It is also interesting to note that the 2019 scenario that explicitly excluded BCS releases (2019RO) indicated that although HP, PC, PM, and TR reefs were indeed negatively affected by flooding coastal rivers in 2019, the freshwater discharges attributable to the double-opening of the BCS (2019Full) created a 5.5-fold increase (17 days → 93 days) in the maximum number of consecutive days when near-bottom salinity was ≤ 5.0 at Henderson Point and Pass Christian, a 6.3-fold increase (12 days → 76 days) at Pass Marianne, and a 10.9-fold increase (7 days → 76 days) at Telegraph Reef (Table 8).

Table 8. Hydrodynamic model results from the various BCS discharge scenarios tested, indicating the total number of days when mean daily near-bottom salinity ≤ 5.0 (or the maximum number of consecutive days when mean daily near-bottom salinity ≤ 5.0, in parentheses). Values in bold red indicate those BCS scenarios (and oyster reef locations) where oyster spat mortalities were at least one standard deviation higher than mean oyster spat mortality (i.e. the ecological "tipping point" for oyster spat). Reef location abbreviations are as follows: BB = Biloxi Bay, BR = Buoy Reef, HP = Henderson Point, PC = Pass Christian, PM = Pass Marianne, PR = Pelican Reef, SH = Shearwater, and TR = Telegraph Reef.

	2011	2018	2019A	2019B	2019Full	2019RO	2020
BB	5	0	0	36	85	0	0
	(3)	(0)	(0)	(36)	(75)	(0)	(0)
BR	38	17	28	65	95	0	11
	(36)	(15)	(24)	(33)	(34)	(0)	(10)
HP	**109**	83	**109**	**117**	**177**	48	85
	(59)	(57)	**(59)**	**(102)**	**(93)**	(17)	(57)
PC	**104**	84	**104**	**118**	**174**	45	83
	(59)	(57)	**(59)**	**(102)**	**(93)**	(17)	(57)
PM	70	51	73	**100**	**147**	16	51
	(56)	(49)	(57)	**(99)**	**(76)**	(12)	(31)
PR	40	17	29	61	98	0	14
	(35)	(14)	(23)	(23)	(48)	(0)	(10)
SH	14	0	0	33	85	0	0
	(14)	(0)	(0)	(29)	(75)	(0)	(0)
TR	62	49	61	**96**	**144**	8	46
	(47)	(38)	(46)	**(87)**	**(76)**	(7)	(23)

Tipping Point Scenario: 2011

The 2011 BCS release scenario was characterized by the 43-day opening, with a peak discharge rate of 315,930 cubic feet per second (cfs), resulting in a cumulative discharge of ~330% Lake Pontchartrain volumes of fresh water into the western Mississippi Sound (wMSS). Despite these remarkable discharges in 2011, Ecosim model results indicated that the resultant low salinities induced "tipping point" mortality events only among spat-sized oysters at the Henderson Point (HP) and Pass Christian (PC) reef locations (Fig. 13), although seed- and sack-sized oysters were negatively affected at many other locations in the 2011 scenario. HSI_{Sal} analyses certainly reflect the depression of habitat suitability for spat oysters in response to dramatically lower salinities at HP and PC caused by the 2011 BCS releases, as indicated by salinities ≤ 5 lasting at these sites for more than three consecutive months (Figure 16).

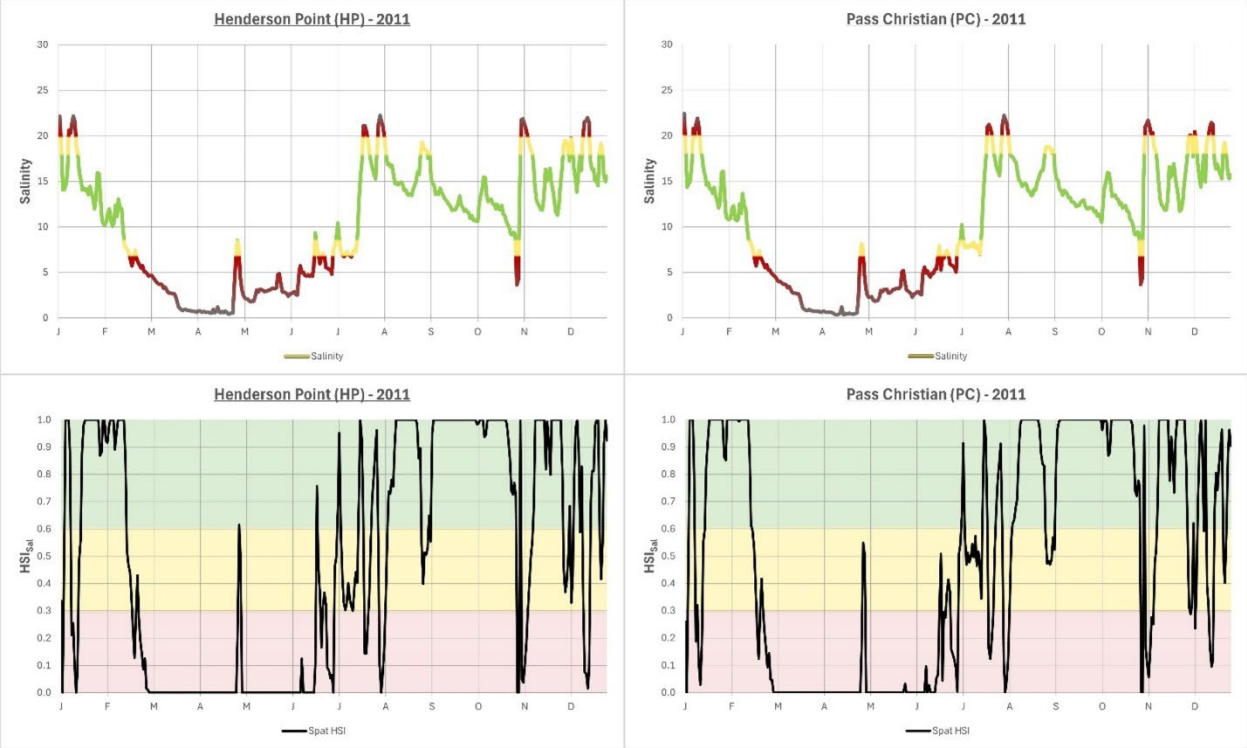

Figure 16. Scenario 2011 near-bottom mean daily salinities (top row) and the resultant calculation of HSI_{Sal} for spat-sized oysters (bottom row) at those locations where Ecosim model results indicated a "tipping point" had been reached. Note that color shading reflects the ranges of "good" (1.0-0.6), "fair" (0.6-0.3), and "poor" (0.3-0.0) habitat suitability for spat (adapted from Volety et al. 2009).

Tipping Point Scenario: 2019A

The 1st opening of the BCS in 2019 (scenario 2019A) was similar in duration to the 2011 scenario, lasting 44 days, but discharge rates were lower than in 2011, such that the maximum discharge rate only reached 213,000 cfs, resulting in a lower cumulative discharge of ~230% Lake Pontchartrain volumes of fresh water released into the wMSS compared to the 2011 scenario. Despite lower cumulative discharges of fresh water being delivered to the wMSS, Ecosim model results from 2019A were very similar to those of the 2011 scenario, such that the resultant low salinities induced "tipping point" mortality events only among spat-sized oysters at the Henderson Point (HP) and Pass Christian (PC) reef locations (Figure 17), although seed- and sack-sized oysters were negatively affected at many other locations in the 2019A scenario (Figure 15; again, very similarly to the 2011 scenario).

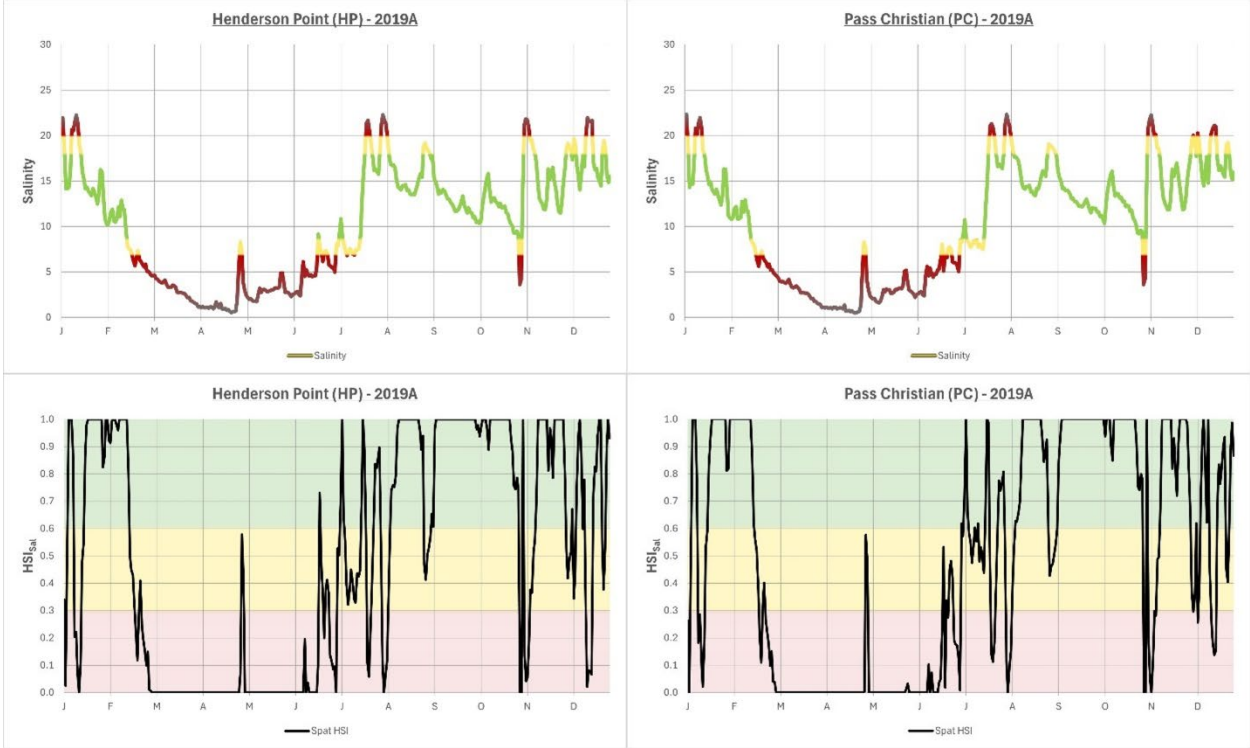

Figure 17. Scenario 2019A near-bottom mean daily salinities (top row) and the resultant calculation of HSI_{Sal} for spat-sized oysters (bottom row) at those locations where Ecosim model results indicated a "tipping point" had been reached. Note that color shading reflects the ranges of "good" (1.0-0.6), "fair" (0.6-0.3), and "poor" (0.3-0.0) habitat suitability for spat (adapted from Volety et al., 2009).

Tipping Point Scenario: 2019B

The 2nd opening of the BCS in 2019 (scenario 2019B) was similar in magnitude to the 2011 scenario, with a cumulative discharge of ~350% Lake Pontchartrain volumes of fresh water released into the wMSS. Although discharge rates were lower than both 2011 and the 1st opening in 2019, reaching a maximum discharge rate of 161,000 cfs, the duration of the 2nd opening was nearly double those of 2011 and 2019A, occurring over a span of 79 days Thus, Ecosim model results from the 2019B scenario indicated a spatial expansion of tipping point mortality events (Figure 18), still occurring only among spat-sized oysters, but now occurring at four reef locations: Henderson Point (HP), Pass Christian (PC), Pass Marianne (PM), and Telegraph Reef (TR). As with prior scenarios, seed- and sack-sized oyster biomass was certainly diminished at all other locations in the 2019B scenario, but not to the extent that any tipping points for seed or sack had been reached. HSI_{Sal} analyses

indicated the expected depression of habitat suitability for spat oysters in response to dramatically lower salinities of the 2019B scenario, with poor habitat suitability persisting across wMSS reefs for 3 (PM, TR) to 4.5 (HP, PC) consecutive months (Figure 18).

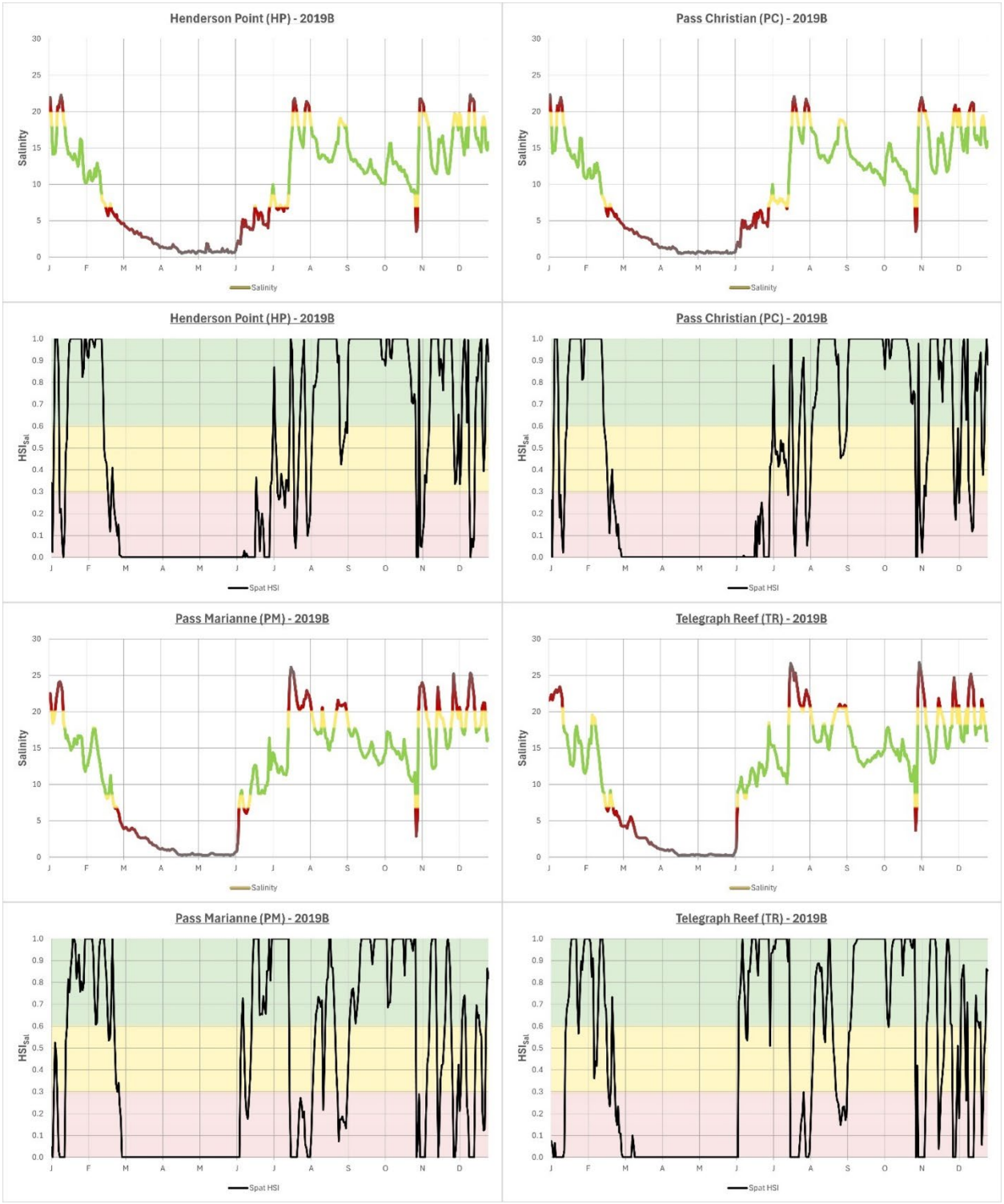

Figure 18. Scenario 2019B near-bottom mean daily salinities (rows 1,3) and the resultant calculation of HSI_{Sal} for spat-sized oysters (rows 2,4) at those locations where Ecosim model results indicated a "tipping point" had been reached. Note that color shading reflects the ranges of "good" (1.0-0.6), "fair" (0.6-0.3), and "poor" (0.3-0.0) habitat suitability for spat (adapted from Volety et al., 2009).

Tipping Point Scenario: 2019Full

The unprecedented double-opening of the BCS in 2019 (scenario 2019Full) occurred over a total of 123 days, slightly more than 33% of the calendar year. Although peak discharge rates were lower than those witnessed in 2011, the extensive duration of the BCS openings throughout 2019 resulted in a total cumulative discharge of ~570% Lake Pontchartrain volumes of fresh water released into the wMSS. Despite these extreme events, Ecosim model results from the 2019Full scenario did not indicate any "tipping point" mortality events any different than those witnessed in the 2019B scenario (Figure 18), still occurring only among spat-sized oysters at the same four reef locations: Henderson Point (HP), Pass Christian (PC), Pass Marianne (PM), and Telegraph Reef (TR). As with prior scenarios, seed- and sack-sized oyster biomass was certainly diminished at all other locations in the 2019Full scenario, but not to the extent that any "tipping points" for seed or sack had been reached. HSI_{Sal} analyses indicated the expected depression of habitat suitability for spat oysters in response to dramatically lower salinities, similar to those of the 2019B scenario, although the full expression of the double opening of the BCS in the 2019Full scenario did indeed preclude the recovery of near-bottom salinities for a 6-month period at the most grievously-affected reef sites (HP, PC; Figure 19). Interestingly, the pause between the double-openings did result in a short-lived recovery of habitat suitability at Pass Marianne (PM) and Telegraph Reef (TR), but it was not enough to alleviate the fact that spat had nonetheless reached their tipping point at these reef sites as well (Figure 19).

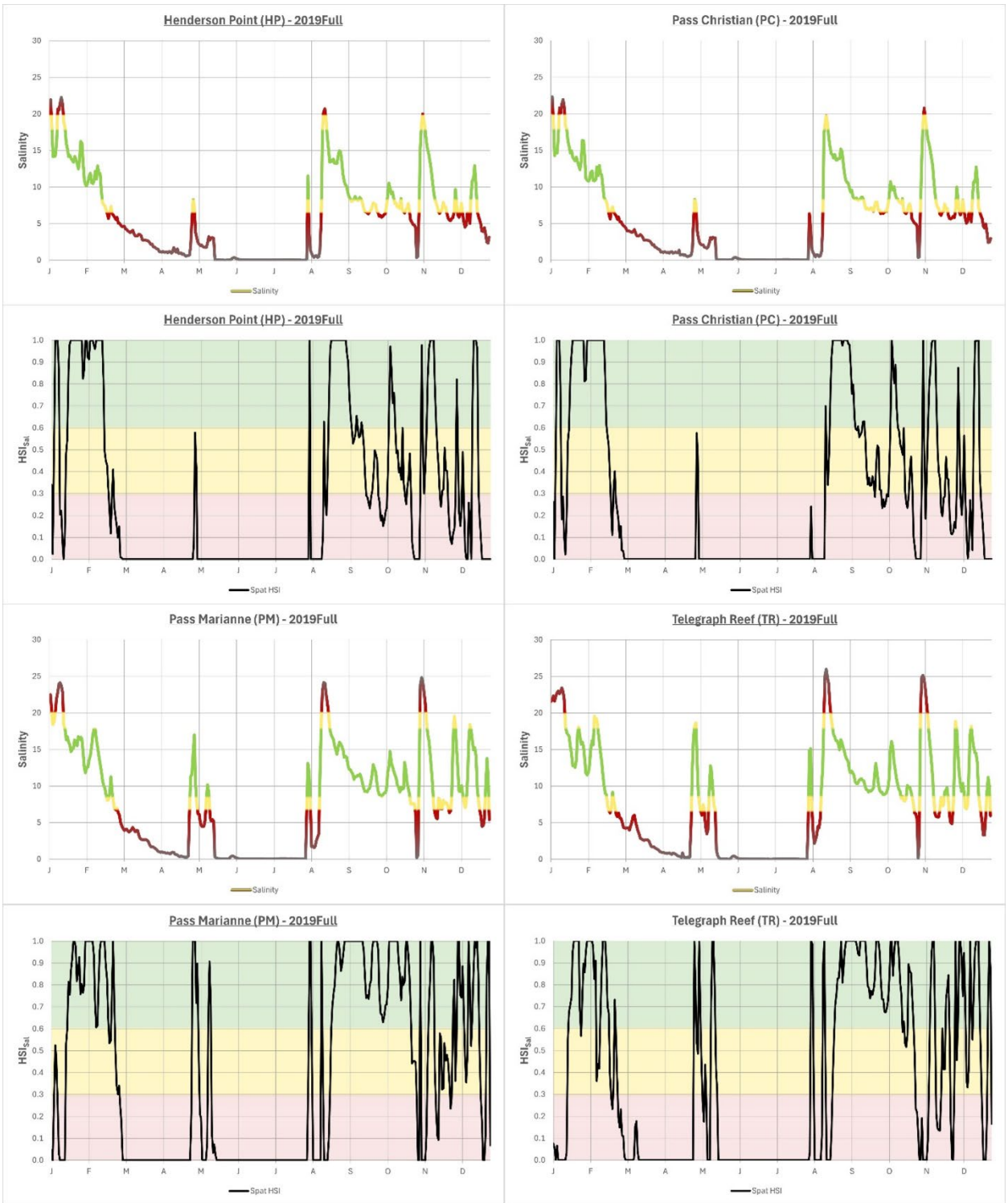

Figure 19. Scenario 2019Full near-bottom mean daily salinities (rows 1,3) and the resultant calculation of HSI_{Sal} for spat-sized oysters (rows 2,4) at those locations where Ecosim model results indicated a "tipping point" had been reached. Note that color shading reflects the ranges of "good" (1.0-0.6), "fair" (0.6-0.3), and "poor" (0.3-0.0) habitat suitability for spat (adapted from Volety et al., 2009).

Summary and Conclusions

BCS operations have led to ecological tipping points for eastern oysters in the Mississippi Sound. In the comparative scenarios simulated in this study, the natural forcing for all simulations provided by the msbCOAWST model are identical – the same 2018 atmospheric forcing, the same climatological riverine forcing, and the same 2018 open boundary conditions. The natural climatological riverine input is representative of typical conditions based on recent climatology covering the years 2011-2020 to isolate the influence of different BCS operations. The double opening of the spillway in 2019 severely affected oyster biomass, with the modeled double opening scenario leading to the lowest oyster biomass values at six of the eight Mississippi oyster reefs included in this study (Biloxi Bay, Henderson Point, Pass Christian, Pass Marianne, Shearwater and Telegraph Reef). At Buoy Reef and Pelican Reef, the scenario with the second opening of the spillway right at the start of the scenario led to the lowest oyster biomass.

By analyzing the data from MDMR's field oyster monitoring program, the ecological tipping points were determined to be when spat loses 80.6% of biomass in a year, seed oysters lose 67.7% in a year, and sack oysters lose 62% in a year. Ecological tipping points occurred for oyster spat during the 2011 BCS opening scenario, the 1st 2019 BCS opening scenario, the 2nd 2019 BCS opening scenario, and the 2019 BCS double opening scenario at Henderson Point and Pass Christian reefs. This includes scenarios where the BCS was open for 43 days with a total freshwater discharge volume of 329.6% of Lake Pontchartrain (2011), the BCS was open for 43 days with a total freshwater discharge volume of 219.5% of Lake Pontchartrain (2019A), the BCS was open for 79 days with a total freshwater discharge volume of 346.9% of Lake Pontchartrain (2019B), and the BCS was open for 122 days with a total freshwater discharge volume of 566.4% of Lake Pontchartrain (2019Full).

While spat oysters located at the Pass Marianne and Telegraph Reef locations had seemingly avoided reaching their ecological tipping point during the 2011 BCS opening scenario and the 1st BCS opening scenario of 2019, the 2nd 2019 opening scenario and the 2019 double opening scenario did result in losses past this ecological threshold. The

biomass losses of spat oysters at the other reefs included in this study (Biloxi Bay, Buoy Reef, Pelican Reef, and Shearwater) did not go past their tipping point during any of the BCS opening scenarios included in this study. This means that the ecological tipping point cannot simply be expressed in a volume of freshwater inflow or a duration of the opening; the timing of the opening and the location of the reef play a role as well. Other factors that we did not examine, such as different atmospheric forcings, are likely to play a role as well in what effects a BCS opening has on Mississippi oyster reefs.

Reefs in the eastern portion of the model domain—Biloxi Bay and Shearwater—were less affected by all opening scenarios than reefs in the west, demonstrating proximity effects of the opening on oyster mortality. Seed and sack oysters experienced good conditions in Biloxi Bay during all BCS openings, indicating that Biloxi Bay is a good relay location when a BCS opening appears inevitable. Additionally, as evidenced by lower mortality at Buoy Reef and Pelican Reef compared to Henderson Point, Pass Christian, Pass Marianne, and Telegraph Reef, reefs that are a few kilometers east of the western reefs may already have lessened proximity effects from the BCS, and are likely protected by increased influences from marine waters entering the Sound. The accompanying hydrodynamic report can provide insights into how hydrodynamics may have caused this difference. Although there were less effects of freshwater inflow on oysters at Buoy Reef and Pelican Reef, these reefs are only 0.192 and 0.408 km^2, respectively, and not historically as productive compared to their larger western Sound counterparts. The extreme reductions in environmental quality and oyster biomass experienced at the western reefs during long and voluminous BCS discharges are impactful, given that the two most historically productive and largest reefs in the Mississippi Sound, Pass Christian and Pass Marianne, are western reefs.

The 2018 and 2020 opening scenarios had the least impact on biomass across all size classes at all reefs compared to all other BCS openings scenarios, reflective of the shorter duration and lower freshwater discharge volume for these two scenarios. These openings did not cause ecological tipping points for any of the size classes at any of the reefs and only resulted in poor conditions for spat at two reefs (Henderson Point and Pass

Christian), with fair to good conditions at all other reefs for all life stages. Conservative spillway operations can therefore result in acceptable effects on oysters in the Mississippi Sound. While this study demonstrates that ecological tipping points are specific to size classes of oysters and locations of the reefs, the developed models allow us to determine ahead of time which reefs are most likely to be affected, and to what extent, when a BCS opening is proposed in future years. Our current results should be viewed as representing the minimum expected ecological impact of spillway operations, with future modeling efforts needed to fully incorporate the impacts of nutrient loadings, hypoxia, and sediment-related stressors for a more complete understanding of BCS effects. The shortest opening duration when a tipping point had been reached for spat was 43 days, and the smallest discharge volume when a tipping point had been reached for spat was 219.5% of Lake Pontchartrain based on historic opening scenarios. Using the information from the scenarios we have run in this study, a BCS opening duration up to 29 days (2020) with a total freshwater discharge volume up to 86.6% of Lake Pontchartrain (2018) would allow for oyster biomass losses to remain above their ecological tipping points for all life stages at all reefs included in our study.

References

Acosta, A. (2000). Estimation of growth and mortality of bay anchovy, *Anchoa mitchilli*, in Florida Bay, Florida USA. *Proc. 51st Gulf and Caribbean Fisheries Institute, St. Croix, US Virgin Islands, November 1998. Fort Pierce, Florida*. https://core.ac.uk/download/pdf/19208736.pdf

Althauser, L. (2003). *An Ecopath/Ecosim analysis of an estuarine food web: Seasonal energy flow and response to river-flow related perturbations* [Louisiana State University]. https://repository.lsu.edu/gradschool_theses/1449

Andrews, J. D., & Hewatt, W. G. (1957). Oyster mortality studies in Virginia. II. The fungus disease caused by *Dermocystidium marinum* in oysters of Chesapeake Bay. *Ecological Monographs*, *27*(1), 2–25.

Aragão, J. A. N., Cintra, I. H. A., De Araújo Silva, K. C., & Petrere Júnior, M. (2021). Reproduction and recruitment of the brown shrimp *Penaeus subtilis* in the Amazon River continental shelf. *Arquivos de Ciências Do Mar*, *54*(1), 163–183. https://doi.org/10.32360/acmar.v54i1.41690

Ayvazian, S., Mulvaney, K., Zarnoch, C., Palta, M., Reichert-Nguyen, J., McNally, S., Pilaro, M., Jones, A., Terry, C., & Fulweiler, R. W. (2021). Beyond bioextraction: The role of oyster-mediated denitrification in nutrient management. *Environmental Science & Technology*, *55*(21), 14457–14465.

Baker Jr., M. S., Wilson, C. A., & Van Gent, D. L. (2001). Age validation of red snapper, *Lutjanus campechanus*, and red drum, *Sciaenops ocellatus*, from the northern Gulf

of Mexico using 210Po/226Ra disequilibria in otoliths. *Proceedings of the 52nd Gulf and Caribbean Fisheries Institute*, 63–73. https://search.hsl.med.nyu.edu

Baker, M. C., Steinhoff, M. A., & Fricano, G. F. (2017). Integrated effects of the Deepwater Horizon oil spill on nearshore ecosystems. *Marine Ecology Progress Series*, *576*, 219–234.

Bare, L. (2001). Leiostomus xanthurus. Animal Diversity Web. https://animaldiversity.org/accounts/Leiostomus_xanthurus/

Barnes, T., Volety, A., Chartier, K., Mazzotti, F., & Pearlstine, L. (2007). A habitat suitability index model for the eastern oyster (*Crassostrea virginica*), a tool for restoration of the Caloosahatchee Estuary, Florida. *Journal of Shellfish Research*, *26*(4), 949–959.

Beamesderfer, R. C. P., & North, J. A. (1995). Growth, natural mortality, and predicted response to fishing for largemouth bass and smallmouth bass populations in North America. *North American Journal of Fisheries Management*, *15*(3), 688–704. https://doi.org/10.1577/1548-8675(1995)015%253C0688:GNMAPR%253E2.3.CO;2

Benjamin, S. G., Weygandt, S. S., Brown, J. M., Hu, M., Alexander, C. R., Smirnova, T. G., Olson, J. B., James, E. P., Dowell, D. C., Grell, G. A., Lin, H., Peckham, S. E., Smith, T. L., Moninger, W. R., Kenyon, J. S., & Manikin, G. S. (2016). *A North American Hourly Assimilation and Model Forecast Cycle: The Rapid Refresh*. https://doi.org/10.1175/MWR-D-15-0242.1

Bentley, J. W., Chagaris, D., Coll, M., Heymans, J. J., Serpetti, N., Walters, C. J., & Christensen, V. (2024). Calibrating ecosystem models to support ecosystem-based

management of marine systems. *ICES Journal of Marine Science*, *81*(2), 260–275. https://doi.org/10.1093/icesjms/fsad213

Bester, C. (2025a, February 5). *Gulf Sturgeon*. Florida Museum. https://www.floridamuseum.ufl.edu/discover-fish/species-profiles/gulf-sturgeon/

Bester, C. (2025b, February 6). *Spotted Seatrout*. Florida Museum. https://www.floridamuseum.ufl.edu/discover-fish/species-profiles/spotted-seatrout/

Blancher II, E. C., Park, R. A., Clough, J. S., Milroy, S. P., Graham, W. M., Rakocinski, C. F., Hendon, J. R., Wiggert, J. D., & Leaf, R. (2017). Establishing nearshore marine secondary productivity baseline estimates for multiple habitats in coastal Mississippi and Alabama using AQUATOX 3.1 NME for use in the Deepwater Horizon natural resource damage assessment. *Ecological Modelling*, *359*, 49–68.

Boudreaux, A. (2013). *Assessment of largemouth bass* Micropterus salmoides *age, growth, gonad development and diet in the upper Barataria estuary* [Master's Thesis]. Nicholls State University.

Branstetter, S., & Stiles, R. (1987). Age and growth estimates of the bull shark, *Carcharhinus leucas*, from the northern Gulf of Mexico. *Environmental Biology of Fishes*, *20*(3), 169–181. https://doi.org/10.1007/BF00004952

Brown, H., Minello, T., Matthews, G., Fisher, M., Anderson, E., Reidel, R., & Leffler, D. (2013). A Comparative Assessment of Gulf Estuarine Systems (CAGES): NOAA Fisheries. *NOAA/NMFS, Editor. NOAA, Galveston, TX*.

Buck, E. H. (2005). *Hurricane Katrina: Fishing and Aquaculture Industries -- Damage and Recovery* (Congressional Research Service Report for Congress Order RS22241; p. 3). https://apps.dtic.mil/sti/html/tr/ADA465457/index.html

Butler, P. A. (1985). *Synoptic Review of the Literature on the Southern Oyster Drill* Thais haemastoma floridana (NOAA Technical Report NMFS 35; p. 9).

Cake Jr, E.W. (1983). *Habitat Suitability Index Models: Gulf of Mexico American Oyster* (U.S. Fish & Wildlife Service Report FWS/OBS-82/10.57).

Cambazoglu, M. K., Armstrong, B. N., & Wiggert, J. D. (2024). Development of a daily coastal ocean model for Mississippi Sound and Bight. *Ocean Dynamics*, *74*(11), 987–1004. https://doi.org/10.1007/s10236-024-01645-4

Cambazoglu, M. K., Soto, I. M., Howden, S. D., Dzwonkowski, B., Fitzpatrick, P. J., Arnone, R. A., Jacobs, G. A., & Lau, Y. H. (2017). Inflow of shelf waters into the Mississippi Sound and Mobile Bay estuaries in October 2015. *Journal of Applied Remote Sensing*, *11*(3), 032410–032410.

Cambazoglu, M. K., Wiggert, J. D., & Pan, C. (2020). *Physical Model of the Mississippi Sound and Bight from 2017-05-14 to 2017-10-25* [Dataset]. GRIIDC. https://doi.org/10.7266/FYMFTNPP

Carlander, K. D. (1969). Handbook of freshwater fishery biology. Volume 1. Life history data on freshwater fishes of the United States and Canada, exclusive of the Perciformes. In *Handbook of freshwater fishery biology*. Iowa State University Press.

Cerco, Carl & Noel, Mark. (2005). *Evaluating ecosystem effects of oyster restoration in Chesapeake Bay* [Report to the Maryland Department of Natural Resources, Annapolis, MD].

Chagaris, D. D., Patterson, W. F., & Allen, M. S. (2020). Relative effects of multiple stressors on reef food webs in the northern Gulf of Mexico revealed via ecosystem modeling. *Frontiers in Marine Science*, *7*, 513. https://doi.org/10.3389/fmars.2020.00513

Chiaverano, L. M., Robinson, K. L., Tam, J., Ruzicka, J. J., Quiñones, J., Aleksa, K. T., Hernandez, F. J., Brodeur, R. D., Leaf, R., Uye, S., Decker, M. B., Acha, M., Mianzan, H. W., & Graham, W. M. (2018). Evaluating the role of large jellyfish and forage fishes as energy pathways, and their interplay with fisheries, in the Northern Humboldt Current System. *Progress in Oceanography*, *164*, 28–36. https://doi.org/10.1016/j.pocean.2018.04.009

Christensen, V., Coll, M., Steenbeek, J., Buszowski, J., Chagaris, D., & Walters, C. (2014). Representing Variable Habitat Quality in a Spatial Food Web Model. *Ecosystems*, *17*, 1397–1412. https://doi.org/10.1007/s10021-014-9803-3

Christensen, V., & Pauly, D. (1992). ECOPATH II — a software for balancing steady-state ecosystem models and calculating network characteristics. *Ecological Modelling*, *61*(3), 169–185. https://doi.org/10.1016/0304-3800(92)90016-8

Christensen, V., & Walters, C. J. (2024). *Ecosystem Modelling with EwE*. The University of British Columbia. https://doi.org/10.14288/24d7-ab68

Christensen, V., Walters, C. J., & Pauly, D. (2008). Ecopath with Ecosim: A user's guide. *Fisheries Centre, University of British Columbia, Vancouver*, 154.

Coen, L. D., Brumbaugh, R. D., Bushek, D., Grizzle, R., Luckenbach, M. W., Posey, M. H., Powers, S. P., & Tolley, S. G. (2007). Ecosystem services related to oyster restoration. *Marine Ecology Progress Series*, *341*, 303–307.

Collins, Mark R. (1985). *Species Profiles: Life Histories and Environmental Requirements of Coastal Fishes and Invertebrates (South Florida)* (Biological Report Nos. 82–4). https://apps.dtic.mil/sti/tr/pdf/ADA162640.pdf

Davis, H. C., & Hidu, H. (1969). Effects of turbidity-producing substances in sea water on eggs and larvae of three genera of bivalve mollusks. *The Veliger*, (4).

Davis, Harry C. & Calabrese, Anthony. (1964). Combined effects of temperature and salinity on development of eggs and growth of larvae of *M. mercenaria*, and *C. virginica*. *Fishery Bulletin*, *63*(3), 643–655.

De Mutsert, K. (2010). *The Effects of a Freshwater Diversion of Nekton Species Biomass Distributions, Food Web Pathways, and Community Structure in a Louisiana Estuary* [Doctoral Dissertation, Louisiana State University and Agricultural & Mechanical College]. https://www.proquest.com/docview/2675220042/abstract/3173B9A078D34312PQ/1

De Mutsert, K., Cowan, J. H., Jr., & Walters, C. J. (2012). Using Ecopath with Ecosim to explore nekton community response to freshwater diversion into a Louisiana estuary. *Marine and Coastal Fisheries*, *4*(1), 104–116. https://doi.org/10.1080/19425120.2012.672366

De Mutsert, K., Lewis, K. A., Buszowski, J., Steenbeek, J., & Milroy, S. (2017). *2017 Coastal Master Plan Modeling: C3-20: Ecopath with Ecosim. Version Final.* (pp. 1–97). Coastal Protection and Restoration Authority.

Dekshenieks, M. M., Hofmann, E. E., Klinck, J. M., & Powell, E. N. (1996). Modeling the vertical distribution of oyster larvae in response to environmental conditions. *Marine Ecology Progress Series*, *136*, 97–110. https://doi.org/10.3354/meps136097

Dekshenieks, M. M., Hofmann, E. E., & Powell, E. N. (1993). Environmental effects on the growth and development of eastern oyster, *Crassostrea virginica* (Gmelin, 1791), larvae: A modeling study. *Journal of Shellfish Research*, *12*(2).

DuPaul, William D. & McEachran, John D. (1973). Age and growth of the Butterfish, *Peprilus tricanthus*, in the Lower York River. *Chesapeake Science*, *14*, 205–207. https://doi.org/10.2307/1350608

Eleuterius, C. (1977). Location of the Mississippi Sound oyster reefs as related to salinity of bottom waters during 1973-1975. *Gulf and Caribbean Research*, *6*(1), 17–23. https://doi.org/10.18785/grr.0601.03

Eleuterius, C. K. (1978). Classification of Mississippi Sound as to estuary hydrological type. *Gulf Research Reports*, *6*(2), 185–187.

Erzini, K. (1991). *A compilation of data on variability in length-age in marine fishes* (p. 36) [Working Paper 77]. Fisheries Stock Assessment, Title XII, Collaborative Research Support Program, University of Rhode Island.

Fodrie, F. J., Rodriguez, A. B., Gittman, R. K., Grabowski, J. H., Lindquist, N. L., Peterson, C. H., Piehler, M. F., & Ridge, J. T. (2017). Oyster reefs as carbon sources and sinks. *Proceedings of the Royal Society B: Biological Sciences*, *284*(1859), 20170891.

Fontaine, C. T., & Neal, R. A. (1971). Length-weight relations for three commercially important penaeid shrimp of the Gulf of Mexico. *Transactions of the American Fisheries Society*, *100*(3), 584–586.

Frazier, B. S., Driggers, W. B., Adams, D. H., Jones, C. M., & Loefer, J. K. (2014). Validated age, growth and maturity of the bonnethead *Sphyrna tiburo* in the western North Atlantic Ocean. *Journal of Fish Biology*, *85*(3), 688–712. https://doi.org/10.1111/jfb.12450

Froese, R. (2022). Estimating somatic growth of fishes from maximum age or maturity. *Acta Ichthyologica et Piscatoria*, *52*(2), 125–133. https://doi.org/10.3897/aiep.52.80093

Froese, R., & Pauly, D. (2025). *FishBase*. https://fishbase.se/

Galtsoff, P. S. (1964). The American oyster *Crassostrea virginica* Gmelin. *United States Fishery Bulletin*, *64*, 1–480.

Garton, D., & Stickle, W. B. (1980). Effects of salinity and temperature on the predation rate of *Thais haemastoma* on *Crassostrea virginica* spat. *The Biological Bulletin*, *158*(1), 49–57.

GDAR. (2013). *GDAR 01—Gulf of Mexico Blue Crab Stock Assessment Report* (p. 291).

GDAR. (2024). *GDAR 04/SEDAR 97—Gulf Menhaden Stock Assessment 2024 Update Assessment Report* (p. 77).

Geers, T. M. (2012). *Developing an ecosystem-based approach to management of the Gulf menhaden fishery using Ecopath with Ecosim* [Master's Thesis, Stony Brook University]. Stony Brook Theses and Dissertations Collection (437). https://commons.library.stonybrook.edu/stony-brook-theses-and-dissertations-collection/437

Geers, T. M., Pikitch, E. K., & Frisk, M. G. (2016). An original model of the northern Gulf of Mexico using Ecopath with Ecosim and its implications for the effects of fishing on ecosystem structure and maturity. *Deep Sea Research Part II: Topical Studies in Oceanography*, *129*, 319–331.

Gilby, B. L., Olds, A. D., Peterson, C. H., Connolly, R. M., Voss, C. M., Bishop, M. J., Elliott, M., Grabowski, J. H., Ortodossi, N. L., & Schlacher, T. A. (2018). Maximizing the benefits of oyster reef restoration for finfish and their fisheries. *Fish and Fisheries*, *19*(5), 931–947.

Gledhill, J. H., Barnett, A. F., Slattery, M., Willett, K. L., Easson, G. L., Otts, S. S., & Gochfeld, D. J. (2020). Mass mortality of the eastern oyster *Crassostrea virginica* in the western Mississippi Sound following unprecedented Mississippi River flooding in 2019. *Journal of Shellfish Research*, *39*(2), 235–244.

Govekar, P. D., Griffin, C., & Beggs, H. (2022). Multi-Sensor Sea Surface Temperature Products from the Australian Bureau of Meteorology. *Remote Sensing*, *14*(15). https://doi.org/10.3390/rs14153785

Grabowski, J. H., Powers, S. P., Roman, H., & Rouhani, S. (2017). Potential impacts of the 2010 Deepwater Horizon oil spill on subtidal oysters in the Gulf of Mexico. *Marine Ecology Progress Series*, *576*, 163–174.

Greer, A. T., Shiller, A. M., Hofmann, E. E., Wiggert, J. D., Warner, S. J., Parra, S. M., Pan, C., Book, J. W., Joung, D., & Dykstra, S. (2018). Functioning of coastal river-dominated ecosystems and implications for oil spill response: From observations to mechanisms and models. *Oceanography*, *31*(3), 90–103.

Gunter, G., & Geyer, R. A. (1955). Studies of fouling organisms in the northwestern Gulf of Mexico. *Publications of the Institute of Marine Science University of Texas*, *4*(1), 36–67.

Haidvogel, D. B., Arango, H., Budgell, W. P., Cornuelle, B. D., Curchitser, E., Di Lorenzo, E., Fennel, K., Geyer, W. R., Hermann, A. J., & Lanerolle, L. (2008). Ocean forecasting in terrain-following coordinates: Formulation and skill assessment of the Regional Ocean Modeling System. *Journal of Computational Physics*, *227*(7), 3595–3624.

Hart, R. A. (2015a). *Stock Assessment Update for White Shrimp (*Litopenaeus setiferus*) in the U.S. Gulf of Mexico for 2014* (p. 21) [NOAA Technical Memorandum].

Hart, R. A. (2015b). *Stock Assessment Updated for Brown Shrimp (*Farfantepenaeus aztecus*) in the U.S. Gulf of Mexico for 2014* (p. 19) [NOAA Technical Memorandum].

Hendon, J. R., Wiggert, J. D., & Hendon, J. M. (2019). *Monitoring 2019 Bonnet Carre Spillway Impacts—Final Report*. Mississippi Dept. of Marine Resources.

Hijuelos, A. C., Moss, L., Sable, S. E., O'Connell, A. M., & Geaghan, J. P. (2016). *2017 Coastal Master Plan: C3-18 – Largemouth Bass, Micropterus salmoides, Habitat*

Suitability Index Model. Version II (pp. 1–25). Coastal Protection and Restoration Authority.

Hijuelos, A. C., Sable, S. E., O'Connell, A. M., & Geaghan, J. P. (2014). *2017 Coastal Master Plan: Habitat Suitability Index Models, Eastern Oyster (Subtask 3.4.5.3), Version 1*. Coastal Protection and Restoration Authority.

Hilling, C. D., Bunch, A. J., Greenlee, R. S., Orth, D. J., & Jiao, Y. (2018). Natural mortality and size structure of introduced blue catfish in Virginia tidal rivers. *Journal of the Southeastern Association of Fish and Wildlife Agencies*, *5*, 30–38.

Hoenig, J. M. (1979). *The vertebral centra of sharks and their use in age determination* [Unpublished master's thesis]. University of Rhode Island.

Hofman, E. E., Klinck, J. M., Powell, E. N., Boyles, S., & Ellis, M. (1994). Modeling oyster populations II. Adult size and reproductive effort. *Journal of Shellfish Research*, *13*(1), 165–182.

Hofstetter, R. P. (1990). *The Texas Oyster Fishery* (No. 40). Texas Parks and Wildlife Department.

Humphries, A. T., Ayvazian, S. G., Carey, J. C., Hancock, B. T., Grabbert, S., Cobb, D., Strobel, C. J., & Fulweiler, R. W. (2016). Directly measured denitrification reveals oyster aquaculture and restored oyster reefs remove nitrogen at comparable high rates. *Frontiers in Marine Science*, *3*, 74. Publicly Available Content Database (2307424288). https://doi.org/10.3389/fmars.2016.00074

Indian River Lagoon National Estuary Program. (n.d.). *Indian River Lagoon Species Inventory*. Retrieved December 1, 2024, from https://irlspecies.org/taxa/index.php?taxon=6982&cl=32

Jacobs, G. A. (2017). *Gulf of Mexico 1 km resolution numerical model simulation with USGS observed river flows, January-February 2016* [Dataset]. Distributed by: GRIIDC, Harte Research Institute, Texas A&M University–Corpus Christi. https://doi.org/10.7266/N7542KZP

Jacobs, G. A., Huntley, H. S., Kirwan Jr, A. D., Lipphardt Jr, B. L., Campbell, T., Smith, T., Edwards, K., & Bartels, B. (2016). Ocean processes underlying surface clustering. *Journal of Geophysical Research: Oceans*, *121*, 180–197. https://doi.org/10.1002/2015JC011140

Kellogg, M. L., Cornwell, J. C., Owens, M. S., & Paynter, K. T. (2013). Denitrification and nutrient assimilation on a restored oyster reef. *Marine Ecology Progress Series*, *480*, 1–19. https://doi.org/10.3354/meps10331

Kirk, J. P. (2008). *Gulf sturgeon movements in and near the Mississippi River gulf outlet* (Technical Report Nos. 08–18). http://hdl.handle.net/11681/6874

Klein, J. C., Powell, E. N., Kreeger, D. A., Zhang, X., Pace, S. M., Kuykendall, K. M., & Thomas, R. L. (2024). Model estimation of eastern oyster larval performance from food quantity and quality measures in western Mississippi Sound. *Marine Ecology Progress Series*, *745*, 73–94. https://doi.org/10.3354/meps14675

Klima, E. F. (1974). A white shrimp mark-recapture study. *Transactions of the American Fisheries Society*, *103*(1), 107–113. https://doi.org/10.1577/1548-8659(1974)103%253C107:AWSMS%253E2.0.CO;2

Kreeger, D. A., Gatenby, C. M., & Bergstrom, P. W. (2018). Restoration potential of several native species of bivalve molluscs for water quality improvement in mid-Atlantic watersheds. *Journal of Shellfish Research*, *37*(5), 1121–1157. https://doi.org/10.2983/035.037.0524

La Peyre, M. K., Casas, S., & La Peyre, J. (2006). Salinity effects on viability, metabolic activity and proliferation of three *Perkinsus* species. *Diseases of Aquatic Organisms*, *71*(1), 59–74. https://doi.org/10.3354/dao071059

La Peyre, M. K., Eberline, B. S., Soniat, T. M., & La Peyre, J. F. (2013). Differences in extreme low salinity timing and duration differentially affect eastern oyster (*Crassostrea virginica*) size class growth and mortality in Breton Sound, LA. *Estuarine, Coastal and Shelf Science*, *135*, 146–157. https://doi.org/10.1016/j.ecss.2013.10.001

La Peyre, M. K., Marshall, D. A., & Sable, S. (2021). *Oyster model inventory: Identifying critical data and modeling approaches to support restoration of oyster reefs in coastal U.S. Gulf of Mexico waters* (Report Nos. 2021–1063; Open-File Report, p. 52). USGS Publications Warehouse. https://doi.org/10.3133/ofr20211063

La Peyre, M. K., Miller, L. S., Miller, S., & Melancon, E. (2017). Comparison of oyster populations, shoreline protection service, and site characteristics at seven created fringing reefs in Louisiana: Key parameters and responses to consider. In D. M. Bilkovic, M. M. Mitchell, & M. K. La Peyre (Eds.), *Living shorelines: The science and*

management of nature-based coastal protection. CRC Research Press. https://pubs.usgs.gov/publication/70192002

Lenihan, H. S. (1999). Physical–biological coupling on oyster reefs: How habitat structure influences individual performance. *Ecological Monographs*, *69*(3), 251–275. https://doi.org/10.1890/0012-9615(1999)069%255B0251:PBCOOR%255D2.0.CO;2

Lewis, K. A., Christian, R. R., Martin, C. W., Allen, K. L., McDonald, A. M., Roberts, V. M., Shaffer, M. N., & Valentine, J. F. (2022). Complexities of disturbance response in a marine food web. *Limnology and Oceanography*, *67*(S1), S352–S364. https://doi.org/10.1002/lno.11790

Linhoss, A. C., Camacho, R., & Ashby, S. (2016). Oyster Habitat Suitability in the Northern Gulf of Mexico. *Journal of Shellfish Research*, *35*(4), 841–849. https://doi.org/10.2983/035.035.0412

Link, J. S. (2010). Adding rigor to ecological network models by evaluating a set of pre-balance diagnostics: A plea for PREBAL. *Ecological Modelling*, *221*(12), 1580–1591. https://doi.org/10.1016/j.ecolmodel.2010.03.012

Loosanoff, V. L. (1962). Effects of turbidity on some larval and adult bivalves. *Proceedings of the Gulf and Caribbean Fisheries Institute*, *14*, 80–94.

Loosanoff, V. L., & Tommers, F. D. (1948). Effect of suspended silt and other substances on rate of feeding of oysters. *Science*, *107*, 69–70.

Lough, R. G. (1975). A re-evaluation of the combined effects of temperature and salinity on survival and growth of bivalve larvae using response surface techniques. *Fishery Bulletin*, *73*(1), 86–94.

Louisiana Sea Grant. (1996). *Conchs* (20(12); Sea Grant Program Lagniappe Report, p. 7).

Luo, J., & Musick, J. A. (1991). Reproductive biology of the bay anchovy in Chesapeake Bay. *Transactions of the American Fisheries Society*, *120*(6), 701–710. https://doi.org/10.1577/1548-8659(1991)120%253C0701:RBOTBA%253E2.3.CO;2

Mackenzie Jr., C. L. (2006). Mississippi oysters after Katrina. *Underwater Naturalist*, *27*(3), 15–18.

Mackin, J. G. (1961). Oyster diseases caused by *Dermocystidium marinum* and other microorganisms in Louisiana. *Publications of the Institute of Marine Science*, *7*, 132–229.

Mann, R. (2001). Restoration of the oyster resource in Chesapeake Bay: The role of oyster reefs in population enhancement, water quality improvement and support of diverse species-rich communities. *Bulletin of the Aquaculture Association of Canada*, *101*(1), 38–42.

Matlock, G. C. & Garcia, M. A. (1983). Stomach contents of selected fishes from Texas bays. *Contributions in Marine Science*, *26*, 95–110.

Morris, R. L., La Peyre, M. K., Webb, B. M., Marshall, D. A., Bilkovic, D. M., Cebrian, J., McClenachan, G., Kibler, K. M., Walters, L. J., Bushek, D., Sparks, E. L., Temple, N. A., Moody, J., Angstadt, K., Goff, J., Boswell, M., Sacks, P., & Swearer, S. E. (2021). Large-scale variation in wave attenuation of oyster reef living shorelines and the influence of inundation duration. *Ecological Applications*, *31*(6), e02382. https://doi.org/10.1002/eap.2382

Muncy, R. J. (1984). *Species Profiles: Life Histories and Environmental Requirements of Coastal Fishes and Invertebrates (South Atlantic): White Shrimp* (FWS/OBS-82/11.27; p. 29). United States Fish and Wildlife Service. https://www.dnr.sc.gov/marine/species/assets/SpeciesProfileWhiteShrimp.pdf

Murphy, M. D., & Taylor, R. G. (1989). Reproduction and growth of black drum, *Pogonias cromis*, in northeast Florida. *Gulf of Mexico Science*, *10*(2), 6.

Murphy, Michael D. & Chittenden Jr., Mark E. (1991). Reproduction, age and growth, and movements of the Gulf butterfish *Peprilus burti*. *Fishery Bulletin*, *89*, 101–116.

Nakamura, I., & Parin, N. V. (1993). *FAO species catalogue. Vol.15. Snake mackerels and cutlassfishes of the world (Families Gempylidae and Trichiuridae). An annotated and illustrated catalogue of the snake mackerels, snoeks, escolars, gemfishes, sackfishes, domine, oilfish, cutlassfishes, scabbardfishes, hairtails and frostfishes known to date* (1st ed., Vol. 15). https://openknowledge.fao.org/server/api/core/bitstreams/9353996e-28d8-4377-a252-e501a70763d0/content/t0539e.htm

Nelson, G. (2002). Age, growth, mortality, and distribution of pinfish (*Lagodon rhomboides*) in Tampa Bay and adjacent Gulf of Mexico waters. *Fishery Bulletin*, *100*(3), 582–592.

Nemeth, D. J., Jackson, J. B., Knapp, A. R., & Purtlebaugh, C. H. (2006). Age and growth of sand seatrout (*Cynoscion arenarius*) in the estuarine waters of the eastern Gulf of Mexico. *Gulf of Mexico Science*, *24*(1), 45–60. https://doi.org/10.18785/goms.2401.07

Nepal, V., & Fabrizio, M. C. (2019). High salinity tolerance of invasive blue catfish suggests potential for further range expansion in the Chesapeake Bay region. *PLOS ONE*, *14*(11), e0224770. https://doi.org/10.1371/journal.pone.0224770

NOAA Eastern Oyster Biological Review Team. (2007). *Status review of the eastern oyster (*Crassostrea virginica*)* (p. 105) [NOAA Technical Memo NMFS F/SPO-88].

NOAA Fisheries. (2025, August 20). *Red Snapper Species Directory*. (Southeast). https://www.fisheries.noaa.gov/species/red-snapper

NOAA Office of Science and Technology. (2011). *Gulf of Mexico Oyster Atlas* (Harte Research Institute for Gulf of Mexico Studies at Texas A&M University-Corpus Christi) [Map]. NOAA National Centers for Environmental Information. http://gulfatlas.noaa.gov/about

NOAA Office of Science and Technology. (2023). *Commercial Fisheries Statistics*. https://www.fisheries.noaa.gov/national/sustainable-fisheries/commercial-fisheries-landings/

NOAA Office of Science and Technology. (2025). *Marine Mammal Stock Assessment Reports by Species/Stock*. https://www.fisheries.noaa.gov/national/marine-mammal-protection/marine-mammal-stock-assessment-reports-species-stock#cetaceans---dolphins

NOAA Office of Sustainable Fisheries. (2023). *Fishery Disaster Determinations*. https://www.fisheries.noaa.gov/national/funding-and-financial-services/fishery-disaster-determinations

Okey, T. A., Vargo, G. A., Mackinson, S., Vasconcellos, M., Mahmoudi, B., & Meyer, C. A. (2004). Simulating community effects of sea floor shading by plankton blooms over the West Florida Shelf. *Ecological Modelling, Placing Fisheries in Their Ecosystem Context*, *172*(2), 339–359. https://doi.org/10.1016/j.ecolmodel.2003.09.015

Palomares, M. L. D., & Pauly, D. (2025). *SeaLifeBase*. https://sealifebase.org/

Palomares, M. L. D., Sorongon, P. M. E., Hunter, Andrea, & Pauly, Daniel. (2008). *Growth of marine mammals* (Von Bertalanffy Growth Parameters of Non-Fish Marine Organisms, pp. 2–26). Fisheries Centre. University of British Columbia. https://doi.org/10.14288/1.0074762

Park, R. A., & Clough, J. S. (2018). *AQUATOX (Release 3.2) – Modeling Environmental Fate and Ecological Effects in Aquatic Ecosystems, Volume 2* (Technical Documentation EPA/600/B-18/241; p. 359). United States Environmental Protection Agency.

Parker, M., & Bricker, S. (2020). Sustainable oyster aquaculture, water quality improvement, and ecosystem service value potential in Maryland Chesapeake Bay. *Journal of Shellfish Research*, *39*(2), 269–281. https://doi.org/10.2983/035.039.0208

Parra, S. M., Sanial, V., Boyette, A. D., Cambazoglu, M. K., Soto, I. M., Greer, A. T., Chiaverano, L. M., Hoover, A., & Dinniman, M. S. (2020). Bonnet Carré Spillway freshwater transport and corresponding biochemical properties in the Mississippi Bight. *Continental Shelf Research*, *199*, 104114. https://doi.org/10.1016/j.csr.2020.104114

Parrack, Michael L. (1979). Aspects of brown shrimp, *Penaeus aztecus*, growth in the northern Gulf of Mexico. *Fishery Bulletin*, *76*(4), 827–837.

Patillo, M., Rozas, L. P., & Zimmerman, R. J. (1995). *A review of salinity requirements for selected invertebrates and fishes of US Gulf of Mexico estuaries* [Final report to the Environmental Protection Agency, Gulf of Mexico Program]. US Department of Commerce, National Oceanic and Atmospheric Administration, National Marine Fisheries Service, Southeast Fisheries Science Center, Galveston Laboratory.

Pauly, D. (1978). *A preliminary Compilation of fish length growth parameters* [Report]. Institut für Meereskunde. https://doi.org/10.3289/ifm_ber_55

Pauly, D. (1979). *Gill size and temperature as governing factors in fish growth: A generalization of von Bertalanffy's growth formula* [Report]. Institut für Meereskunde. https://doi.org/10.3289/ifm_ber_63

Pauly, Daniel. (1985). The population dynamics of short-lived species, with emphasis on squids. *NAFO Scientific Council Studies*, *9*, 143–154.

Perez, J. A. A., de Aguiar, D. C., & Oliveira, U. C. (2002). Biology and population dynamics of the long-finned squid *Loligo plei* (Cephalopoda: Loliginidae) in southern Brazilian waters. *Fisheries Research*, *58*(3), 267–279. https://doi.org/10.1016/S0165-7836(01)00397-6

Peterson, N. R., VanDeHey, J. A., & Willis, D. W. (2010). Size and age at maturity of bluegill (*Lepomis macrochirus*) in southeastern South Dakota impoundments. *Journal of Freshwater Ecology*, *25*(2), 303–312. https://doi.org/10.1080/02705060.2010.9665081

Phyto'pedia—The Phytoplankton Encyclopaedia Project. (2012). https://phytoplankton.eoas.ubc.ca/

Piazza, B. P., Banks, P. D., & La Peyre, M. K. (2005). The potential for created oyster shell reefs as a sustainable shoreline protection strategy in Louisiana. *Restoration Ecology*, *13*(3), 499–506.

Poirier, L. A., Clements, J. C., Coffin, M. R. S., Craig, T., Davidson, J., Miron, G., Davidson, J. D. P., Hill, J., & Comeau, L. A. (2021). Siltation negatively affects settlement and gaping behaviour in eastern oysters. *Marine Environmental Research*, *170*, 105432. https://doi.org/10.1016/j.marenvres.2021.105432

Posadas, B. (2020). Economic impacts of coastal hazards on Mississippi commercial oyster fishery from 2005 to 2016. *Journal of Ocean and Coastal Economics*, *6*(1). https://doi.org/10.15351/2373-8456.1115

Potts, Jennifer C. & Manooch III, Charles S. (2002). Estimated ages of red porgy (*Pagrus pagrus*) from fishery-dependent and fishery-independent data and a comparison of growth parameters. *Fishery Bulletin*, *100*(1), 81–89.

Powell, E. N., Klinck, J., & Hofmann, E. (1996). Modeling diseased oyster populations. II. Triggering mechanisms for *Perkinsus marinus* epizootics. *Journal of Shellfish Research*, *15*(1). https://digitalcommons.odu.edu/ccpo_pubs/160

Powell, E. N., Klinck, J., Hofmann, E., & Ray, S. (1994). Modeling oyster populations. IV. Rates of mortality, population crashes, and management. *Fishery Bulletin*, *92*(2). https://digitalcommons.odu.edu/ccpo_pubs/84

Powell, E. N., Mann, R., Ashton-Alcox, K. A., Kim, Y., & Bushek, D. (2016). The allometry of oysters: Spatial and temporal variation in the length–biomass relationships for

Crassostrea virginica. *Journal of the Marine Biological Association of the United Kingdom*, *96*(5), 1127–1144. https://doi.org/10.1017/S0025315415000703

Ragone Calvo, L. M., Wetzel, R. I., & Burreson, E. M. (2000). Development and verification of a model for the population dynamics of the protistan parasite, *Perkinsus marinus*, within its host, the eastern oyster, *Crassostrea virginica*, in Chesapeake Bay. *Journal of Shellfish Research*, *20*(1), 231–241.

Rao, K. V. S. (2011). Age and growth of "Ghol", *Pseudosciaena diacanthus* (Lacépède) in Bombay and Saurashtra waters. *Indian Journal of Fisheries*, *13*(1 & 2), 251–292.

Reagan Jr, R. E., & Wingo, W. M. (1985). *Species profiles: Life histories and environmental requirements of coastal fishes and invertebrates (Gulf of Mexico) - southern flounder. [*Paralichtys lethostigma*]* (NP-5901733). Mississippi State Univ., Mississippi State (USA). Dept. of Wildlife and Fisheries. https://www.osti.gov/biblio/5570193

Ridgway, S. H., & Fenner, C. A. (1982). Weight-length relationships of wild-caught and captive Atlantic bottlenose dolphins. *Journal of the American Veterinary Medical Association*, *181*(11), 1310–1315.

Rose, K. A., McLean, R. I., & Summers, J. K. (1989). Development and monte carlo analysis of an oyster bioaccumulation model applied to biomonitoring data. *Ecological Modelling*, *45*(2), 111–132. https://doi.org/10.1016/0304-3800(89)90087-2

Rozas, L. P., & Minello, T. J. (1997). Estimating densities of small fishes and decapod crustaceans in shallow estuarine habitats: A review of sampling design with focus on gear selection. *Estuaries*, *20*(1), 199–213. https://doi.org/10.2307/1352731

Ruzicka, J. J., Brodeur, R. D., & Wainwright, T. C. (2007). Seasonal Food Web Models for the Oregon Inner-shelf Ecosystem: Investigating the Role of Large Jellyfish. *CalCOFI Report*, 106–128.

Rybovich, M. M. (2014). *Growth and mortality of spat, seed, and market-sized oysters (*Crassostrea virginica*) in low salinities and high temperatures* [Master's Thesis, Louisiana State University]. LSU Master's Theses. https://repository.lsu.edu/gradschool_theses/3690

Sagarese, S. R., Lauretta, M. V., & Walter, J. F. (2017). Progress towards a next-generation fisheries ecosystem model for the northern Gulf of Mexico. *Ecological Modelling*, *345*, 75–98. https://doi.org/10.1016/j.ecolmodel.2016.11.001

Satterfield, E. (2017). *Reassessment of the Red Drum Stock in Mississippi Coastal Waters: The Role of Ages 3-5 Year-Class Fish* [Master's Thesis]. The University of Southern Mississippi.

SEDAR. (2013). *SEDAR 34-HMS Atlantic Sharpnose Shark Stock Assessment Report* (p. 298).

SEDAR. (2018). *SEDAR 63-Gulf Menhaden Stock Assessment Report* (p. 352).

SEDAR. (2024a). *SEDAR 74-Gulf of Mexico Red Snapper Stock Assessment Report* (p. 733).

SEDAR. (2024b). *SEDAR 77-HMS Hammerhead Sharks Stock Assessment Report* (p. 901).

Sergeant, D. E., Caldwell, D. K., & Caldwell, M. C. (1973). Age, growth, and maturity of bottlenosed dolphin (*Tursiops truncatus*) from northeast Florida. *Journal of the Fisheries Research Board of Canada*, *30*(7), 1009–1011. https://doi.org/10.1139/f73-165

Serpetti, N., Baudron, A. R., Burrows, M. T., Payne, B. L., Helaouët, P., Fernandes, P. G., & Heymans, J. J. (2017). Impact of ocean warming on sustainable fisheries management informs the Ecosystem Approach to Fisheries. *Scientific Reports*, *7*(1), 13438. https://doi.org/10.1038/s41598-017-13220-7

Shchepetkin, A. F., & McWilliams, J. C. (2005). The regional oceanic modeling system (ROMS): A split-explicit, free-surface, topography-following-coordinate oceanic model. *Ocean Modelling*, *9*(4), 347–404. https://doi.org/10.1016/j.ocemod.2004.08.002

Sheikh, P. A. (2005). *The Impact of Hurricane Katrina on Biological Resources* (Congressional Research Service Report for Congress Order RL33117; pp. 1–9).

Shlossman, Philip A. & Chittenden Jr., Mark E. (1981). Reproduction, movements, and population dynamics of the sand seatrout, *Cynoscion arenarius*. *Fishery Bulletin*, *79*(4), 649–669.

Sinnickson, D., Chagaris, D., & Allen, M. (2021). Exploring impacts of river discharge on forage fish and predators using Ecopath with Ecosim. *Frontiers in Marine Science*, *8*, 689950. https://doi.org/10.3389/fmars.2021.689950

Soniat, T. M. (1985). Changes in levels of infection of oysters by *Perkinsus marinus*, with special reference to the interaction of temperature and salinity upon parasitism. *Northeast Gulf Science*, *7*(2), 171–174.

Soniat, T. M., Conzelmann, C. P., Byrd, J. D., Roszell, D. P., Bridevaux, J. L., Suir, K. J., & Colley, S. B. (2013). Predicting the effects of proposed Mississippi River diversions

on oyster habitat quality; application of an oyster habitat suitability index model. *Journal of Shellfish Research*, *32*(3), 629–638.

Soniat, T. M., Klinck, J. M., Powell, E. N., & Hofmann, E. E. (2012). Understanding the success and failure of oyster populations: Periodicities of *Perkinsus marinus*, and oyster recruitment, mortality, and size. *Journal of Shellfish Research*, *31*(3), 635–646. https://doi.org/10.2983/035.031.0307

Soniat, T. M., Powell, E., Hofmann, E., & Klinck, J. (1998). Understanding the Success and Failure of Oyster Populations: The Importance of Sampled Variables and Sample Timing. *Journal of Shellfish Research*, *17*(4). https://digitalcommons.odu.edu/ccpo_pubs/89

Soto Ramos, I. M., Crooke, B., Seegers, B., Cetinić, I., Cambazoglu, M. K., & Armstrong, B. (2023). Spatial and temporal characterization of cyanobacteria blooms in the Mississippi Sound and their relationship to the Bonnet Carré Spillway openings. *Harmful Algae*, *127*, 102472. https://doi.org/10.1016/j.hal.2023.102472

Sparre, P., & Venema, S. C. (1998). Introduction to tropical fish stock assessment. Part 1. Manual. *FAO Fish. Tech. Paper.*, *306*, 1–407.

St. Amant, L. S. (1957). *The Southern Oyster Drill* (Louisiana Wildlife and Fisheries Commission 7th Biennial Report, pp. 81–85).

Stanic, S., Wiggert, J. D., Bernard, L., McKenna, J., Sunkara, V., Braud, J., & Diercks, A. (2024). Coastal CUBEnet: An integrated observation and modeling system for sustainable Northern Gulf of Mexico coastal areas. *Frontiers in Marine Science*, *11*. https://doi.org/10.3389/fmars.2024.1400511

Stanley, J. G., & Sellers, M. A. (1986). *Species profiles: Life histories and environmental requirements of coastal fishes and invertebrates (Gulf of Mexico)—American oyster* (Technical Report TR EL-82-4). U.S. Army Corps of Engineers.

Stenzel, H. B. (1971). *Treatise on invertebrate paleontology: Part N (Vol. 3 of 3) Mollusca 6: Bivalvia: Oysters*.

Stevenson, Jill T. & Secor, David H. (1999). Age determination and growth of Hudson River Atlantic sturgeon, *Acipenser oxyrinchus*. *Fishery Bulletin*, *97*, 153–166.

Sumer, C., Teksam, I., Karatas, H., Beyhan, T., & Aydın, C. (2013). Growth and reproduction biology of the blue crab, *Callinectes sapidus* Rathbun, 1896, in the Beymelek Lagoon (southwestern coast of Turkey). *Turkish Journal of Fisheries and Aquatic Sciences*, *13*, 675–684. https://doi.org/10.4194/1303-2712-v13_4_13

Supan, J., & Voisin, M. (2006). The Louisiana oyster recovery plan: A response to Hurricanes Katrina and Rita. *Journal of Shellfish Research*, *25*(2), 780.

Texas Parks & Wildlife Department. (n.d.). *Pinfish (*Lagodon rhomboides*)*. Texas Parks & Wildlife. Retrieved March 11, 2025, from https://tpwd.texas.gov/huntwild/wild/species/pinfish/

Turner, J. S. (2021). *Water Clarity and Suspended Particle Dynamics in the Chesapeake Bay: Local Effects of Oyster Aquaculture, Regional Effects of Reduced Shoreline Erosion, and Long-Term Trends in Remotely Sensed Reflectance* [Doctoral Dissertation]. The College of William & Mary.

United States Army Corps of Engineers. (2021, April 14). *Bonnet Carré Spillway Overview, Spillway Operation Information*.

https://www.mvn.usace.army.mil/Missions/Mississippi-River-Flood-Control/Bonnet-Carre-Spillway-Overview/Spillway-Operation-Information/

U.S. Fish and Wildlife Service (USFWS). (1981). *Standards for the Development of Habitat Suitability Index Models* (USFWS Technical Report 103 ESM; p. 81).

U.S. Fish and Wildlife Service (USFWS). (1982). *Gulf Coast Ecological Inventory Map: Mobile, Alabama, Mississippi, Louisiana Area* [Map]. https://digital.library.unt.edu/ark:/67531/metadc66684/

U.S. Geological Survey. (2021). *National Water Information System data available on the World Wide Web* [Dataset]. http://dx.doi.org/10.5066/F7P55KJN

VanderKooy, S. J. (2012). *The oyster fishery of the Gulf of Mexico, United States: A fisheries management plan (2012 Revision)* (Report for the Gulf States Marine Fisheries Commission, National Oceanographic and Atmospheric Administration).

Veenstra, J., Southwell, M., Dix, N., Marcum, P., Jackson, J., Burns, C., Herbert, C., & Kemper, A. (2021). High carbon accumulation rates in sediment adjacent to constructed oyster reefs, Northeast Florida, USA. *Journal of Coastal Conservation*, *25*(4), 40. https://doi.org/10.1007/s11852-021-00829-0

Vignier, J., Rolton, A., Soudant, P., Chu, F.-L. E., Robert, R., & Volety, A. K. (2018). Evaluation of toxicity of Deepwater Horizon slick oil on spat of the oyster *Crassostrea virginica*. *Environmental Science and Pollution Research International*, *25*(2), 1176–1190. https://doi.org/10.1007/s11356-017-0476-2

Volety, A. K., Savarese, M., Tolley, S. G., Arnold, W. S., Sime, P., Goodman, P., Chamberlain, R. H., & Doering, P. H. (2009). Eastern oysters (*Crassostrea virginica*) as an indicator

for restoration of Everglades ecosystems. *Ecological Indicators*, *9S*, 120–136. https://doi.org/10.1016/j.ecolind.2008.06.005

von Bertalanffy, L. (1938). A quantitative theory of organic growth (inquiries on growth laws. II). *Human Biology*, *10*(2), 181–213.

Walters, C., Martell, S. J. D., Christensen, V., & Mahmoudi, B. (2008). An Ecosim model for exploring Gulf of Mexico ecosystem management options: Implications of including multistanza life-history models for policy predictions. *Bulletin of Marine Science*, *83*(1), 251–271.

Waltz, C. Wayne, Roumillat, William A., & Wenner, Charles A. (1982). Biology of the whitebone porgy, *Calamus leucosteus*, in the South Atlantic Bight. *Fishery Bulletin*, *80*(4), 863–874.

Warner, J. C., Armstrong, B., He, R., & Zambon, J. B. (2010). Development of a Coupled Ocean–Atmosphere–Wave–Sediment Transport (COAWST) modeling system. *Ocean Modelling*, *35*(3), 230–244. https://doi.org/10.1016/j.ocemod.2010.07.010

Wells, B., & Jones, C. (2002). Reproduction of black drum, *Pogonias cromis*, from the Chesapeake Bay region. *Virginia Journal of Science*, *53*(1), 3–11. https://doi.org/10.25778/ncmy-pm70

Wiggert, J. D., Armstrong, B. N., Cambazoglu, M. K., & Sandeep, K. K. (2022). *Mid-Breton Sediment Diversion (MBrSD) Assessment—Final Report* (p. 96) [Technical Report]. The University of Southern Mississippi. https://doi.org/10.18785/sose.001

Appendix

Environmental Response Thresholds for Eastern Oyster (*Crassostrea virginica*)

Table A1. Temperature response thresholds among various age classes of the eastern oyster (Crassostrea virginica) in productive U.S. Gulf and Atlantic reef areas (n.d. = no data).

Life Stage	Temperature (°C) Minima	Temperature (°C) Optima	Temperature (°C) Maxima
Larv	*n.d.* [b2007]	20.0 - 30.0 [b2007]	*n.d.* [b2007]
	15.0 [d1964]	27.5 - 32.5 [d1964]	37.5 [*d1964*]
	15.0 [d1993]	32.0 - 35.0 [d1993]	*n.d.* [d1993]
	15.3 [l1975]	32.1 - *n.d.* [l1975]	*n.d.* [l1975]
	17.5 [n2007]	20.0 - 32.5 [n2007]	*n.d.* [n2007]
Spat	8.0 [c2005]	25.0 - 29.0 [c2005]	46.0 [c2005]
	n.d. [h1990]	*n.d.* - *n.d.* [h1990]	32.0 [h1990]
	20.0 [h2014, s1986]	25.0 - 30.0 [h2014, s1986]	*n.d.* [h2014, s1986]
	6.0 [l2016]	*n.d.* - *n.d.* [l2016]	32.0 [l2016]
Seed	6.5 [b2007]	20.0 - 30.0 [b2007]	42.0 [b2007]
	n.d. [c1983]	20.0 - 30.0 [c1983]	34.0 [c1983]
	8.0 [c2005]	25.0 - 29.0 [c2005]	46.0 [c2005]
	n.d. [h1990]	*n.d.* - *n.d.* [h1990]	32.0 [h1990]
	6.0 [l2016]	*n.d.* - *n.d.* [l2016]	32.0 [l2016]
	n.d. [n2007]	20.0 - 30.0 [n2007]	36.0 [n2007]
Sack	6.5 [b2007]	20.0 - 30.0 [b2007]	42.0 [b2007]
	5.0 [c1983]	20.0 - 30.0 [c1983]	34.0 [c1983]
	8.0 [c2005]	25.0 - 29.0 [c2005]	46.0 [c2005]
	1.0 [g1964]	*n.d.* - *n.d.* [g1964]	36.0 [g1964]
	n.d. [h1990]	*n.d.* - *n.d.* [h1990]	32.0 [h1990]
	1.0 [h2014, s1986]	20.0 - 30.0 [h2014, s1986]	49.0 [h2014, s1986]
	6.0 [l2016]	*n.d.* - *n.d.* [l2016]	32.0 [l2016]
	n.d. [n2007]	20.0 - 30.0 [n2007]	36.0 [n2007]

Sources: [b2007]Barnes et al. (2007); [c1983]Cake (1983); [c2005]Cerco & Noel (2005); [d1964]Davis & Calabrese (1964); [d1993]Dekshenieks et al. (1993); [g1964]Galtsoff (1964); [h1990]Hofstetter (1990); [h2014]Hijuelos et al. (2014); [l2016]Linhoss et al. (2016); [n2007]NOAA Technical Report F/SPO-88 (2007); [s1986]Stanley & Sellers (1986)

Table A2. Salinity response thresholds among various age classes of the eastern oyster (Crassostrea virginica) in productive U.S. Gulf and Atlantic reef areas (n.d. = no data).

Life Stage	Salinity Minima	Salinity Optima	Salinity Maxima
Larv	5.0 b2007	20.0 - 29.0 b2007	35.0 b2007
	6.2 d1964	20.4 - 27.5 d1964	*n.d.* d1964
	5.4 l1975	19.0 - *n.d.* l1975	*n.d.* l1975
	5.0 d1993	17.5 - 32.0 d1993	*n.d.* d1993
	n.d. d1996	17.5 - 25.0 d1996	*n.d.* d1996
	5.0 g1964	12.5 – *n.d.* g1964	*n.d.* g1964
Spat	5.0 b2007	12.0 - 27.0 b2007	>35.0 b2007
	4.0 c2005	10.0 - *n.d.* c2005	*n.d.* c2005
	n.d. h1990	15.0 - 30.0 h1990	*n.d.* h1990
	5.0 h2014, p1995	8.0 - 15.0 h2014, p1995	39.0 h2014, p1995
	6.0 l2016	12.0 - 27.0 l2016	*n.d.* l2016
	5.0 v2012	7.5 - *n.d.* v2012	*n.d.* v2012
Seed	5.0 b1954, c1983	10.0 - 20.0 b1954, c1983	40.0 b1954, c1983
	5.0 b2007	14.0 - 28.0 b2007	40.0 b2007
	4.0 c2005	10.0 - *n.d.* c2005	*n.d.* c2005
	n.d. e1977	10.0 - 30.0 e1977	*n.d.* e1977
	5.0 g1955, g1964, s1971	*n.d. - n.d.* g1955, g1964, s1971	40.0 g1955, g1964, s1971
	n.d. h1990	15.0 - 30.0 h1990	*n.d.* h1990
	2.0 h2014, p1995	8.0 - 15.0 h2014, p1995	43.5 h2014, p1995
	6.0 l2016	12.0 - 27.0 l2016	*n.d.* l2016
	5.0 n2007, v2009	14.0 - 28.0 n2207, v2009	42.0 n2007, v2009
	3.5 p1994	7.5 - *n.d.* p1994	*n.d.* p1994
	5.0 v2012	7.5 - *n.d.* v2012	*n.d.* v2012
Sack	5.0 b1954, c1983	10.0 - 20.0 b1954, c1983	40.0 b1954, c1983
	5.0 b2007	**14.0 - 28.0 b2007**	**40.0 b2007**
	4.0 c2005	**10.0 - *n.d.* c2005**	***n.d.* c2005**
	***n.d.* e1977**	**10.0 - 30.0 e1977**	***n.d.* e1977**
	5.0 g1955, g1964, s1971	***n.d. - n.d.* g1955, g1964, s1971**	**40.0 g1955, g1964, s1971**
	***n.d.* h1990**	**15.0 - 30.0 h1990**	***n.d.* h1990**
	2.0 h2014, p1995	**14.0 - 30.0 h2014, p1995**	**43.5 h2014, p1995**
	6.0 l2016	**12.0 - 27.0 l2016**	***n.d.* l2016**
	5.0 n2007, v2009	**14.0 - 28.0 n2207, v2009**	**42.0 n2007, v2009**
	3.5 p1994	**7.5 - *n.d.* p1994**	***n.d.* p1994**
	5.0 v2012	**7.5 - *n.d.* v2012**	***n.d.* v2012**

Sources: b1954Butler (1985); b2007Barnes et al. (2007); c1983Cake (1983); c2005Cerco & Noel (2005); d1964Davis & Calabrese (1964); d1993Dekshenieks et al. (1993); d1996Dekshenieks et al. (1996); e1977Eleuterius (1977); g1955Gunter & Geyer (1955); g1964Galtsoff (1964); h1990Hofstetter (1990); h2014Hijuelos et al. (2014); l1975Lough (1975); l2016Linhoss et al. (2016); n2007NOAA Technical Report F/SPO-88 (2007); p1994Powell et al. (1994); p1995Patillo et al. (1995); s1971Stenzel (1971); v2009Volety et al. (2009); v2012VanderKooy (2012)